Measurement of forward-backward multiplicity correlations in Pb+Pb, *p*+Pb and *pp* collisions with the ATLAS detector

Mingliang Zhou

(Stony Brook University)

for the ATLAS collaboration

ATLAS-CONF-2015-051

Initial Stages Conference, Lisbon

26 May 2016

Motivation: a historical view

- Rapidity correlations is an old story

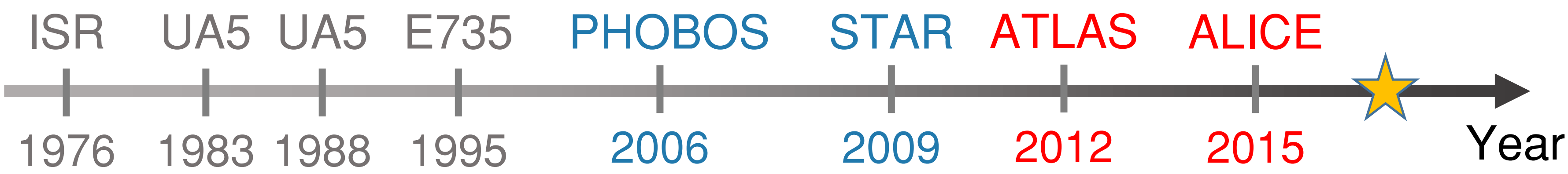

- Physics goal: understand production mechanism in early stage.
  - More details see Longgang and Jiangyong's talks.

Motivation: a historical view

- Rapidity correlations is an old story

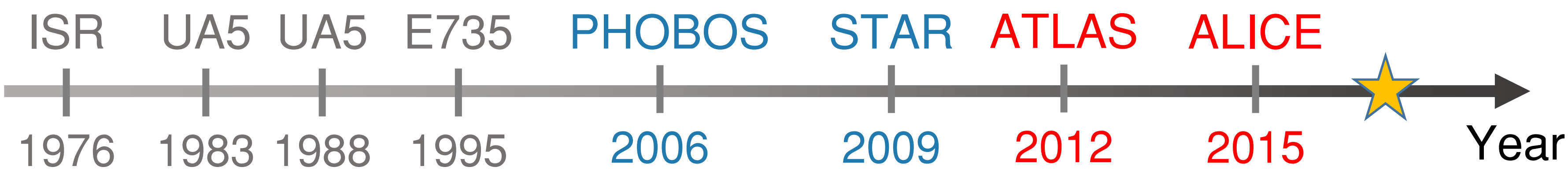

- Physics goal: understand production mechanism in early stage.
  - More details see Longgang and Jiangyong's talks.

- Why we come back to this analysis?
  - Previous methods focused on limited phase space: η and $-\eta$;
  - Short-range correlation and statistical dilution;
  - Few direct comparisons among different systems;

Motivation: a historical view

- Rapidity correlations is an old story

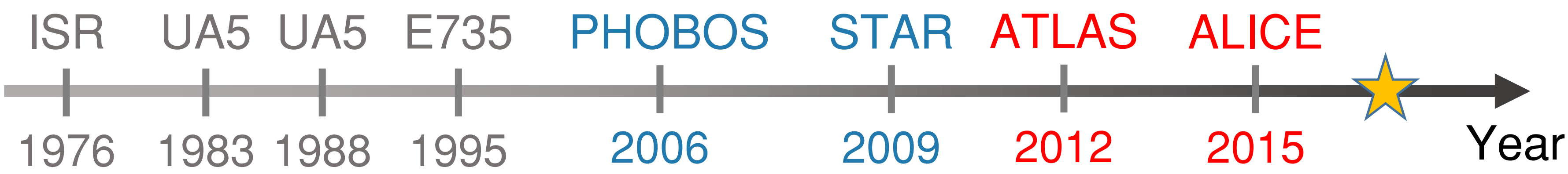

- Physics goal: understand production mechanism in early stage.
  - More details see Longgang and Jiangyong's talks.

- Why we come back to this analysis?
  - Previous methods focused on limited phase space: η and $-\eta$;
  - We used a new observable that covers full η space;
  - Short-range correlation and statistical dilution;
  - We estimated short-range correlation;
  - Few direct comparisons among different systems;
  - We compared from large to small systems.

Pb+Pb, *p*+Pb and *pp* datasets

- Correlation functions calculated using charged particles $p_T > 0.2$ GeV;
- High-multiplicity track (HMT) trigger used to increase statistics;

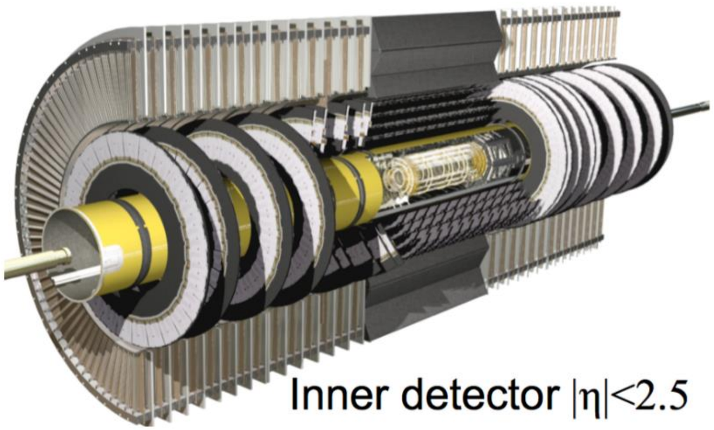

Pb+Pb 2.76 TeV, 2010, MB

p+Pb 5.02 TeV, 2013, MB+HMT

p+p 13 TeV, 2015, MB+HMT

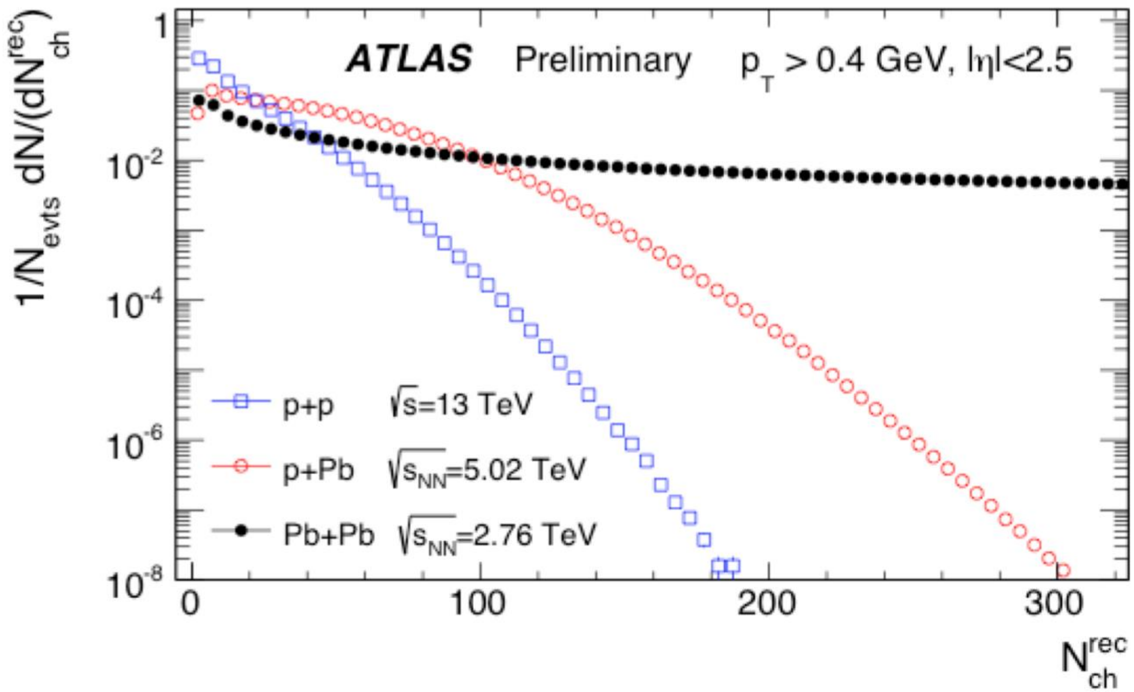

- Analysis carried out in many bins over $10 \leq N_{ch}^{rec} < 300$;
- Results presented as a function efficiency-corrected values N_{ch}.

Pb+Pb, *p*+Pb and *pp* datasets

- Correlation functions calculated using charged particles $p_T > 0.2$ GeV;
- High-multiplicity track (HMT) trigger used to increase statistics;

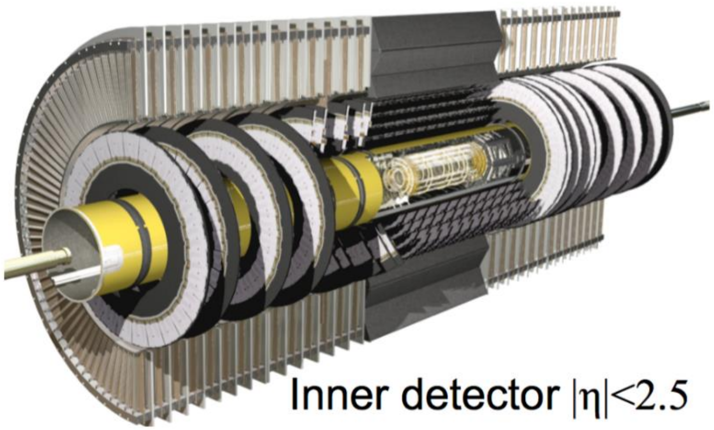

Pb+Pb 2.76 TeV, 2010, MB

p+Pb 5.02 TeV, 2013, MB+HMT

p+p 13 TeV, 2015, MB+HMT

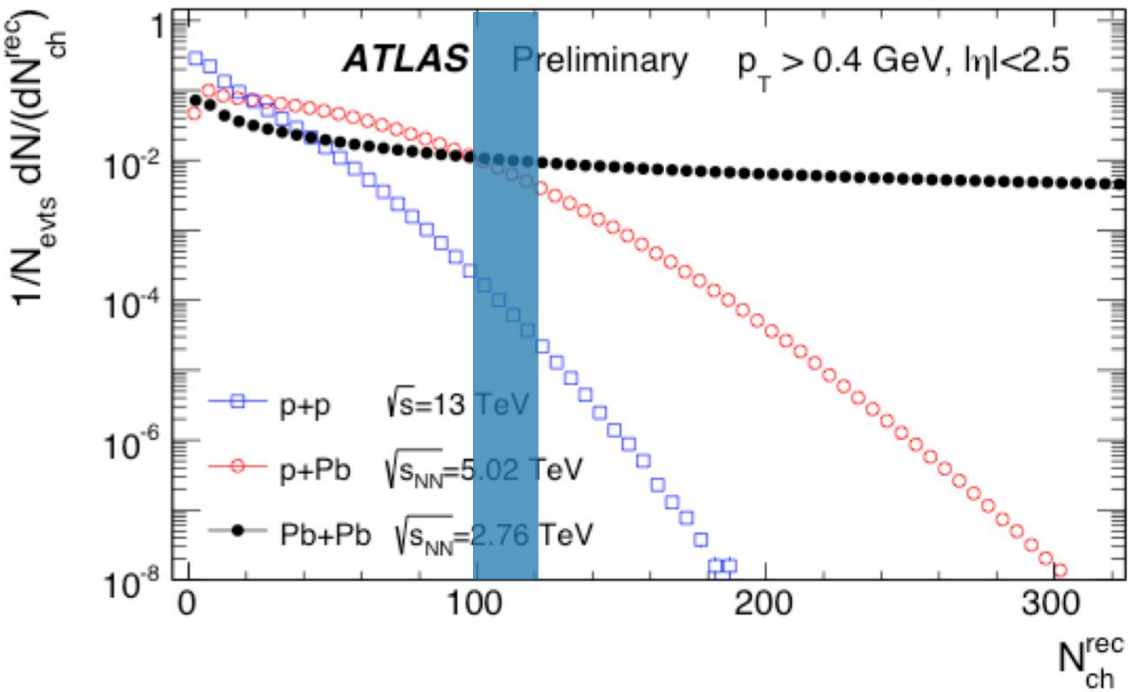

- Analysis carried out in many bins over $10 \leq N_{ch}^{rec} < 300$;
- Results presented as a function efficiency-corrected values N_{ch}.

  - How long-range correlation compare among three systems, at the same N_{ch}?

Observable

- Single particle observable

$$R_s(\eta) \equiv \frac{N(\eta)}{\langle N(\eta) \rangle}$$

Observable

- Single particle observable

$$R_s(\eta) \equiv \frac{N(\eta)}{\langle N(\eta) \rangle}$$

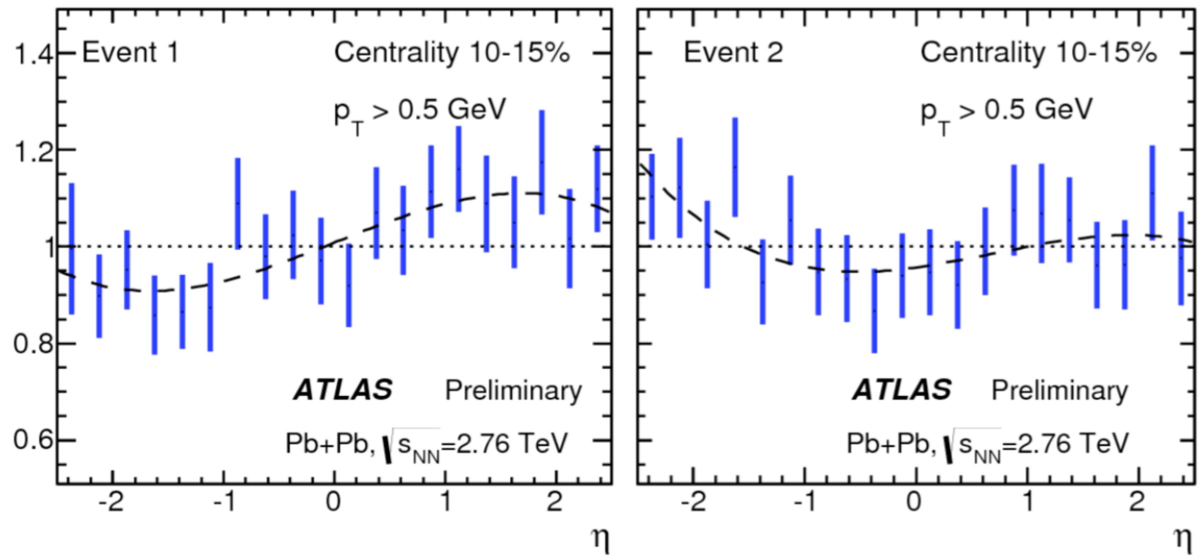

Observable

- Single particle observable

$$R_s(\eta) \equiv \frac{N(\eta)}{\langle N(\eta) \rangle}$$

- Dominated by statistical fluctuations!

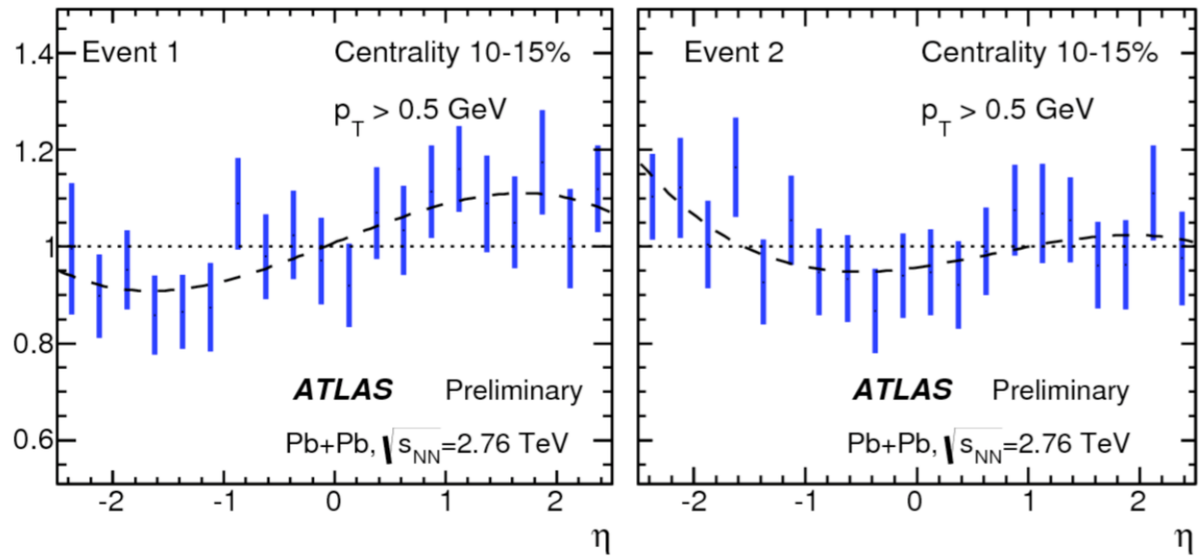

Observable

- Single particle observable

$$R_s(\eta) \equiv \frac{N(\eta)}{\langle N(\eta)\rangle}$$

- Dominated by statistical fluctuations!

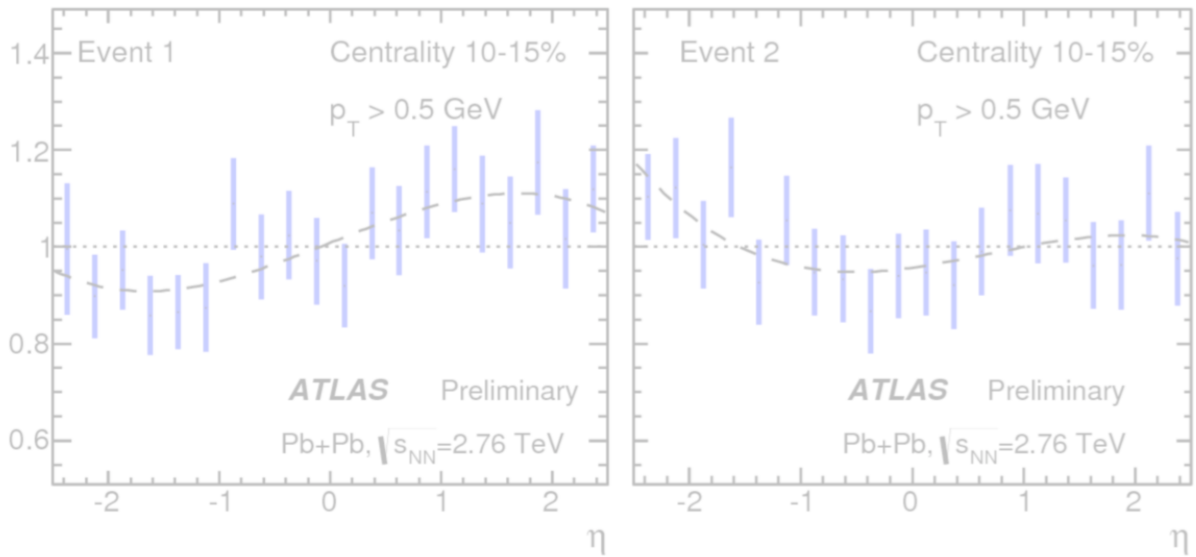

- Two particles observable (correlation function)

$$C(\eta_1, \eta_2) = \frac{\langle N(\eta_1) N(\eta_2)\rangle}{\langle N(\eta_1)\rangle\langle N(\eta_2)\rangle}$$

Observable

- Single particle observable

$$R_s(\eta) \equiv \frac{N(\eta)}{\langle N(\eta) \rangle}$$

- Dominated by statistical fluctuations!

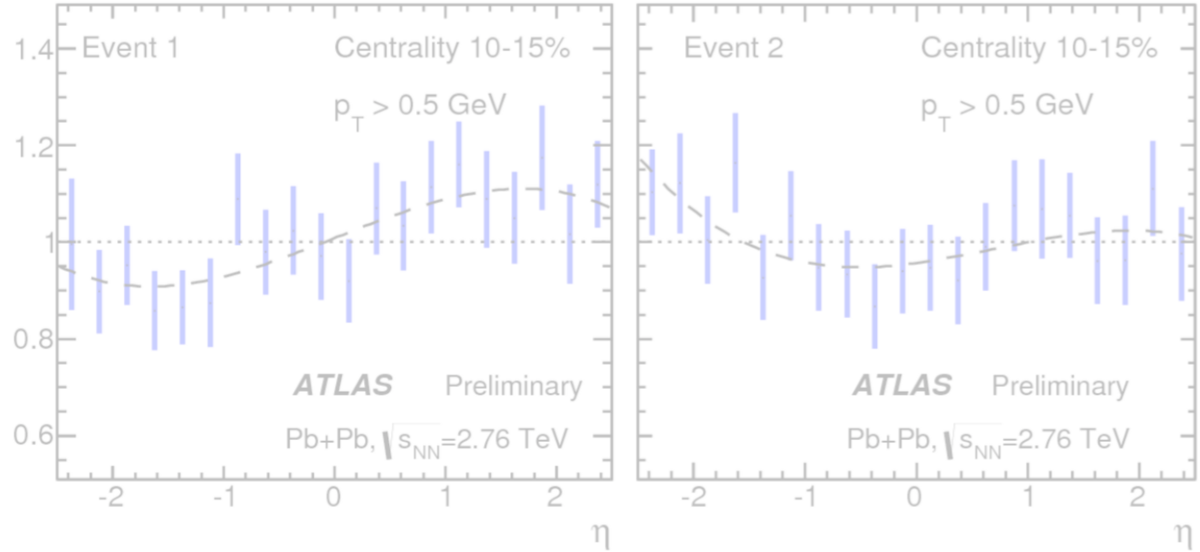

- Two particles observable (correlation function)

$$C(\eta_1, \eta_2) = \frac{\langle N(\eta_1) N(\eta_2) \rangle}{\langle N(\eta_1) \rangle \langle N(\eta_2) \rangle} = \langle R_s(\eta_1) R_s(\eta_2) \rangle$$

Two-particle correlation is related to single-particle distribution.

Observable

- Single particle observable

$$R_s(\eta) \equiv \frac{N(\eta)}{\langle N(\eta)\rangle}$$

- Dominated by statistical fluctuations!

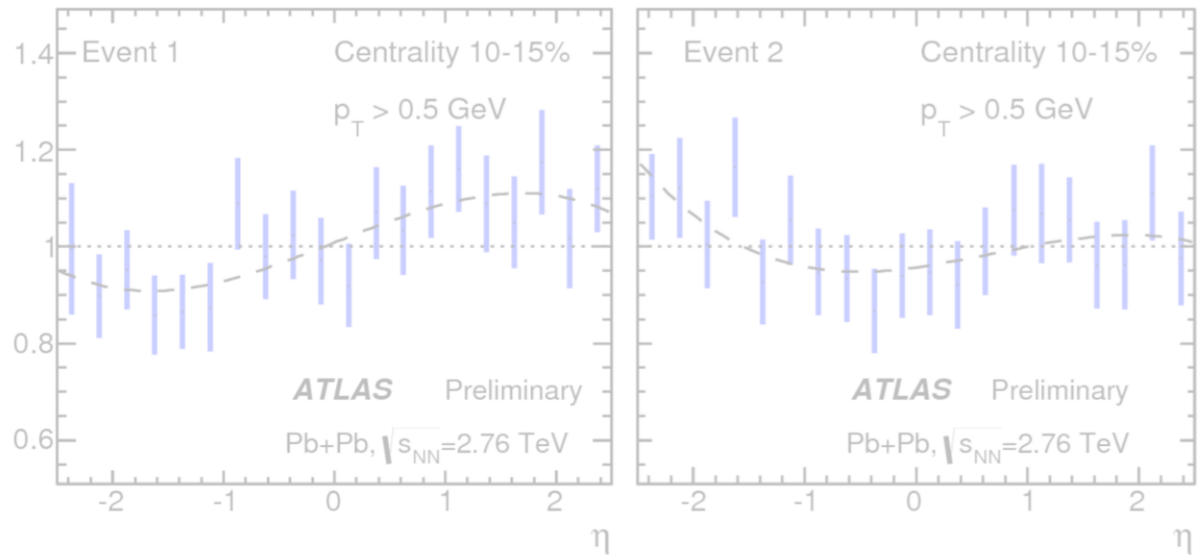

- Two particles observable (correlation function)

$$C(\eta_1,\eta_2) = \frac{\langle N(\eta_1)N(\eta_2)\rangle}{\langle N(\eta_1)\rangle\langle N(\eta_2)\rangle} = \langle R_s(\eta_1)R_s(\eta_2)\rangle$$

Two-particle correlation is related to single-particle distribution.

- Advantage of correlation function
  - Disentangles dynamical fluctuation from statistical fluctuation.
  - Detector effects removed by mixed events;

A. Bzdak and D. Teaney, PRC 87 (2013) 024906

Jia, Jiangyong, Sooraj Radhakrishnan, and MZ. Phys.Rev. C93 (2016) no.4, 044905

FB multiplicity correlation $C(\eta_1, \eta_2)$

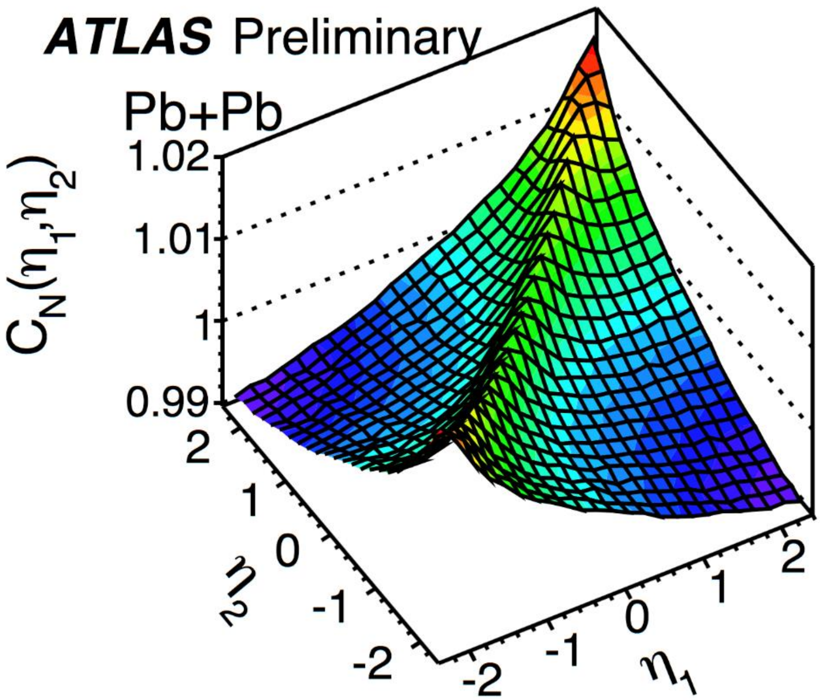

FB multiplicity correlation $C(\eta_1, \eta_2)$

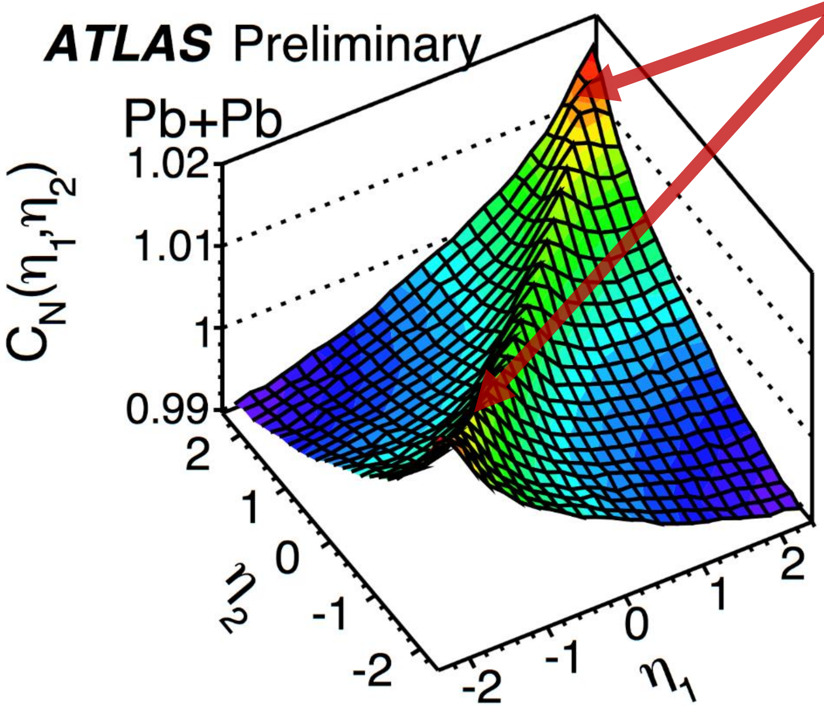

$|\eta_-| \equiv |\eta_1 - \eta_2| \approx 0$

Short-range correlation $\delta_{SRC}(\eta_1, \eta_2)$

reflect correlation in the same source:

jet fragmentation, resonance decay...

FB multiplicity correlation $C(\eta_1, \eta_2)$

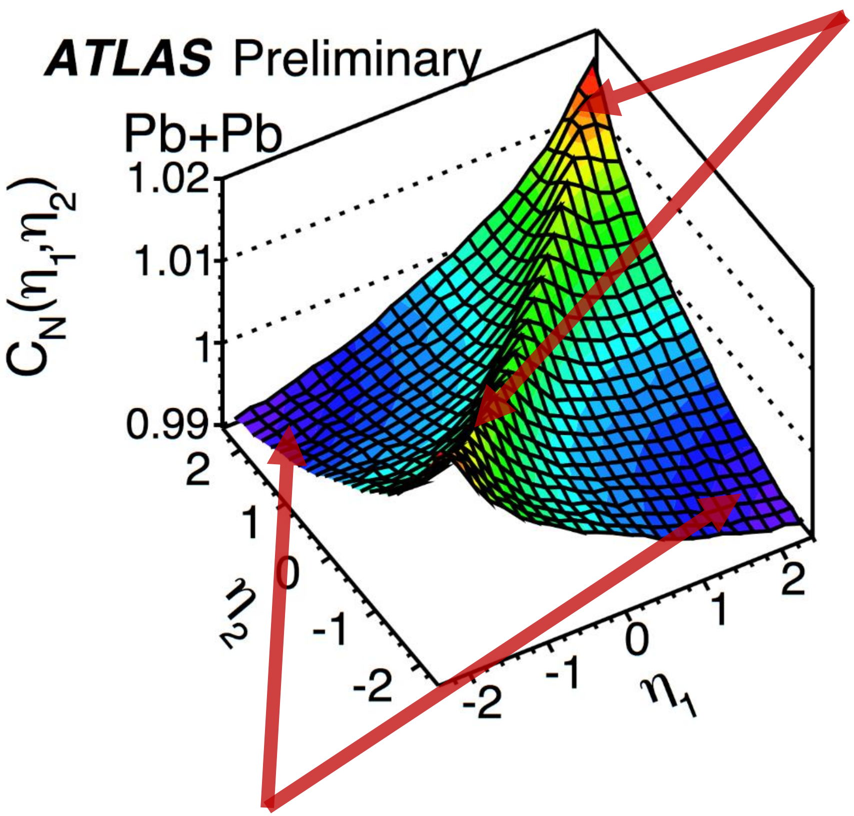

$|\eta_-| \equiv |\eta_1 - \eta_2| \approx 0$

Short-range correlation $\delta_{SRC}(\eta_1, \eta_2)$

reflect correlation in the same source:

jet fragmentation, resonance decay...

$|\eta_-| \equiv |\eta_1 - \eta_2| > 1.5$

Long-range correlation $C_{LRC}(\eta_1, \eta_2)$

reflect FB asymmetric number of sources:

participants, partons, tubes/strings...

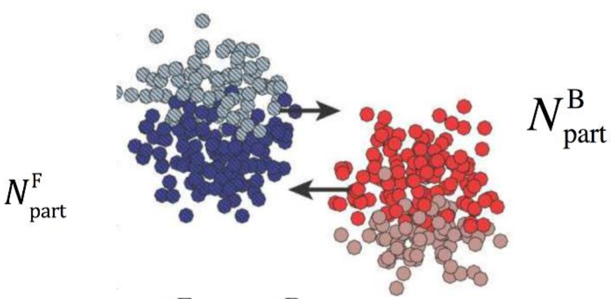

$$A_{\mathrm{part}} = \frac{N^{\mathrm{F}}_{\mathrm{part}} - N^{\mathrm{B}}_{\mathrm{part}}}{N^{\mathrm{F}}_{\mathrm{part}} + N^{\mathrm{B}}_{\mathrm{part}}}$$

FB multiplicity correlation $C(\eta_1, \eta_2)$

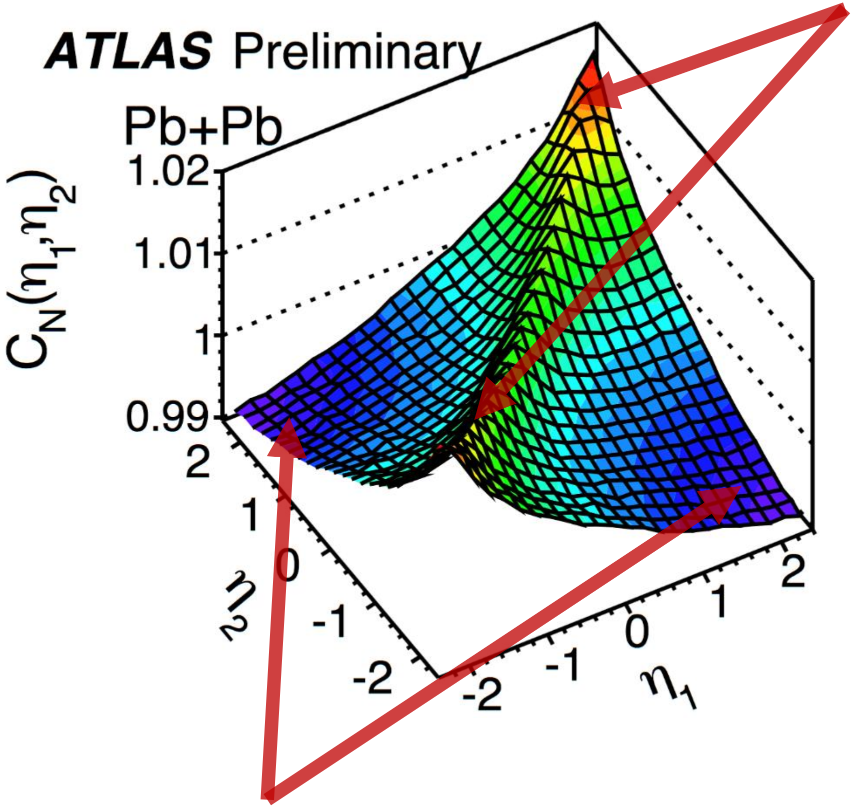

$|\eta_-| \equiv |\eta_1 - \eta_2| \approx 0$

Short-range correlation $\delta_{SRC}(\eta_1, \eta_2)$

reflect correlation in the same source:

jet fragmentation, resonance decay...

- Goal: study the long-range correlation;
- Challenge: hard cut on $|\Delta\eta| < 2$ to suppress SRC will lose information.

$|\eta_-| \equiv |\eta_1 - \eta_2| > 1.5$

Long-range correlation $C_{LRC}(\eta_1, \eta_2)$

reflect FB asymmetric number of sources:

participants, partons, tubes/strings...

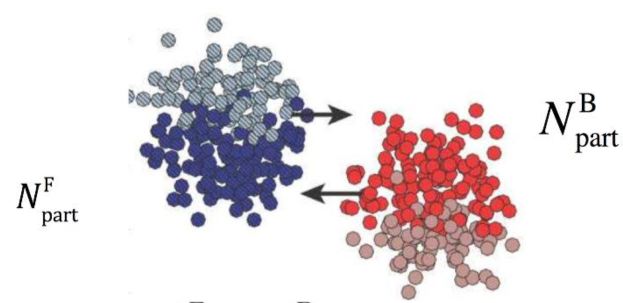

$$A_{\mathrm{part}} = \frac{N^{\mathrm{F}}_{\mathrm{part}} - N^{\mathrm{B}}_{\mathrm{part}}}{N^{\mathrm{F}}_{\mathrm{part}} + N^{\mathrm{B}}_{\mathrm{part}}}$$

Charge dependence of $C(\eta_1, \eta_2)$

- Particles from the same source (SRC) have strong charge dependence.

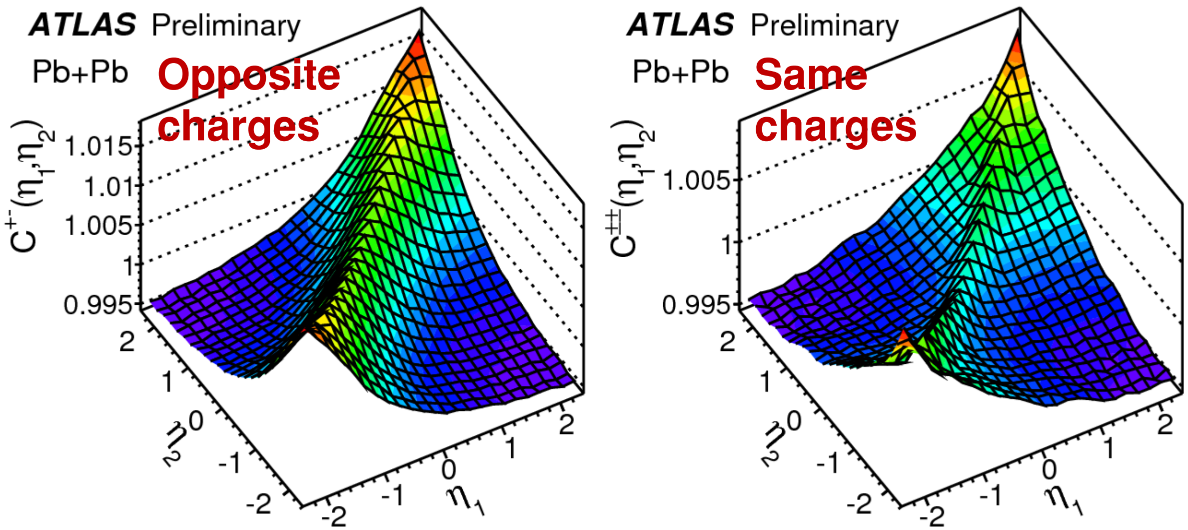

Charge dependence of $C(\eta_1, \eta_2)$

- Particles from the same source (SRC) have strong charge dependence.

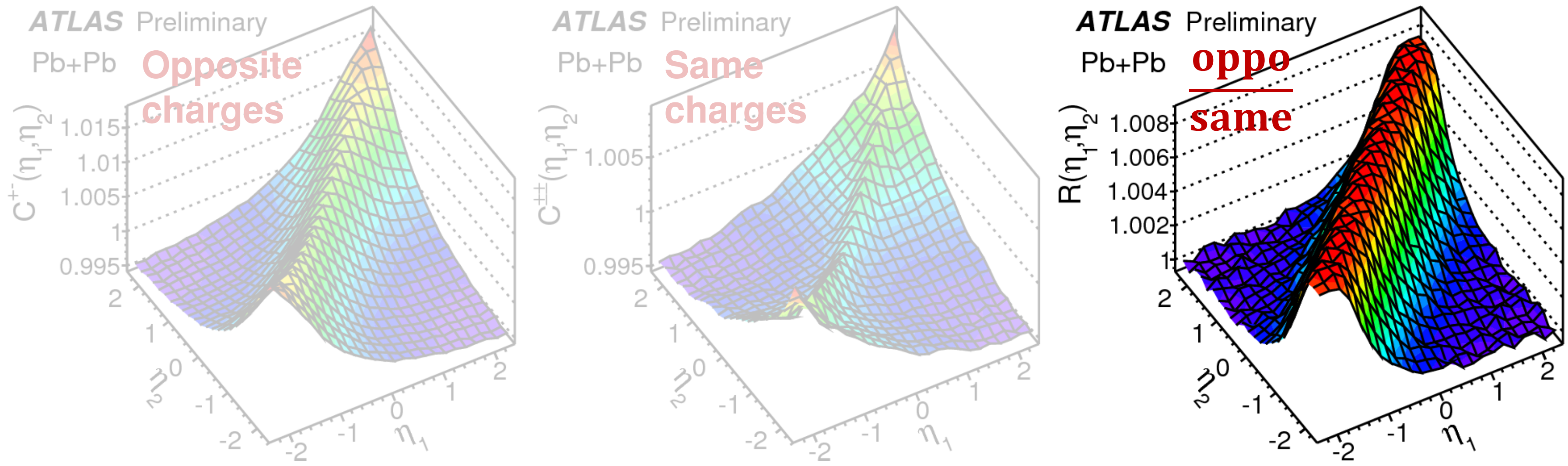

- Ratio of opposite to same charges $R(\eta_1, \eta_2)$
  - Very strong Gaussian-like SRC;
  - Very weak LRC: charge-independent;

Charge dependence of $C(\eta_1, \eta_2)$

- Particles from the same source (SRC) have strong charge dependence.

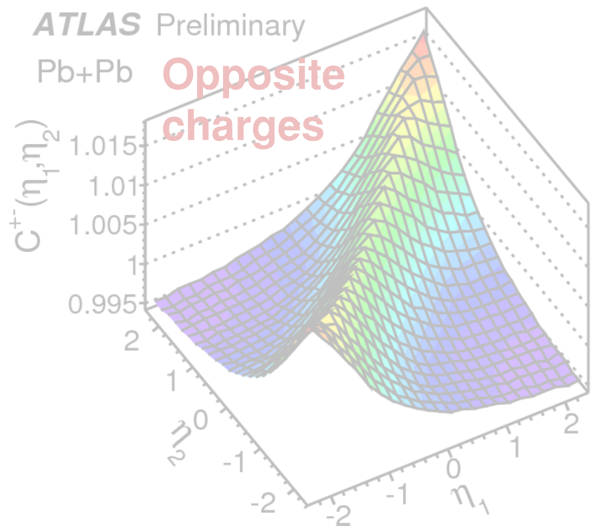

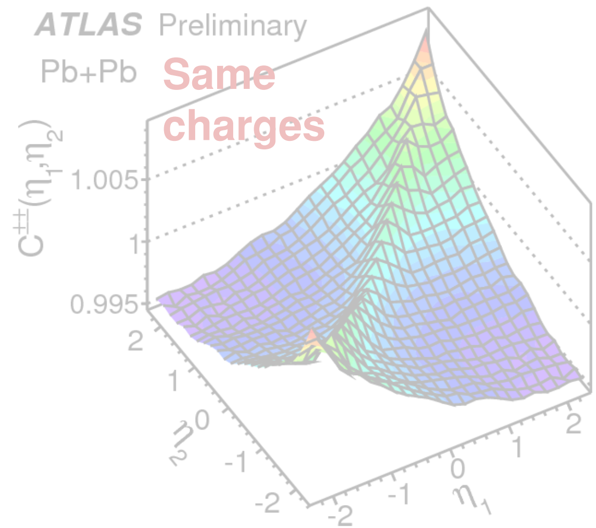

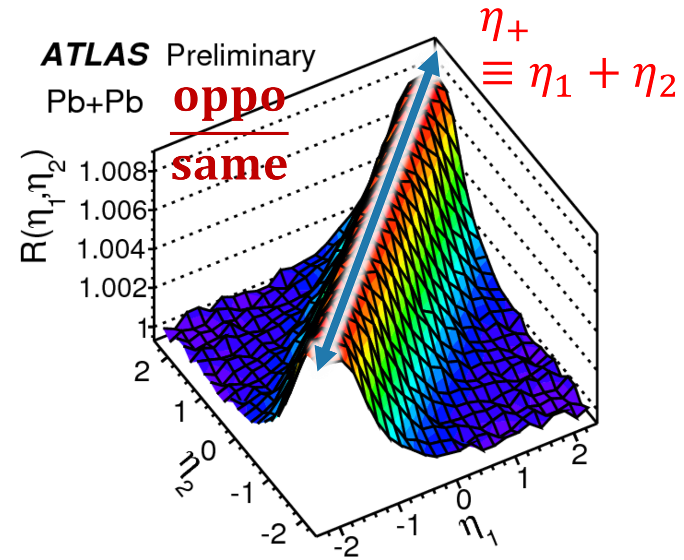

- Ratio of opposite to same charges $R(\eta_1, \eta_2)$
  - Very strong Gaussian-like SRC;
  - Very weak LRC: charge-independent;
- Amplitude of $R(\eta_1, \eta_2)$ along η_+: $f(\eta_+)$, reflects the strength of SRC in the longitudinal direction;

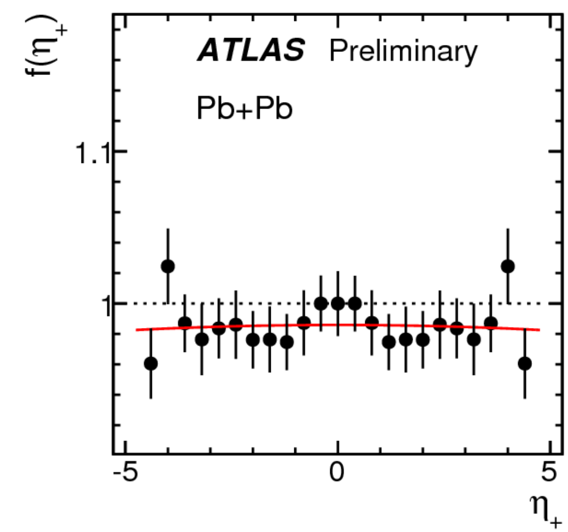

Charge dependence of $C(\eta_1, \eta_2)$

- Particles from the same source (SRC) have strong charge dependence.

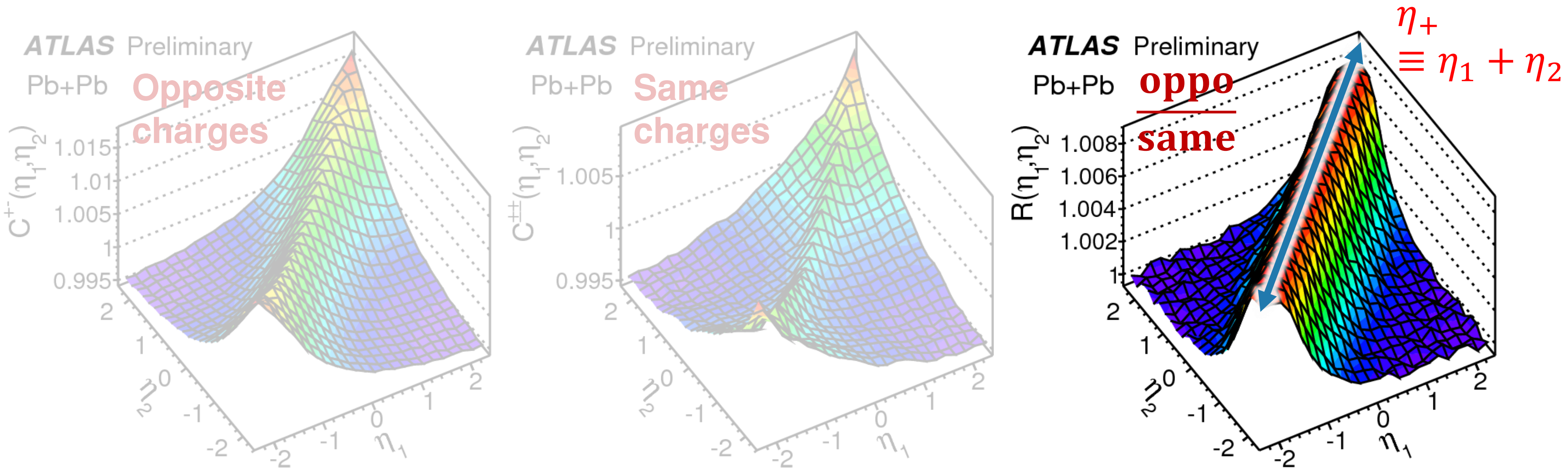

- Ratio of opposite to same charges $R(\eta_1, \eta_2)$
  - Very strong Gaussian-like SRC;
  - Very weak LRC: charge-independent;
- Amplitude of $R(\eta_1, \eta_2)$ along η_+: $f(\eta_+)$, reflects the strength of SRC in the longitudinal direction;
- Assumption: strength of SRC along η_+ is same for same charge and opposite charge.

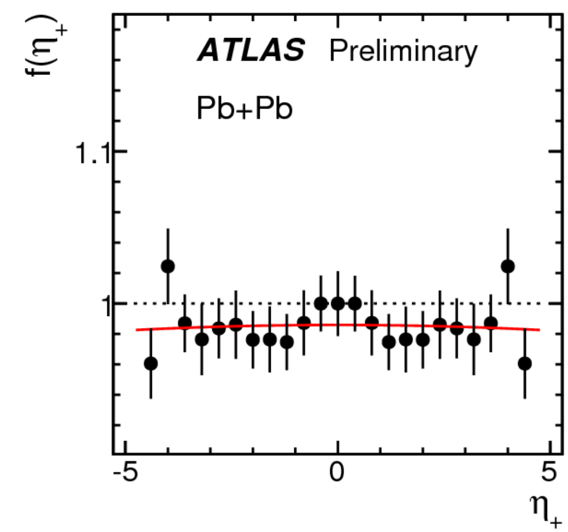

Estimation of short-range correlation

- To estimate SRC, LRC pedestal is estimated first.

Estimation of short-range correlation

- To estimate SRC, LRC pedestal is estimated first.

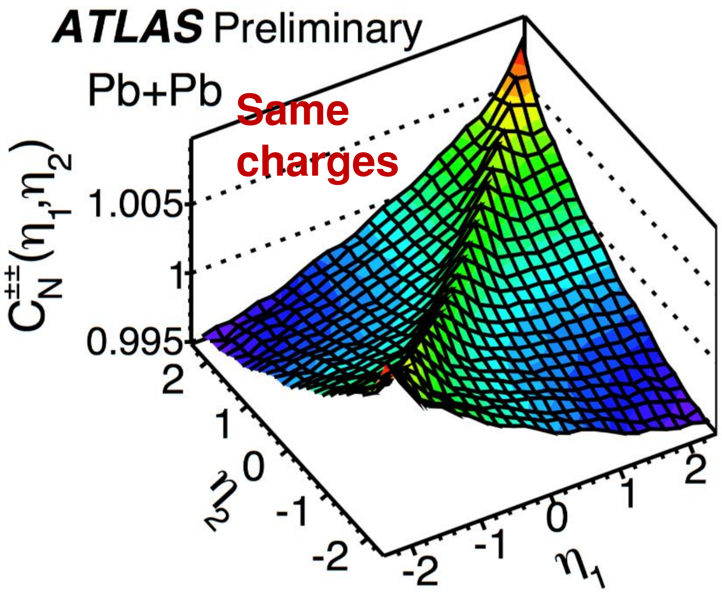

- $C(\eta_1, \eta_2)$ from same charge used to estimate LRC pedestal because of small SRC;

Estimation of short-range correlation

- To estimate SRC, LRC pedestal is estimated first.

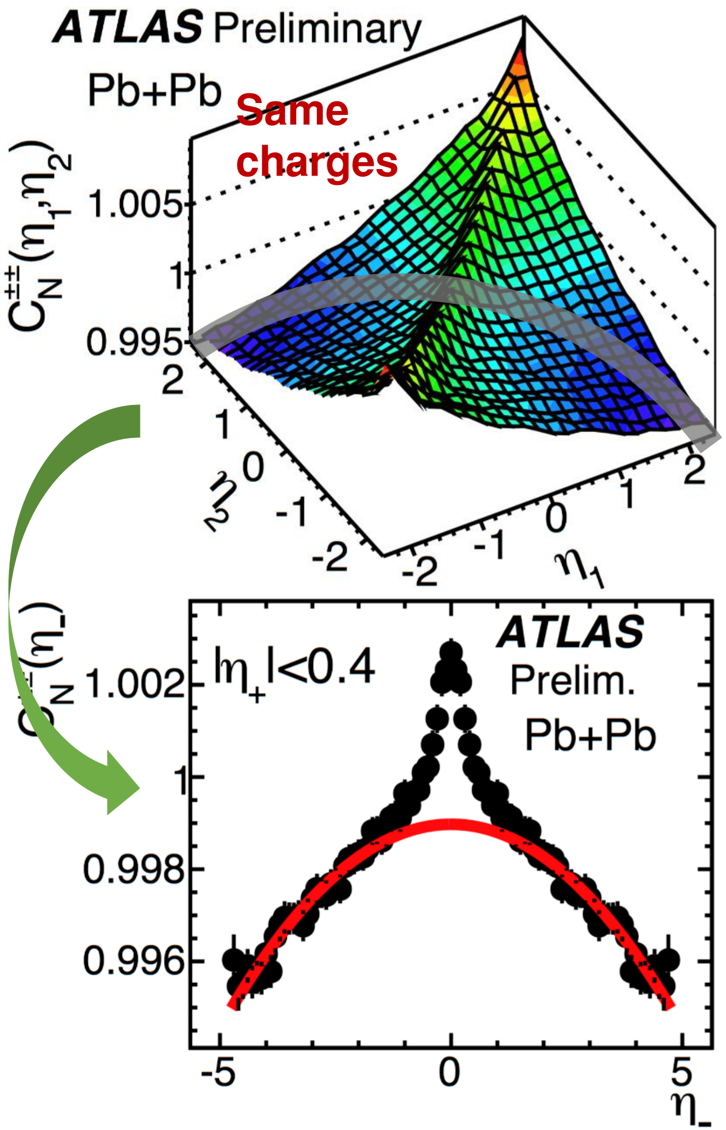

- $C(\eta_1, \eta_2)$ from same charge used to estimate LRC pedestal because of small SRC;
- LRC pedestal is fitted with quadratic function;

Estimation of short-range correlation

- To estimate SRC, LRC pedestal is estimated first.

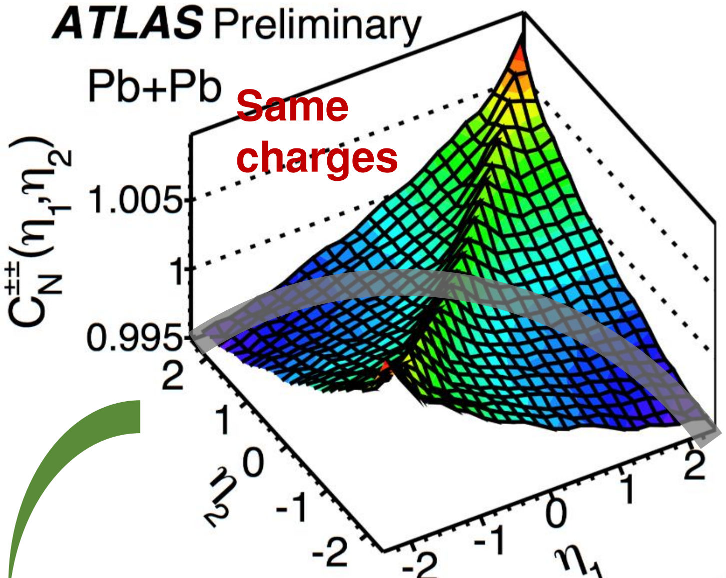

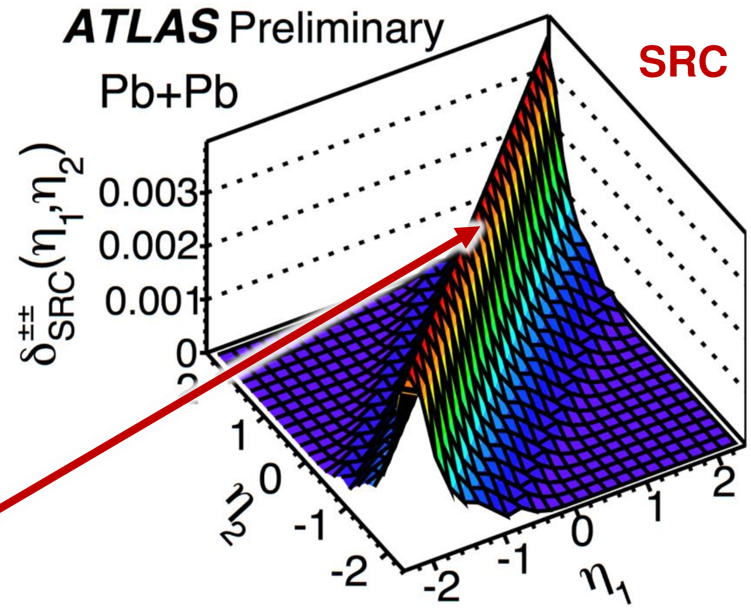

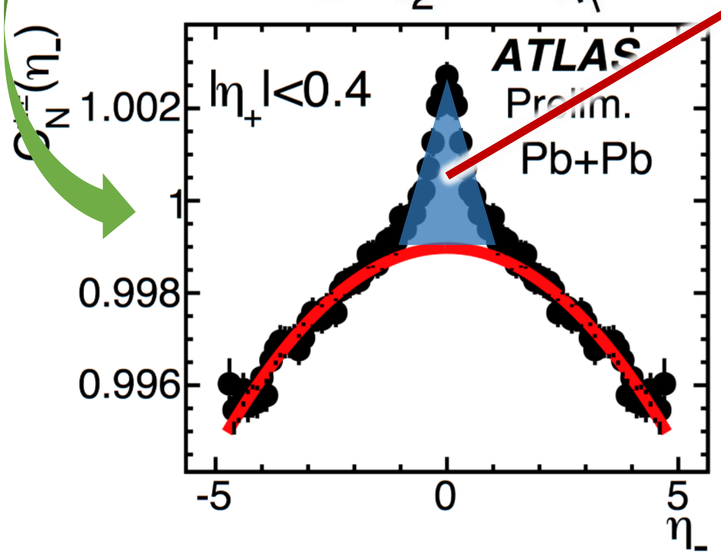

- $C(\eta_1, \eta_2)$ from same charge used to estimate LRC pedestal because of small SRC;
- LRC pedestal is fitted with quadratic function;
- The additional structure upon LRC pedestal determines the shape of SRC;

Estimation of short-range correlation

- To estimate SRC, LRC pedestal is estimated first.

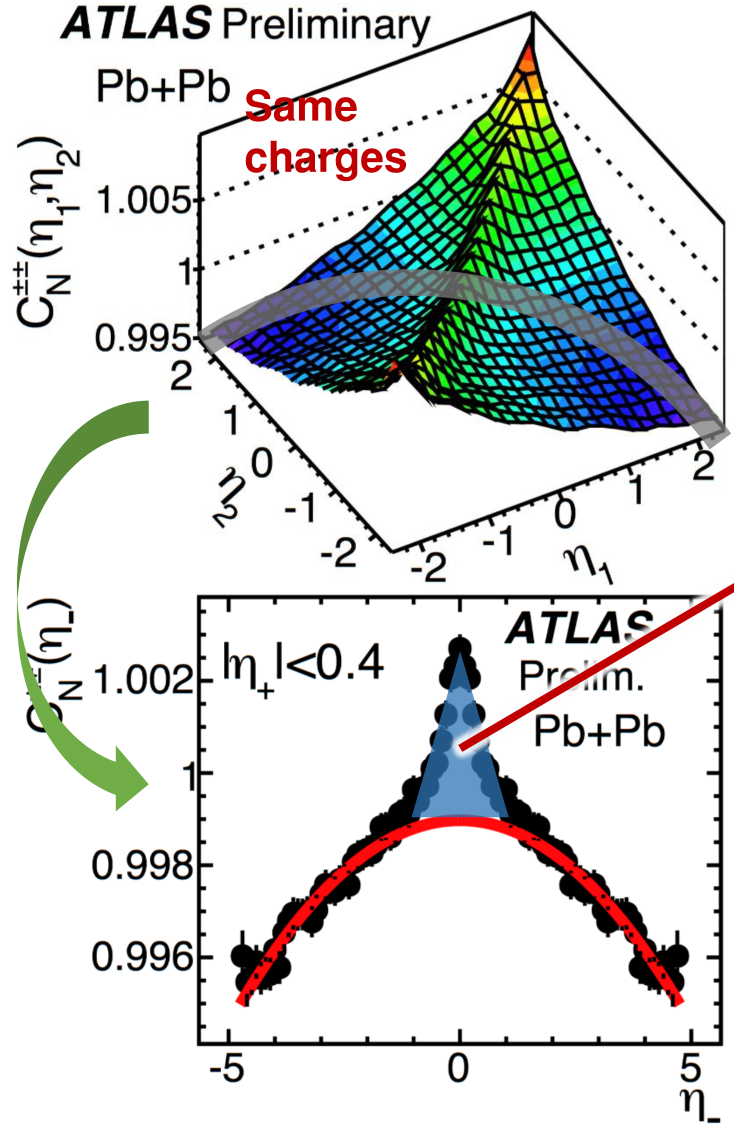

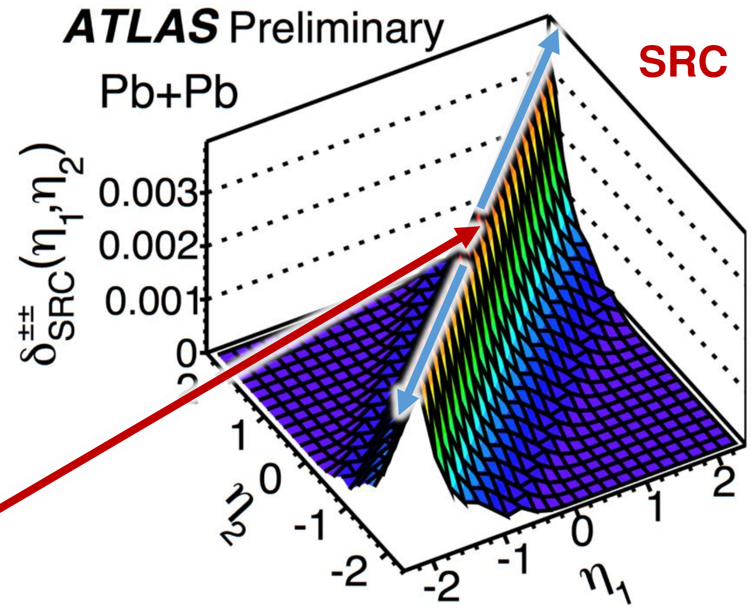

- $C(\eta_1, \eta_2)$ from same charge used to estimate LRC pedestal because of small SRC;
- LRC pedestal is fitted with quadratic function;
- The additional structure upon LRC pedestal determines the shape of SRC;
- The full $\delta_{SRC}(\eta_1, \eta_2)$ is then populated using $f(\eta_+)$ scaling.

Quantify shape fluctuation: Legendre expansion

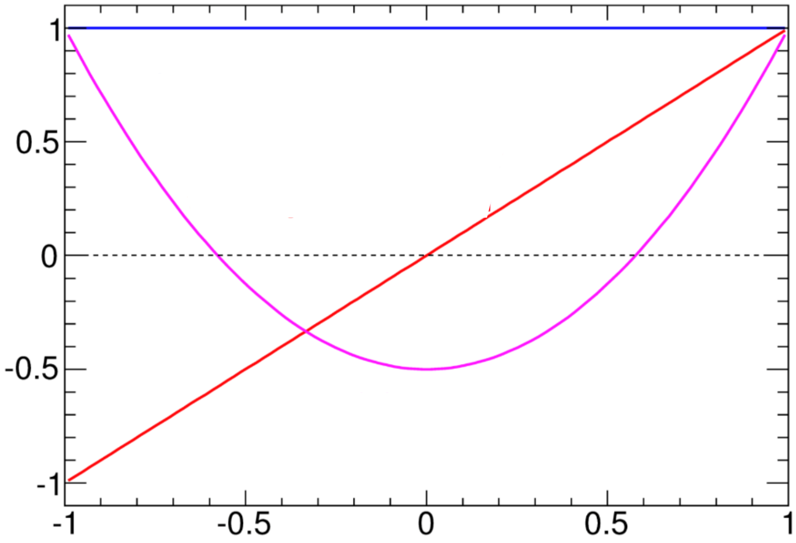

Quantify shape fluctuation: Legendre expansion

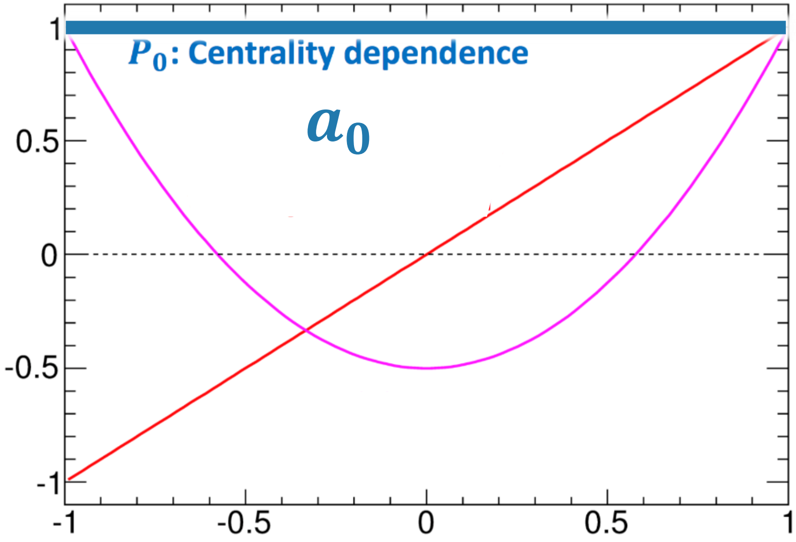

- Analysis focuses on dynamical fluctuation upon average;

$$R_s(\eta) \equiv \frac{N(\eta)}{\langle N(\eta)\rangle} \qquad C(\eta_1,\eta_2) = \frac{\langle N(\eta_1)N(\eta_2)\rangle}{\langle N(\eta_1)\rangle\langle N(\eta_2)\rangle}$$

Quantify shape fluctuation: Legendre expansion

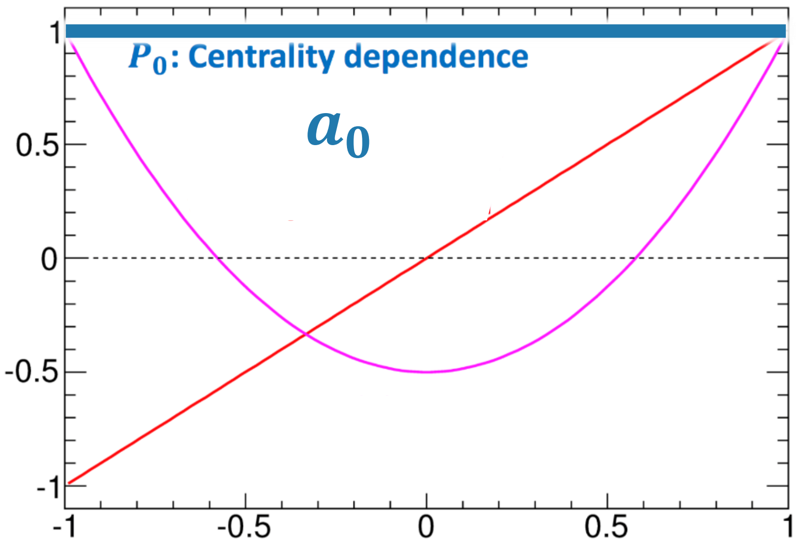

- Analysis focuses on dynamical fluctuation upon average;
- However, average multiplicity changes with centrality;

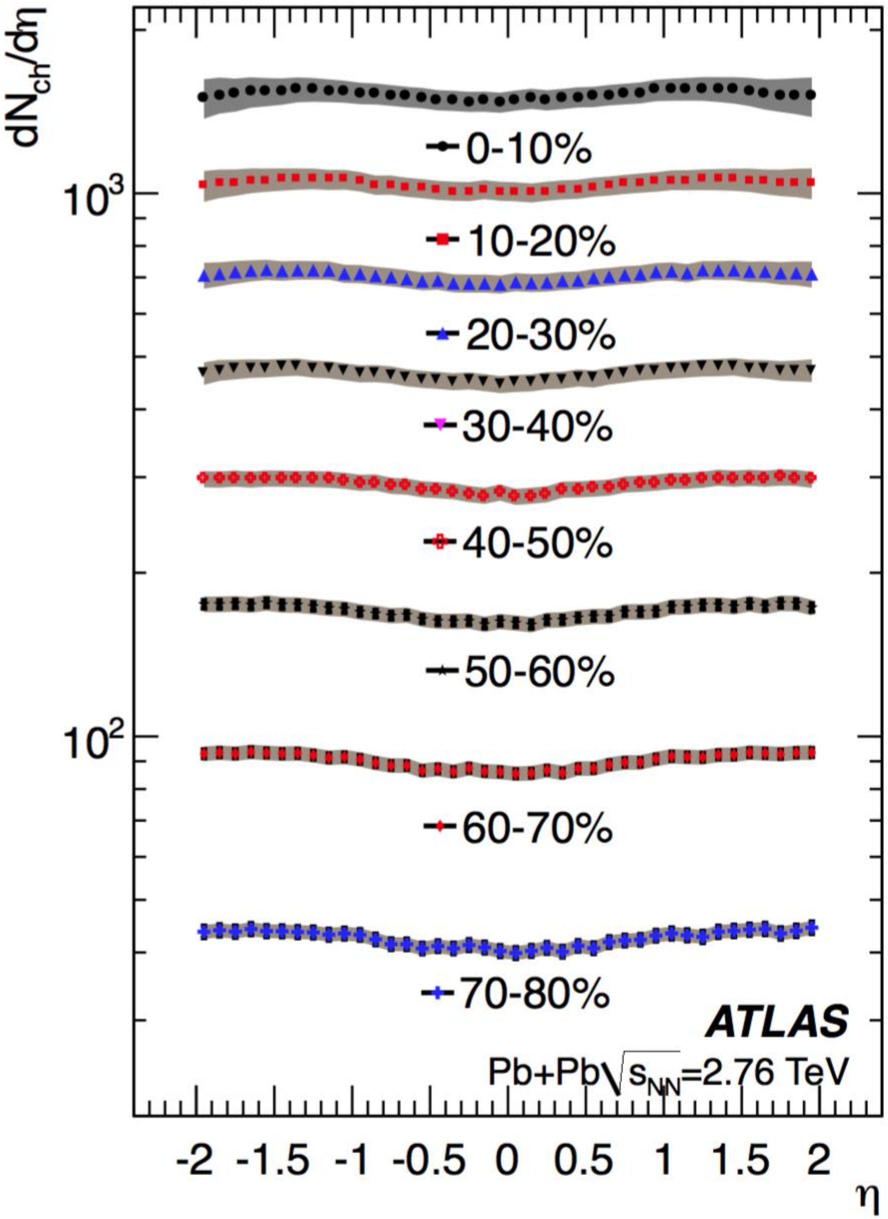

Quantify shape fluctuation: Legendre expansion

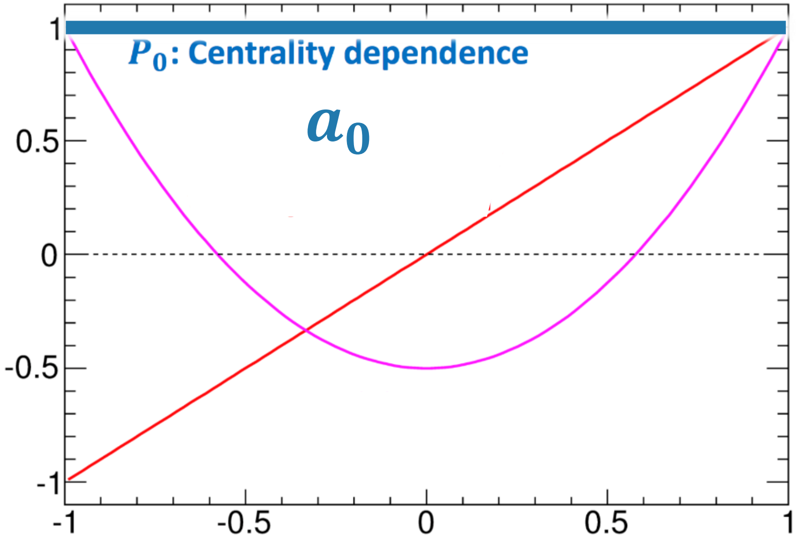

- Analysis focuses on dynamical fluctuation upon average;
- However, average multiplicity changes with centrality;
- The residual centrality dependence is removed by normalizing $C(\eta_1, \eta_2)$

$$C_N(\eta_1, \eta_2) = \frac{C(\eta_1, \eta_2)}{C_p(\eta_1) C_p(\eta_2)}$$

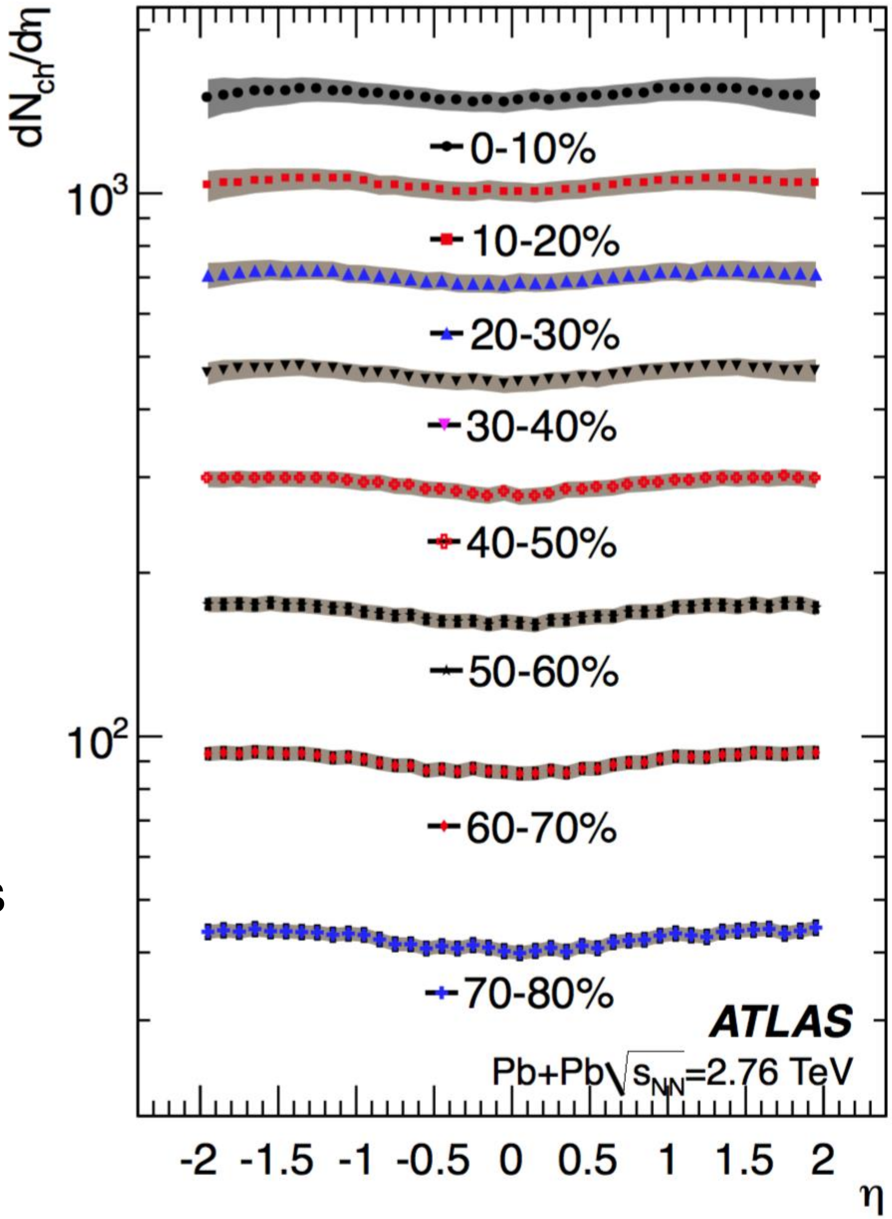

Quantify shape fluctuation: Legendre expansion

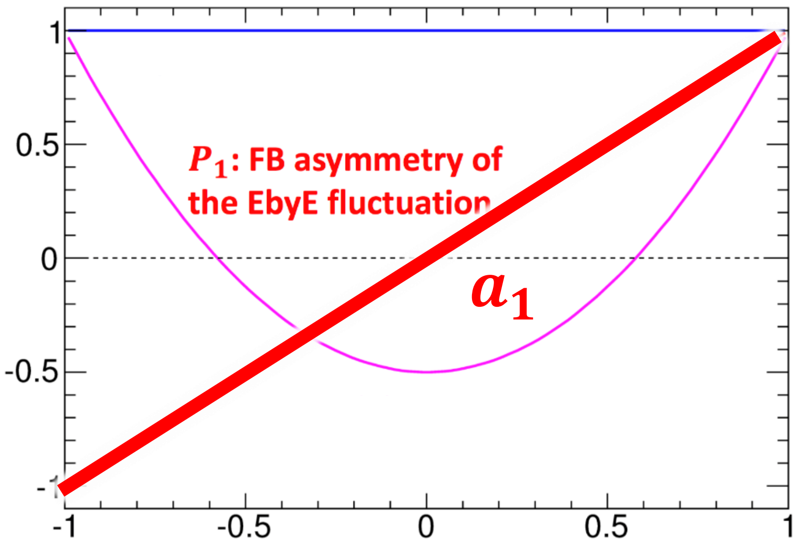

- The linear shape quantifies the FB multiplicity asymmetry;

Quantify shape fluctuation: Legendre expansion

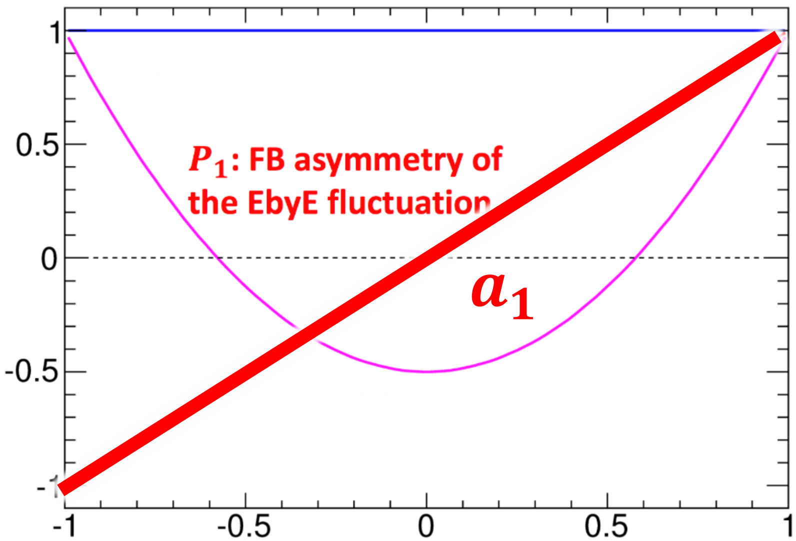

- The linear shape quantifies the FB multiplicity asymmetry;

- HIJING shows strong correlation between final multiplicity asymmetry and initial participant asymmetry;

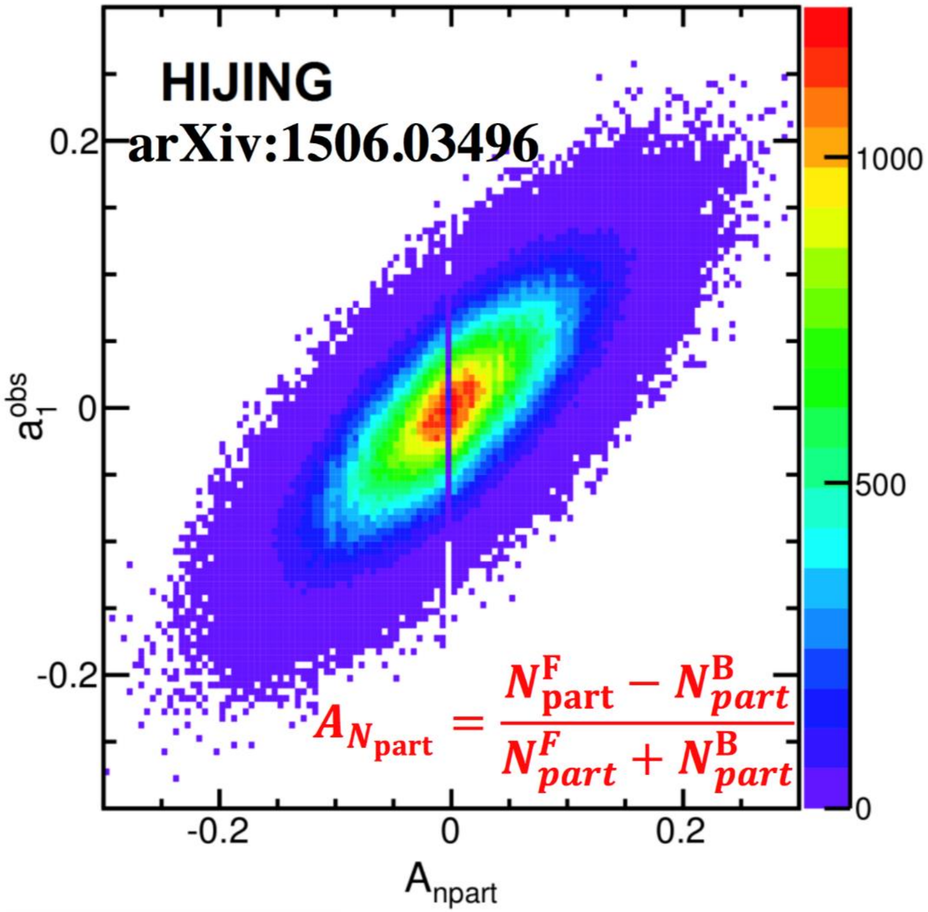

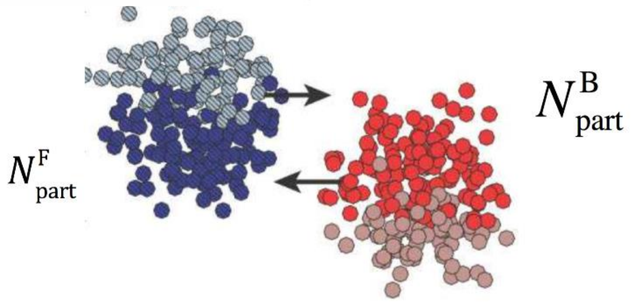

Quantify shape fluctuation: Legendre expansion

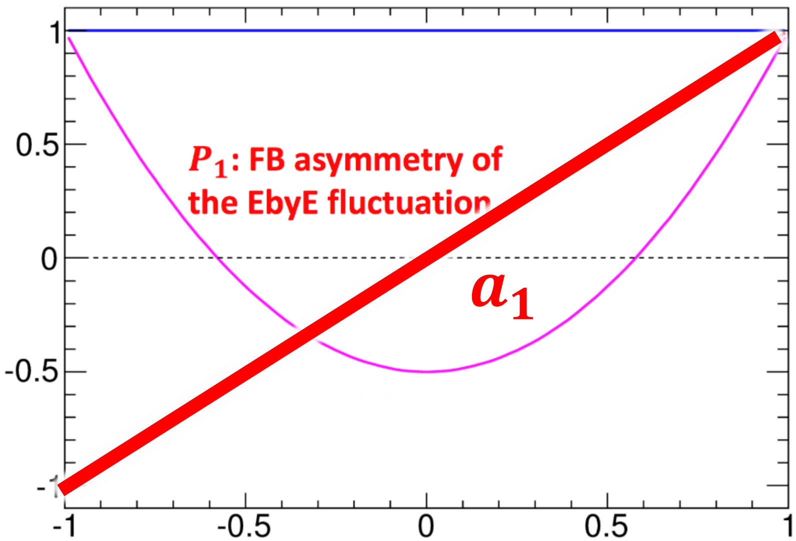

- The linear shape quantifies the FB multiplicity asymmetry;
- HIJING shows strong correlation between final multiplicity asymmetry and initial participant asymmetry;
- As will be shown later, this component dominates the shape fluctuation.

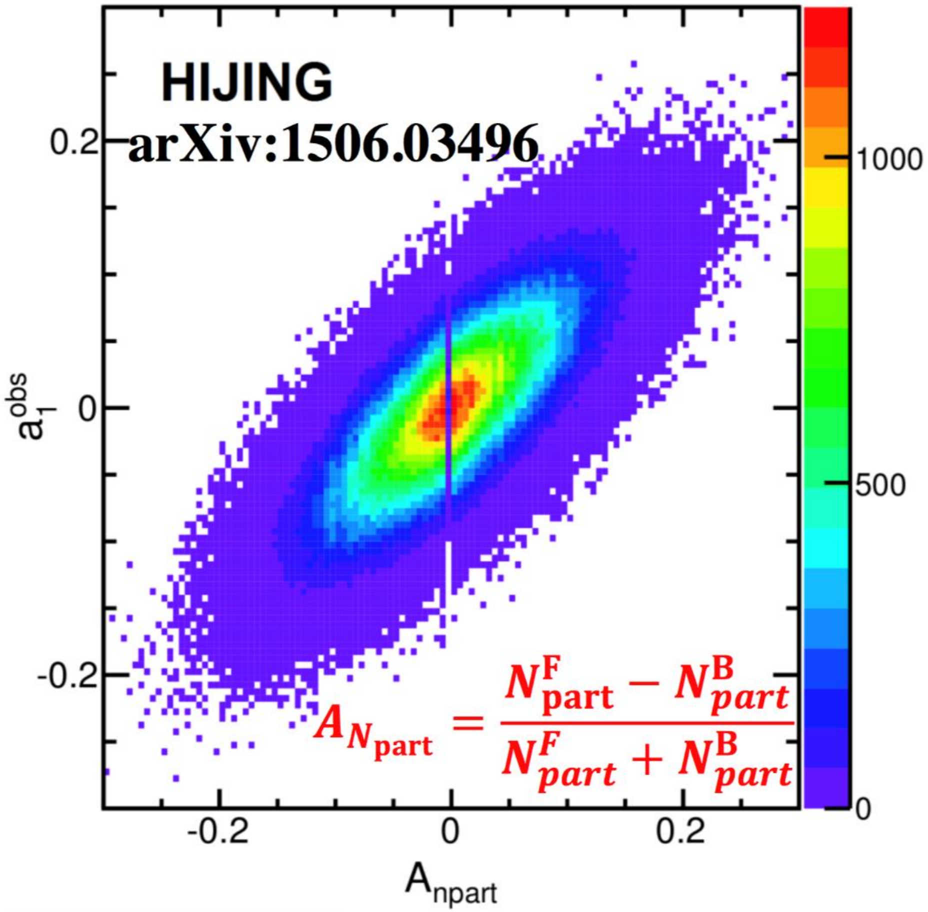

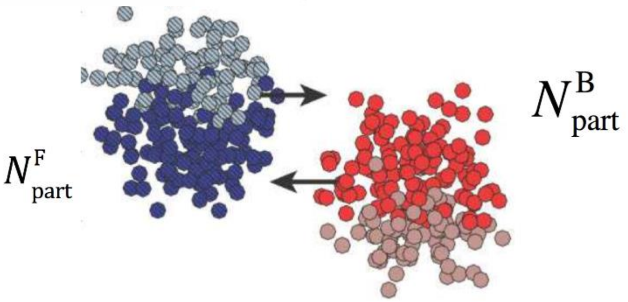

Quantify shape fluctuation: Legendre expansion

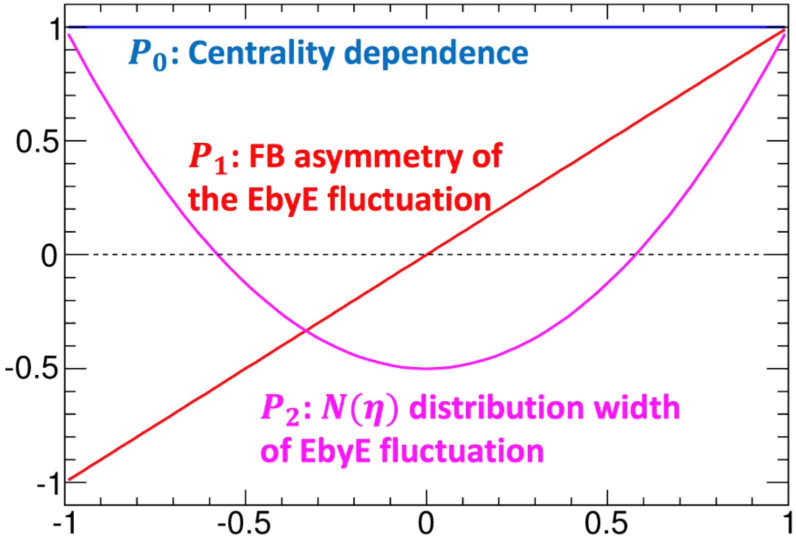

- Expansion of correlation function $C_N(\eta_1, \eta_2)$

$$1 + \sum_{n.m=1}^{\infty} \underline{\langle a_n a_m \rangle} \frac{T_n(\eta_1)T_m(\eta_2) + T_n(\eta_2)T_m(\eta_1)}{2}$$

Quantify shape fluctuation: Legendre expansion

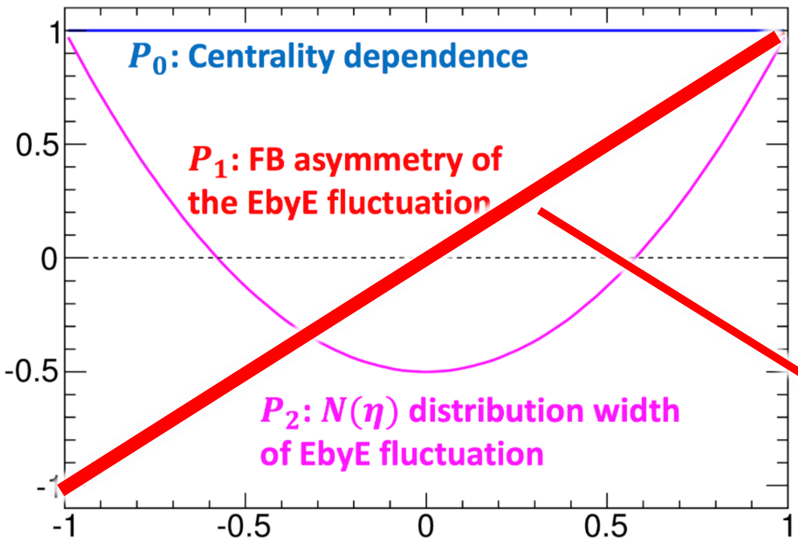

- Expansion of correlation function $C_N(\eta_1, \eta_2)$

$$1 + \sum_{n.m=1}^{\infty} \underline{\langle a_n a_m \rangle} \frac{T_n(\eta_1)T_m(\eta_2) + T_n(\eta_2)T_m(\eta_1)}{2}$$

- If linear shape dominates:

$$C_N(\eta_1, \eta_2) = 1 + \langle a_1^2 \rangle \eta_1 \eta_2$$

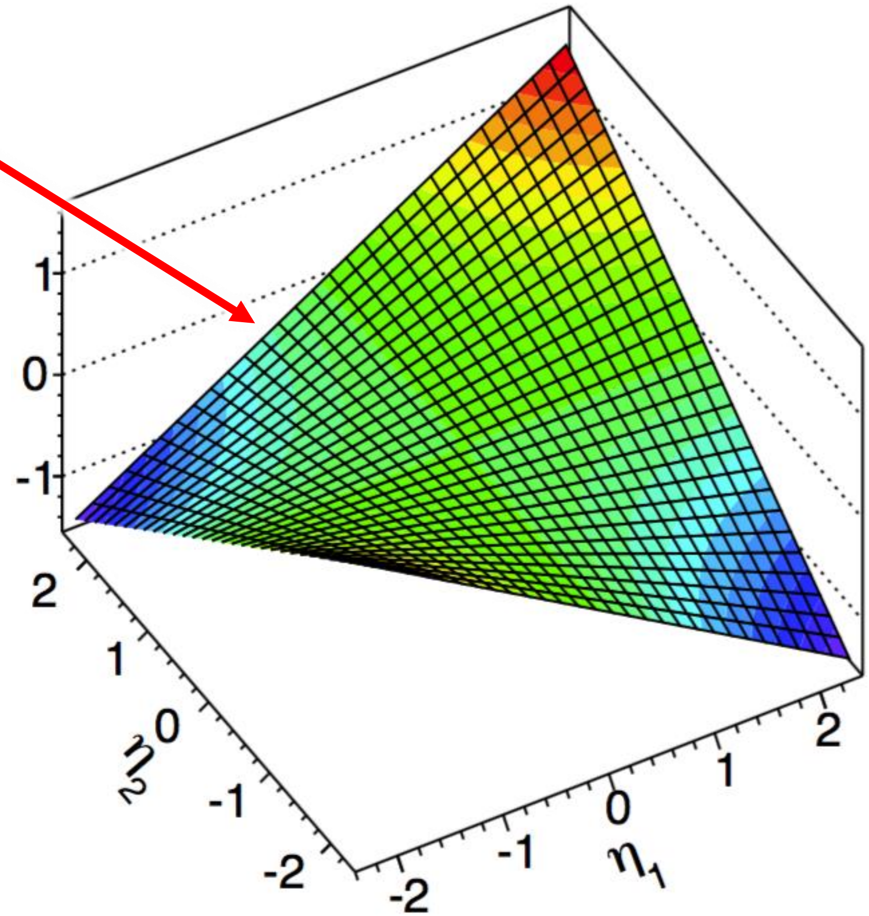

Quantify shape fluctuation: Legendre expansion

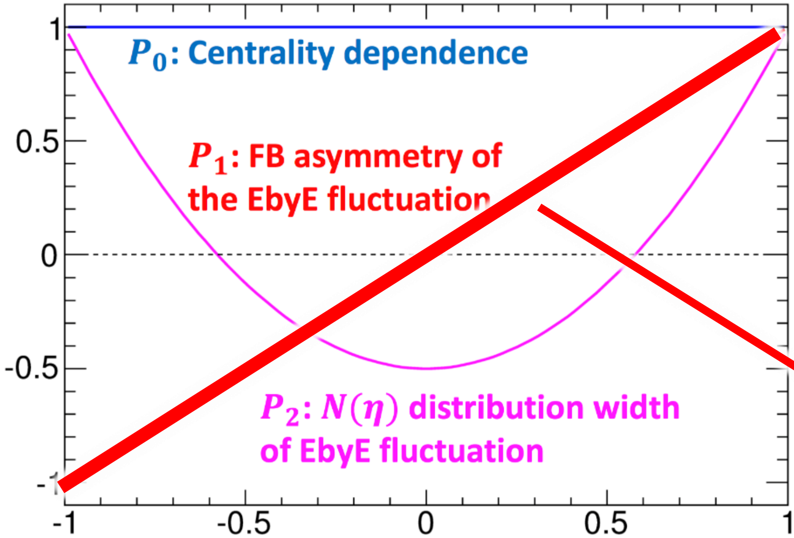

- Expansion of correlation function $C_N(\eta_1, \eta_2)$

$$1 + \sum_{n.m=1}^{\infty} \underline{\langle a_n a_m \rangle} \frac{T_n(\eta_1)T_m(\eta_2) + T_n(\eta_2)T_m(\eta_1)}{2}$$

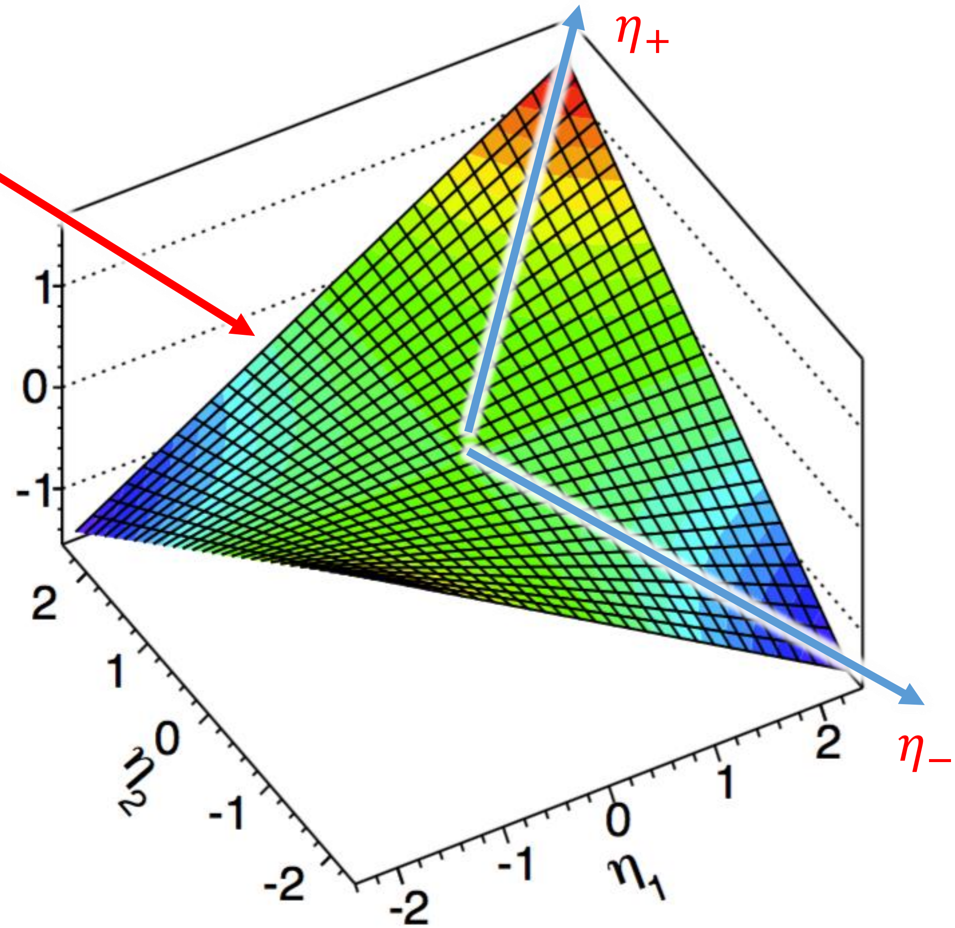

- If linear shape dominates:

$$C_N(\eta_1, \eta_2) = 1 + \langle a_1^2 \rangle \eta_1 \eta_2$$

- Expressed as η_+ and η_-:

$$C_N(\eta_1, \eta_2) = 1 + \frac{\langle a_1^2 \rangle}{4} (\eta_+^2 - \eta_-^2)$$

Results: correlation functions

Raw
$C_N(\eta_1,\eta_2)$

=

Short-range
$\delta_{SRC}(\eta_1,\eta_2)$

+

Long-range
$C_N^{sub}(\eta_1,\eta_2)$

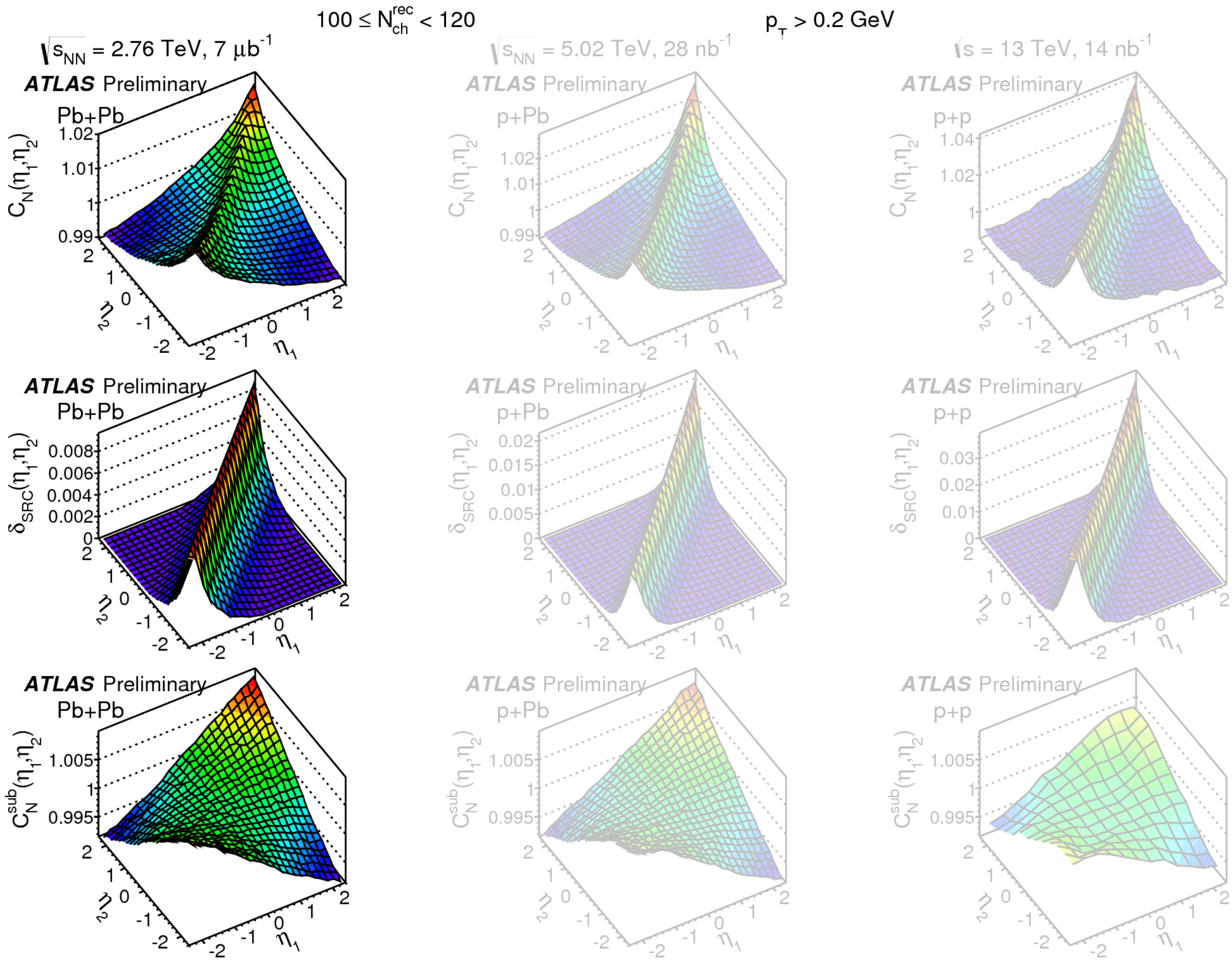

Pb+Pb

p+Pb

pp

Results: correlation functions

Raw
$C_N(\eta_1, \eta_2)$

=

Short-range
$\delta_{SRC}(\eta_1, \eta_2)$

+

Long-range
$C_N^{sub}(\eta_1, \eta_2)$

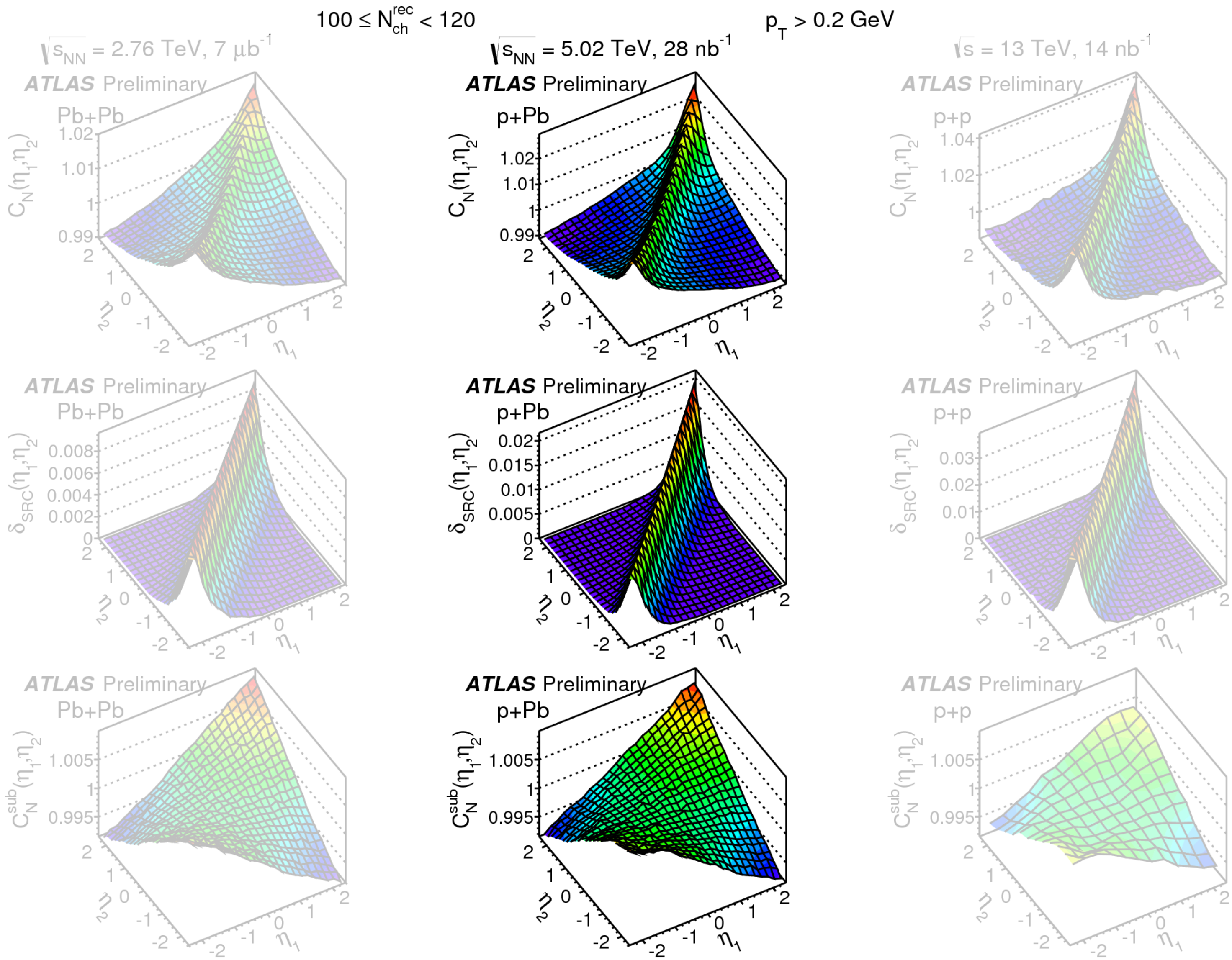

Pb+Pb

p+Pb

pp

Results: correlation functions

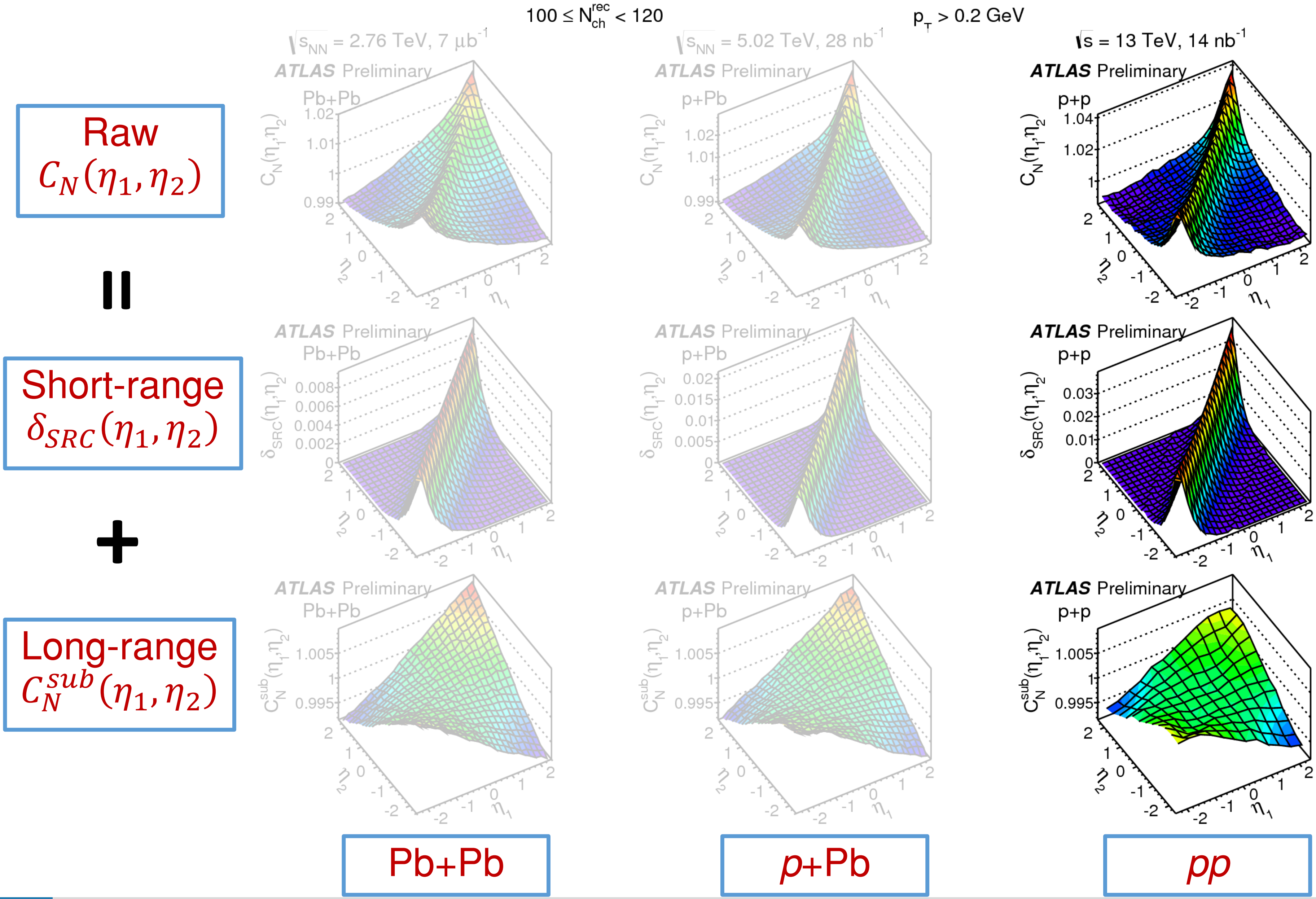

Results: correlation functions

Raw
$C_N(\eta_1, \eta_2)$

=

Short-range
$\delta_{SRC}(\eta_1, \eta_2)$

+

Long-range
$C_N^{sub}(\eta_1, \eta_2)$

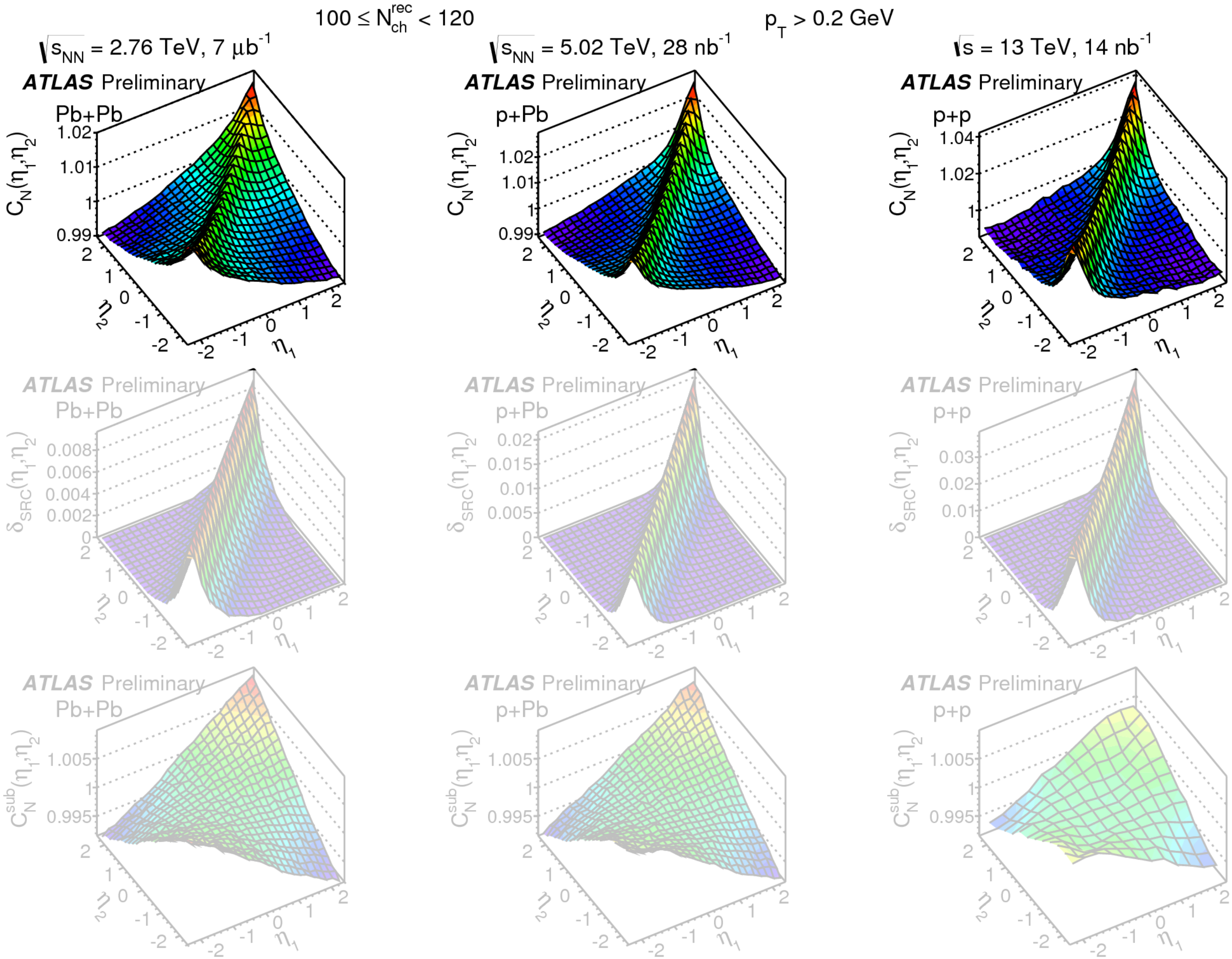

Pb+Pb

p+Pb

pp

Results: correlation functions

Raw
$C_N(\eta_1, \eta_2)$

=

Short-range
$\delta_{SRC}(\eta_1, \eta_2)$

+

Long-range
$C_N^{sub}(\eta_1, \eta_2)$

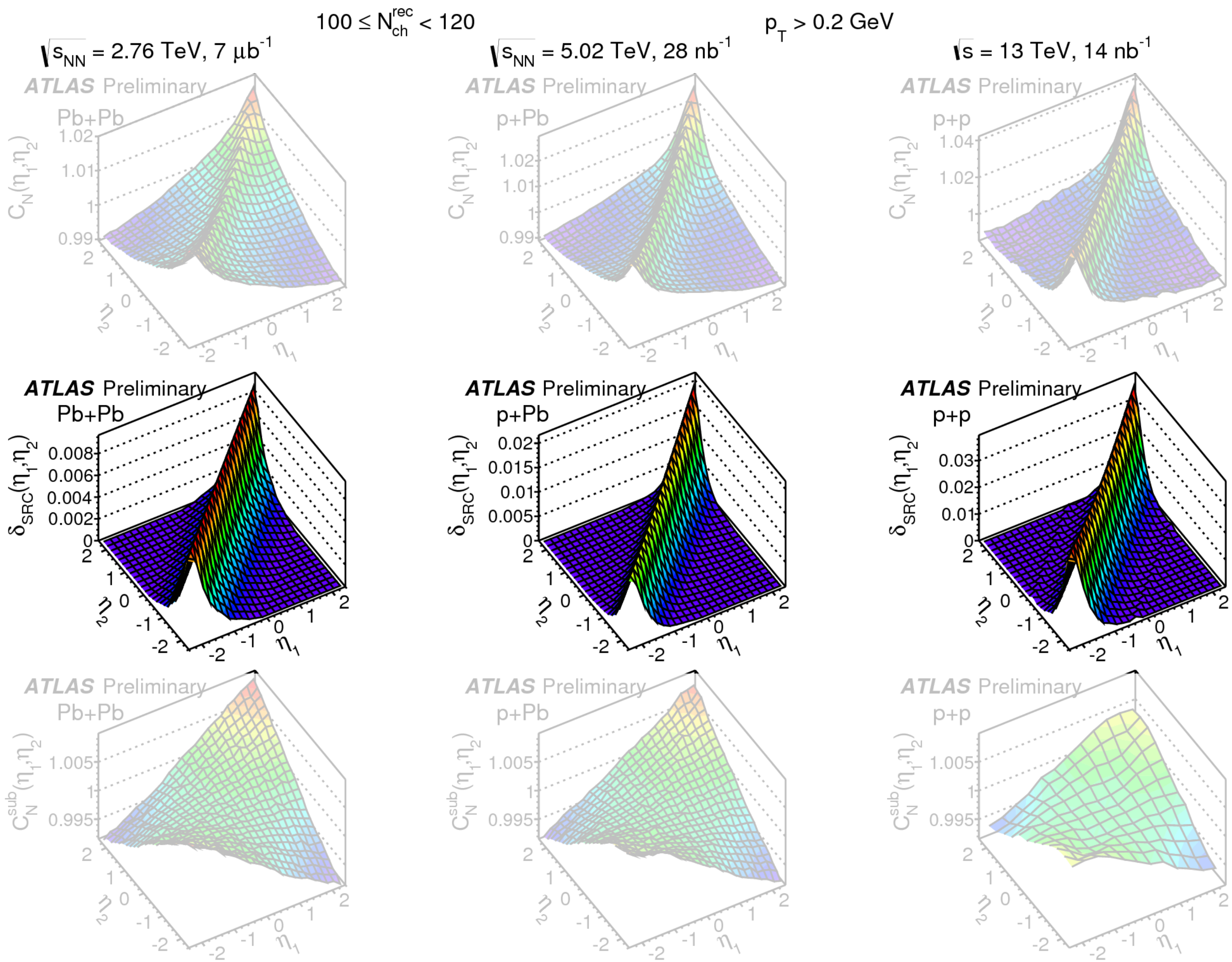

Pb+Pb

p+Pb

pp

Results: correlation functions

Raw
$C_N(\eta_1, \eta_2)$

=

Short-range
$\delta_{SRC}(\eta_1, \eta_2)$

+

Long-range
$C_N^{sub}(\eta_1, \eta_2)$

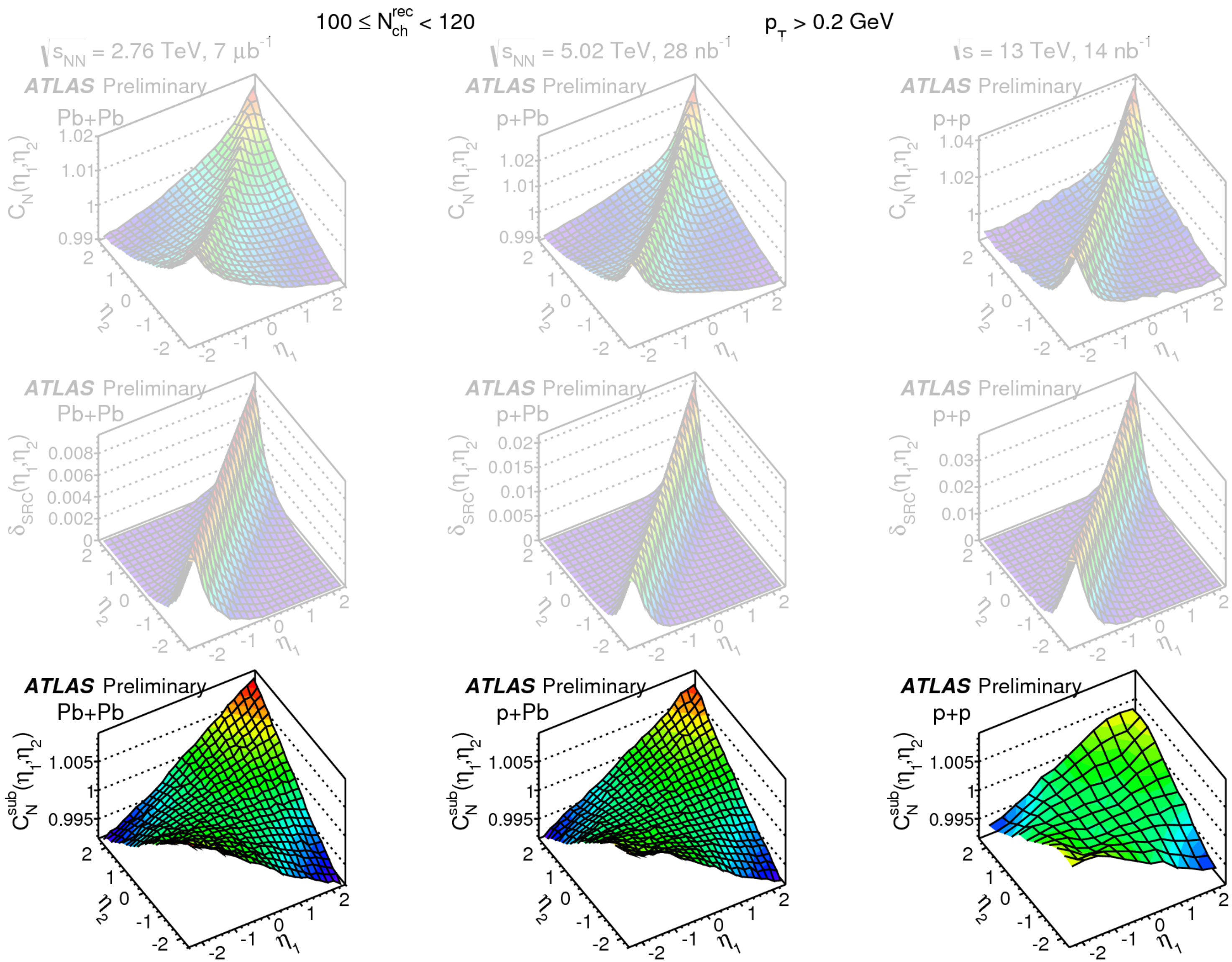

- After SRC subtraction, similar LRC in all three systems!

Results: Legendre spectra before SRC removal

$$1+\sum_{n.m=1}^{\infty}\langle a_n a_m\rangle \frac{T_n(\eta_1)T_m(\eta_2)+T_n(\eta_2)T_m(\eta_1)}{2}$$

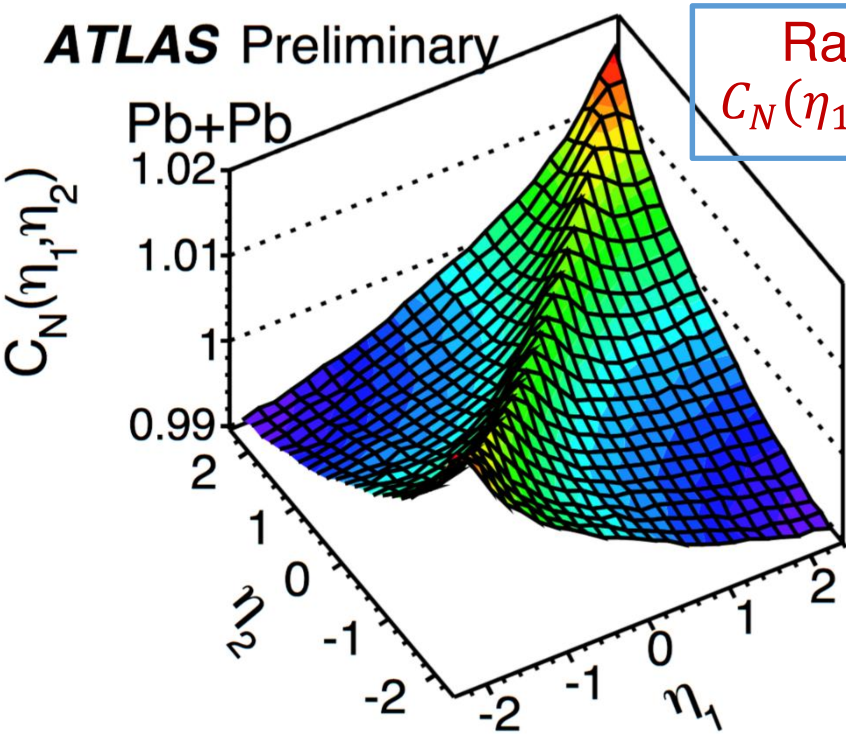

Raw
$C_N(\eta_1,\eta_2)$

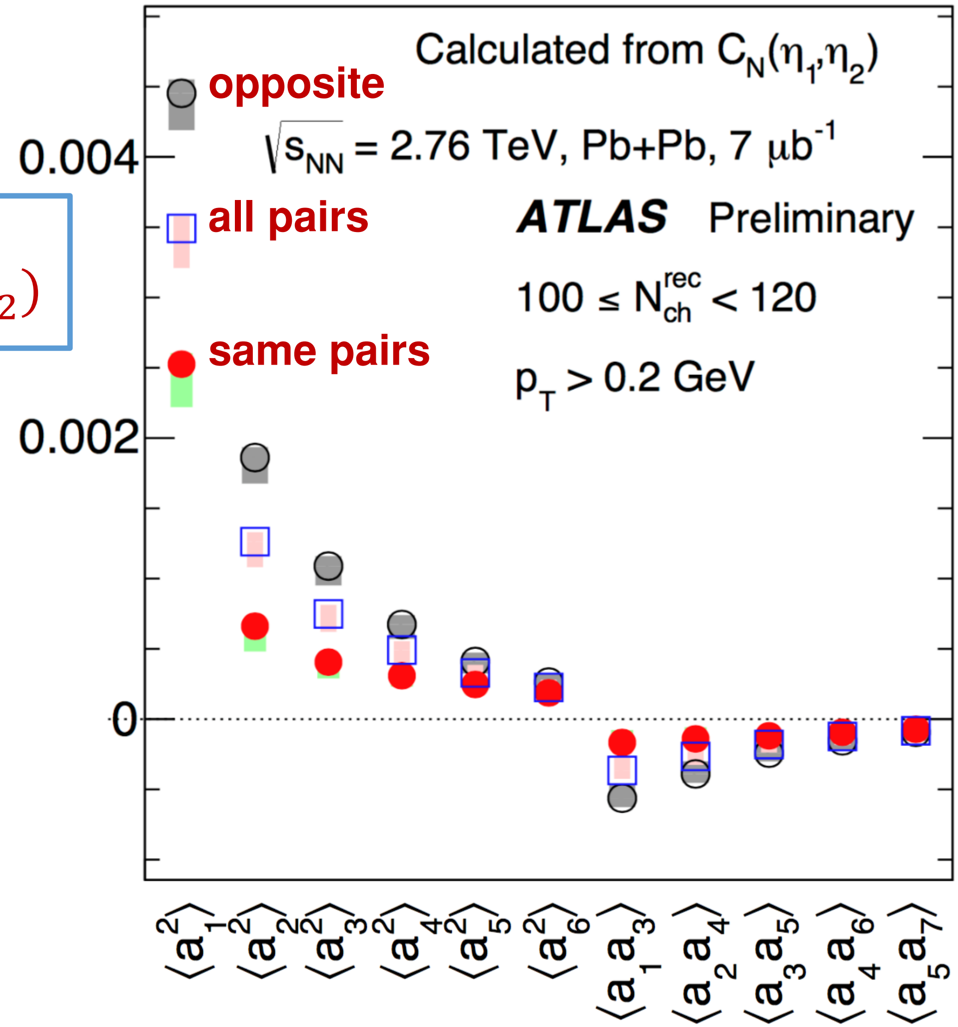

Results: Legendre spectra before SRC removal

$$1+\sum_{n.m=1}^{\infty}\langle a_n a_m\rangle \frac{T_n(\eta_1)T_m(\eta_2)+T_n(\eta_2)T_m(\eta_1)}{2}$$

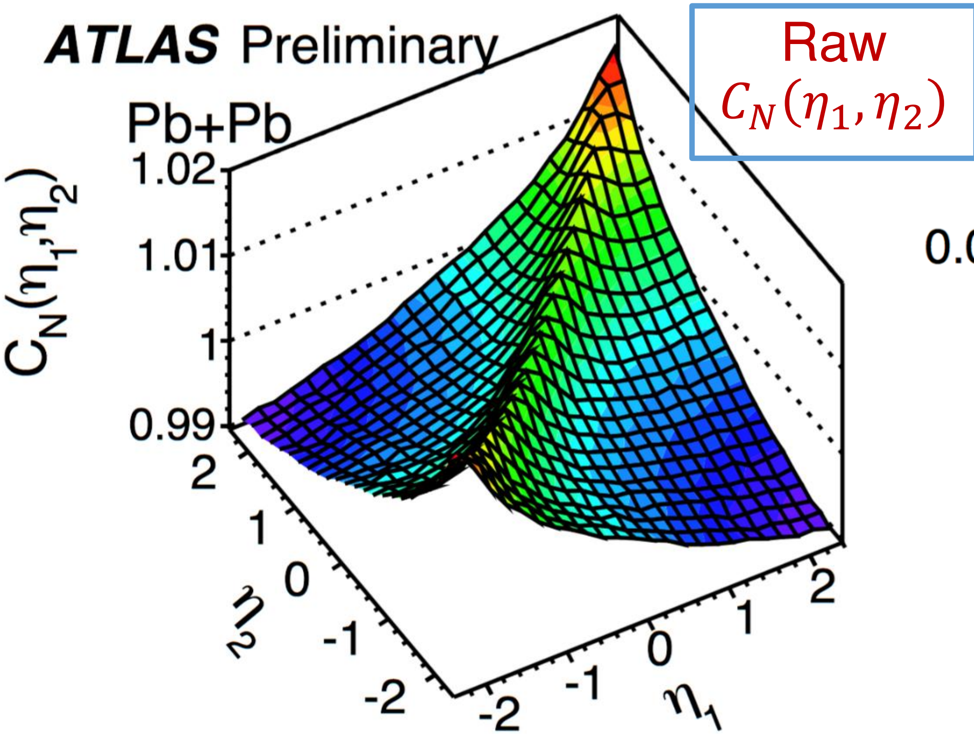

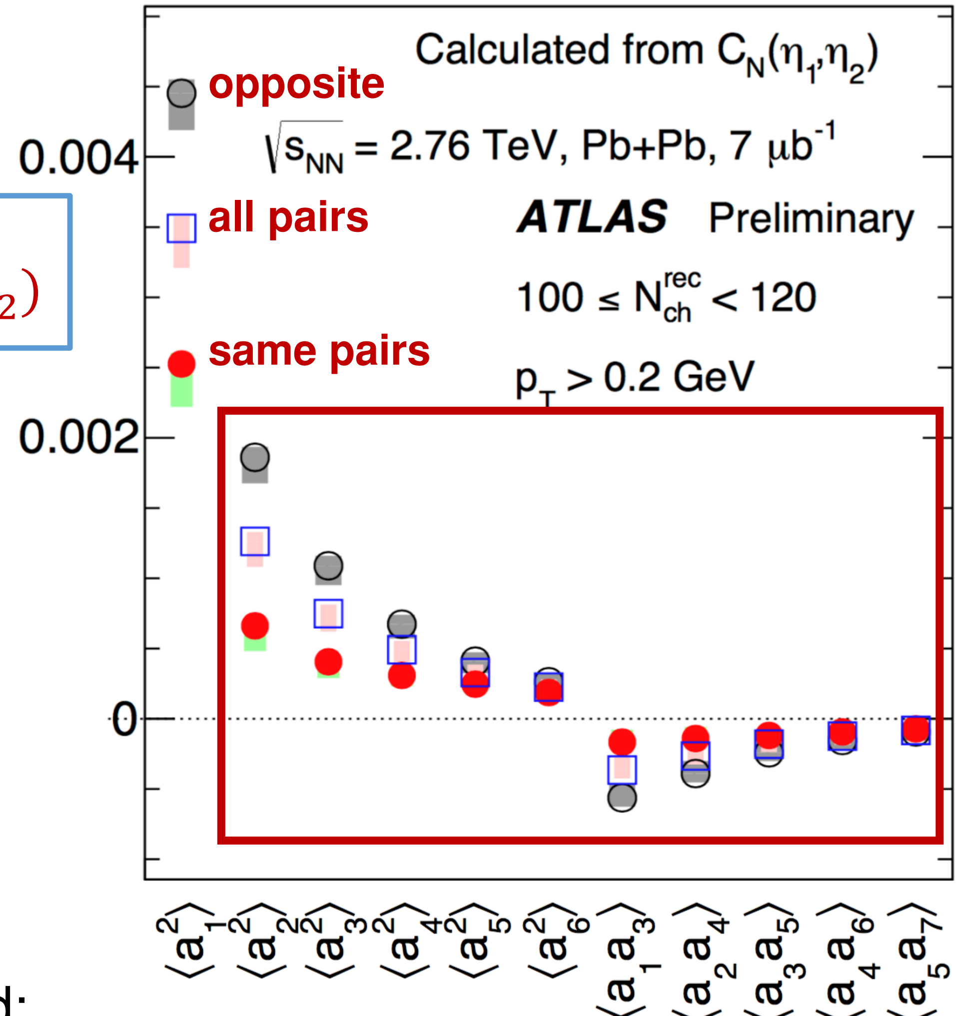

- Higher order coefficients observed;

Results: Legendre spectra before SRC removal

$$1 + \sum_{n.m=1}^{\infty} \langle a_n a_m \rangle \frac{T_n(\eta_1)T_m(\eta_2) + T_n(\eta_2)T_m(\eta_1)}{2}$$

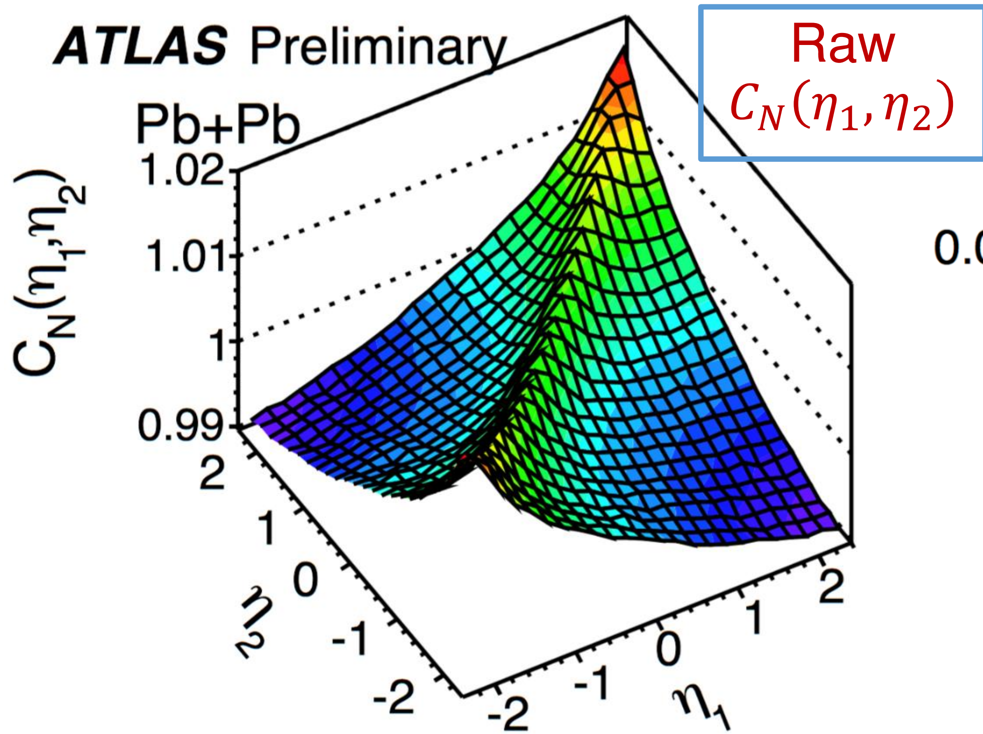

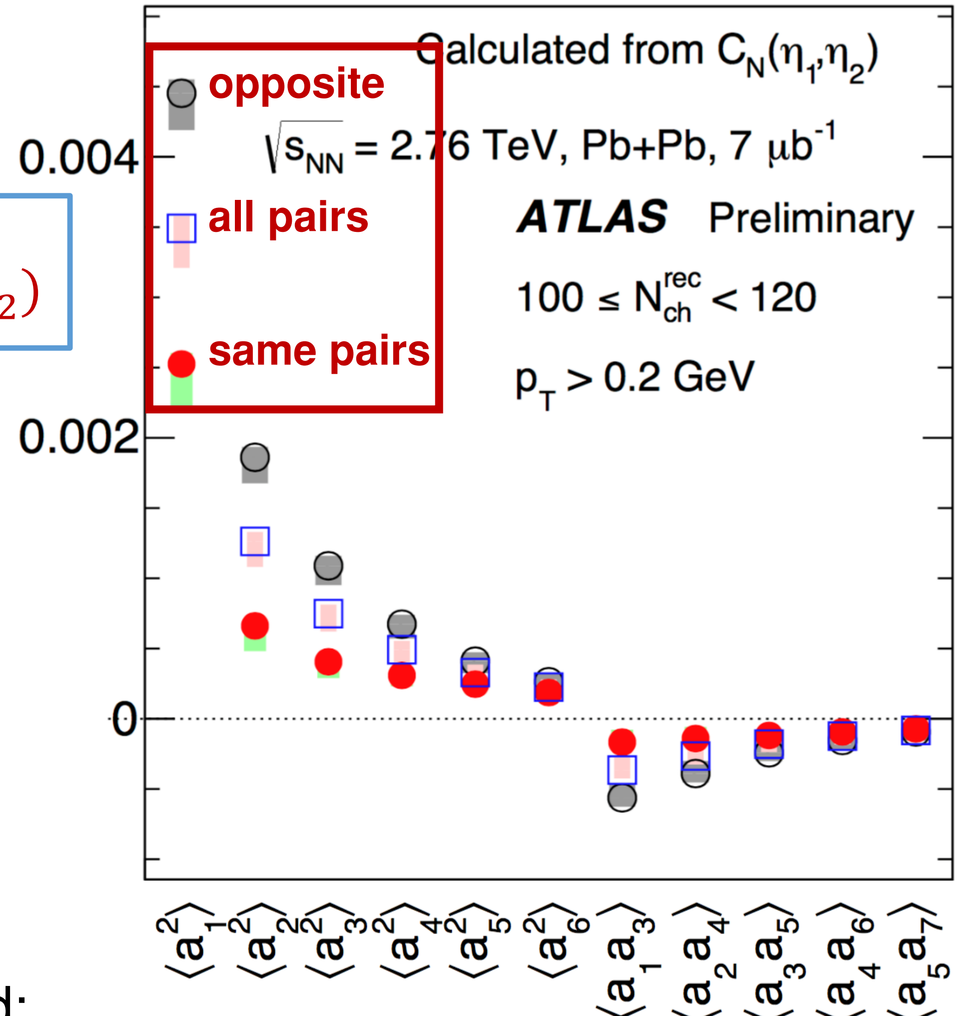

- Higher order coefficients observed;
- Coefficients depend on charge combinations;

Results: Legendre spectra before SRC removal

$$1 + \sum_{n.m=1}^{\infty} \langle a_n a_m \rangle \frac{T_n(\eta_1)T_m(\eta_2) + T_n(\eta_2)T_m(\eta_1)}{2}$$

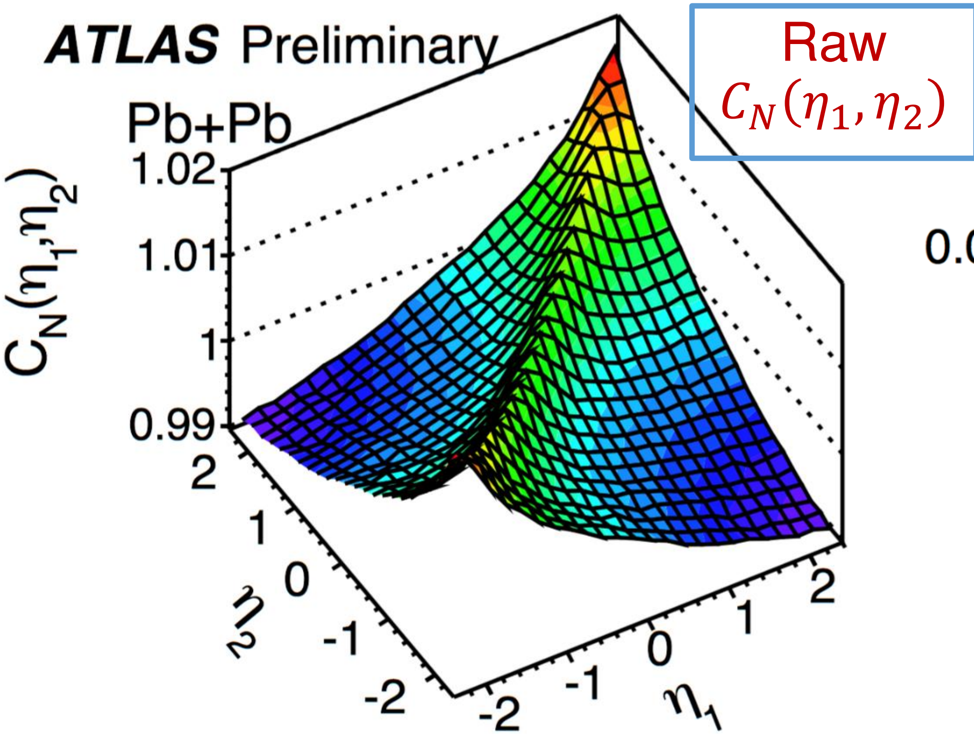

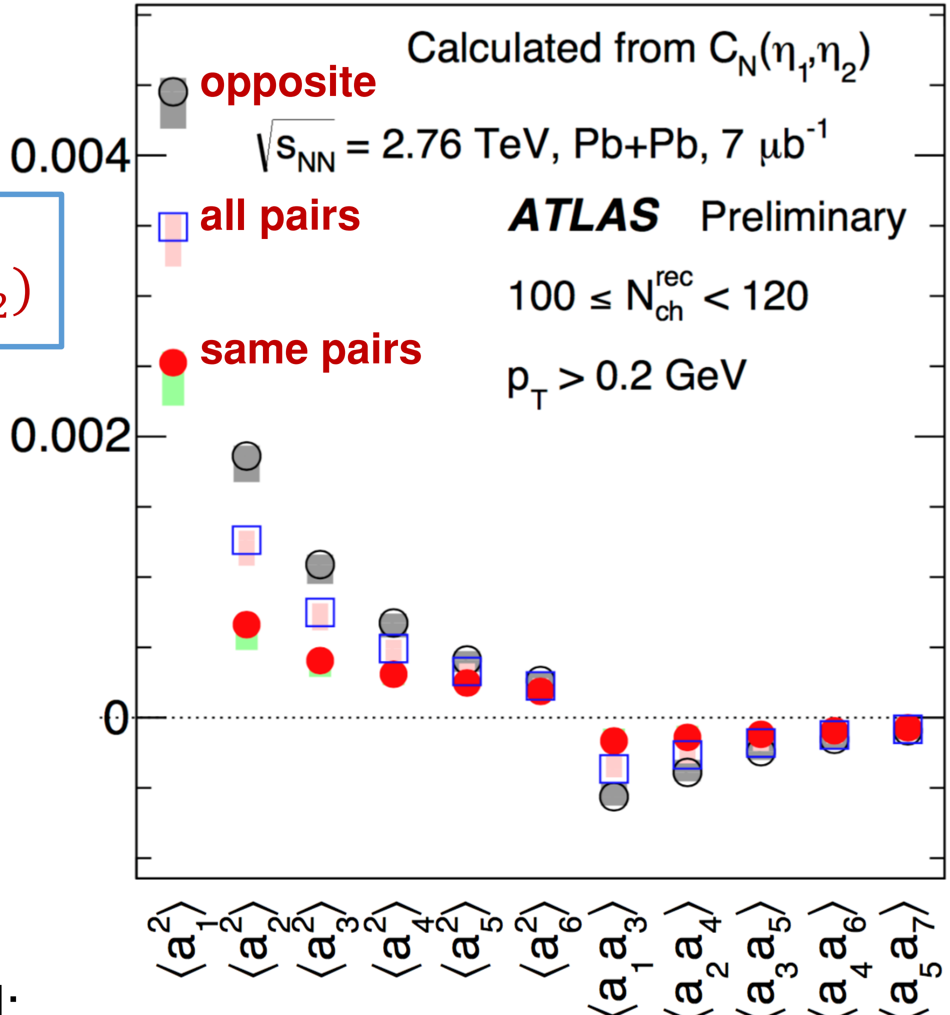

- Higher order coefficients observed;
- Coefficients depend on charge combinations;
- Complicated and very hard to interpret: due to SRC!

Results: Legendre spectra after SRC removal

$$1+\sum_{n.m=1}^{\infty}\langle a_n a_m\rangle \frac{T_n(\eta_1)T_m(\eta_2)+T_n(\eta_2)T_m(\eta_1)}{2}$$

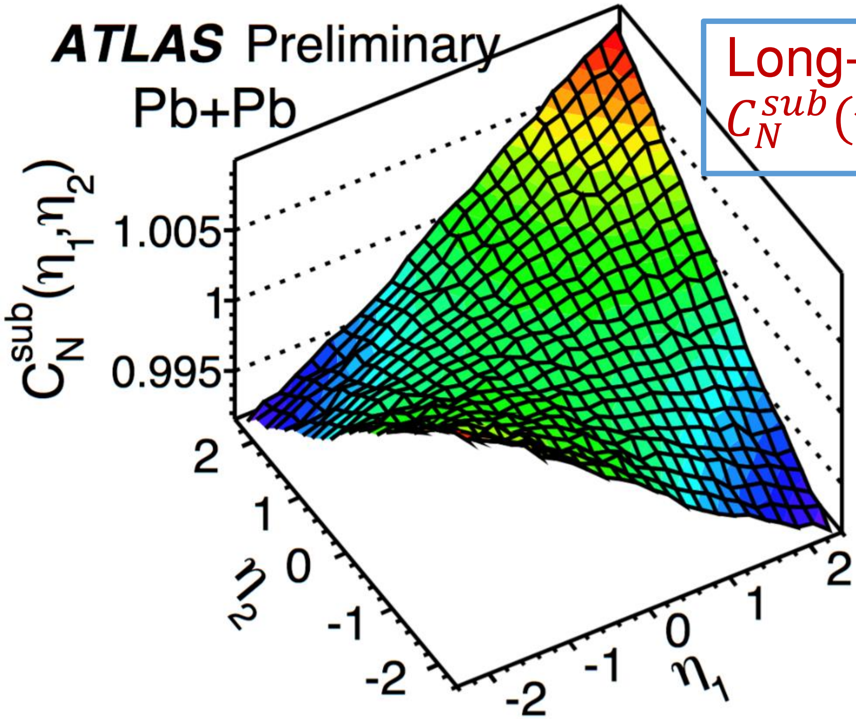

Long-range $C_N^{sub}(\eta_1,\eta_2)$

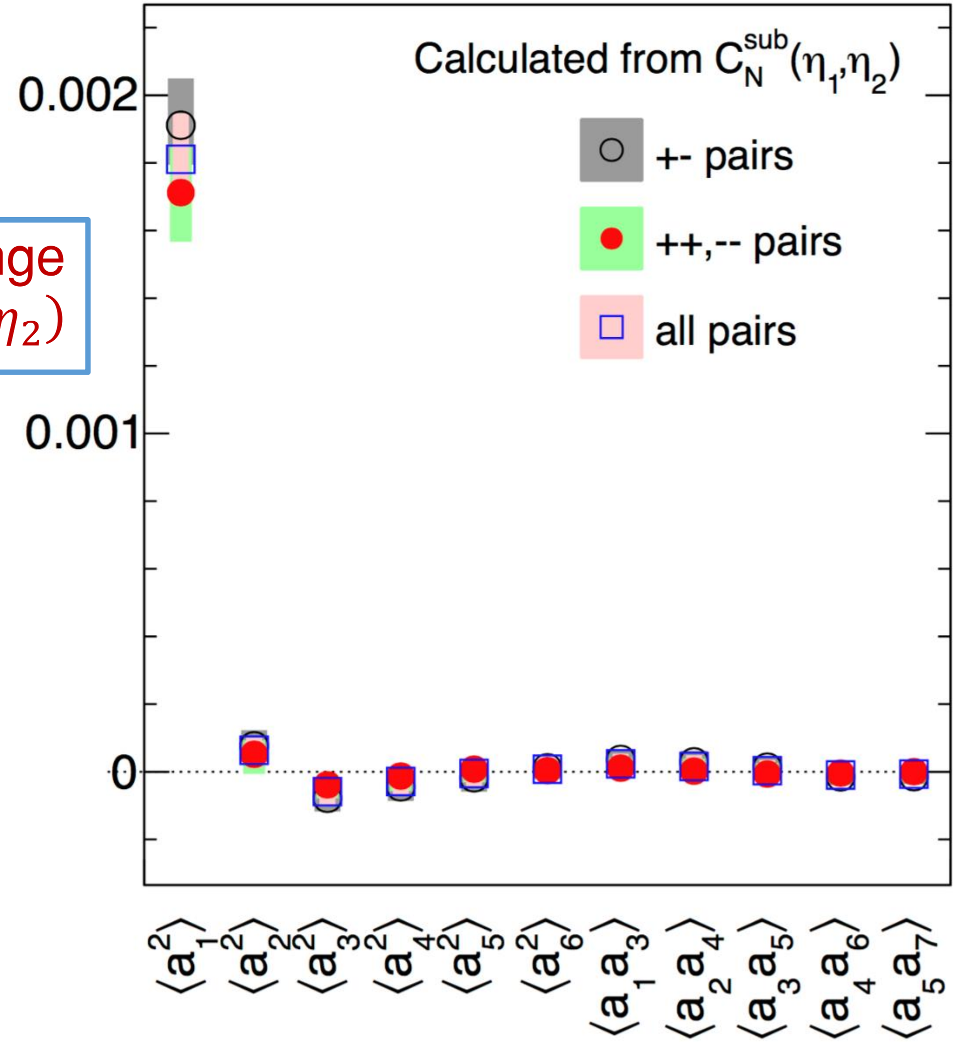

Results: Legendre spectra after SRC removal

$$1+\sum_{n.m=1}^{\infty}\langle a_n a_m\rangle \frac{T_n(\eta_1)T_m(\eta_2)+T_n(\eta_2)T_m(\eta_1)}{2}$$

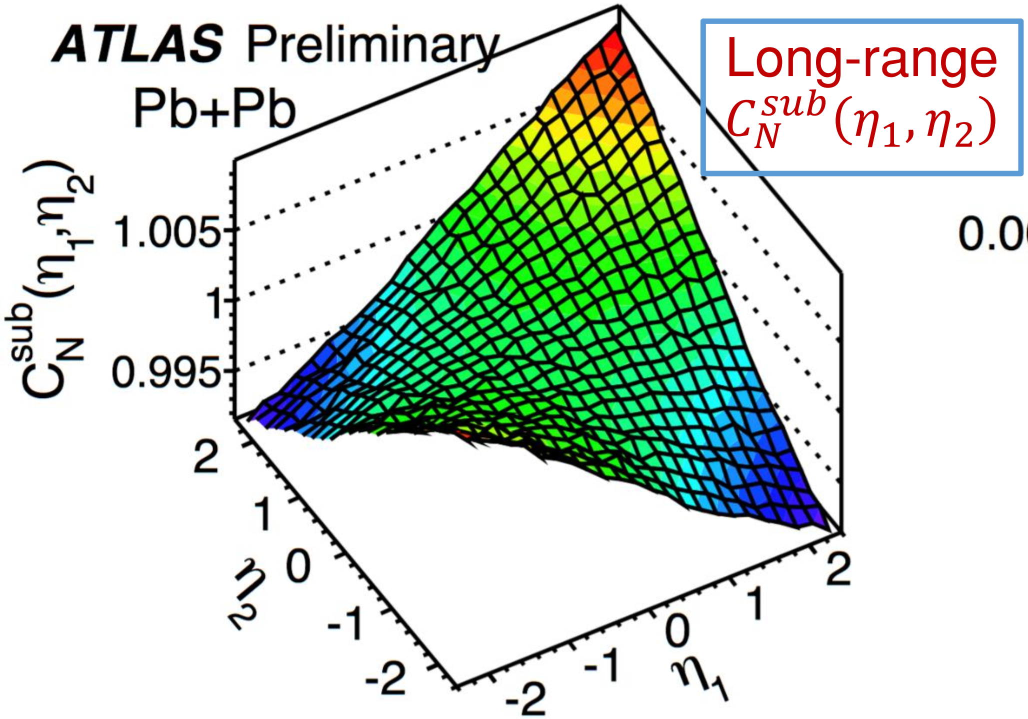

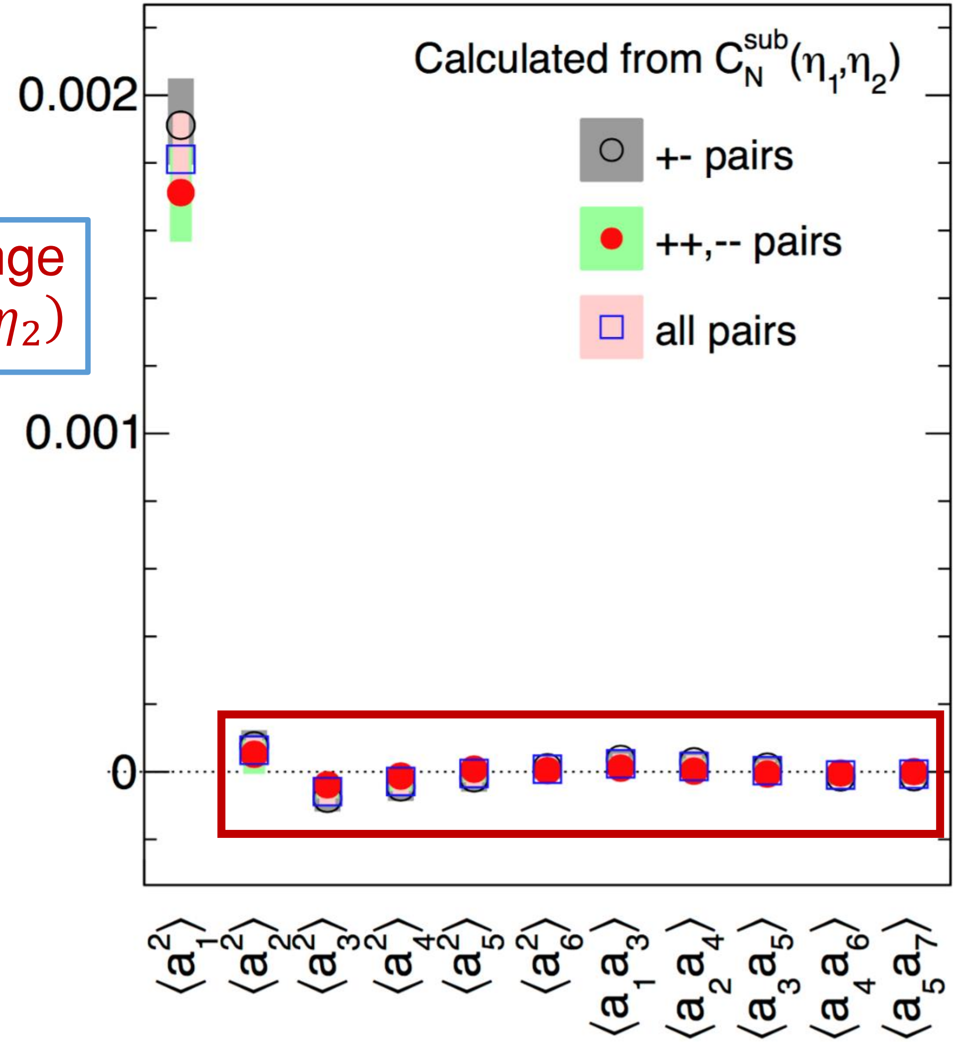

- Higher order coefficients consistent with 0: dominated by a_1;

Results: Legendre spectra after SRC removal

$$1 + \sum_{n.m=1}^{\infty} \langle a_n a_m \rangle \frac{T_n(\eta_1)T_m(\eta_2) + T_n(\eta_2)T_m(\eta_1)}{2}$$

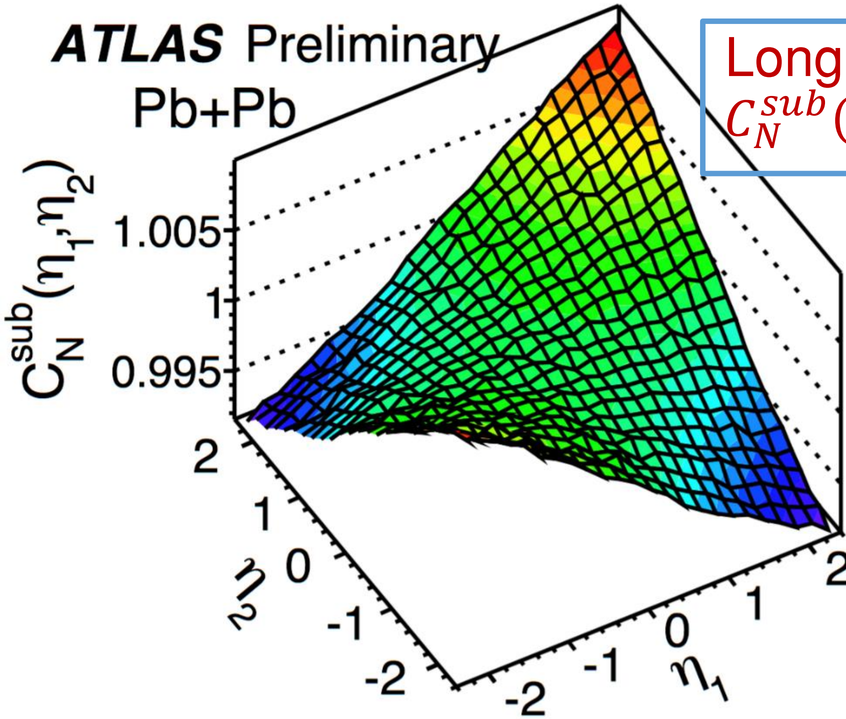

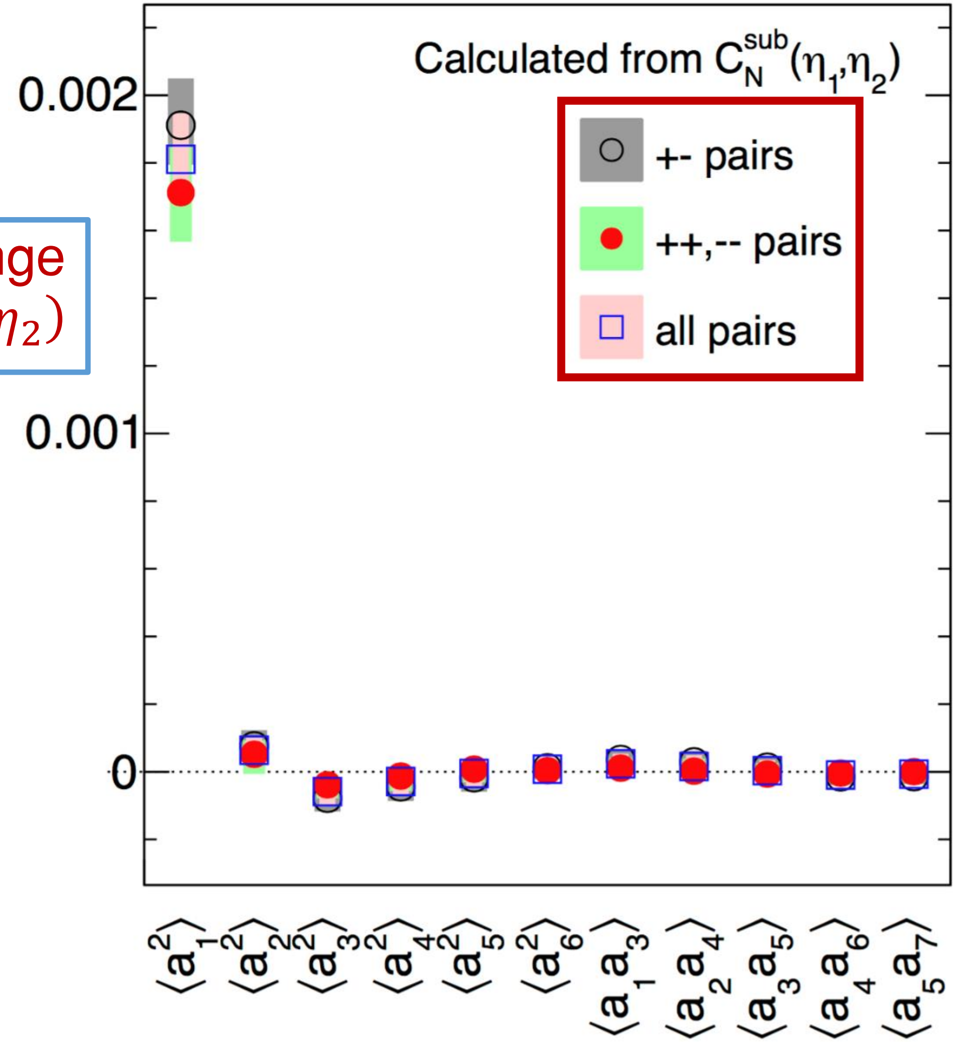

- Higher order coefficients consistent with 0: dominated by a_1;
- Coefficients independent of charge combinations;

Results: Legendre spectra after SRC removal

$$1+\sum_{n.m=1}^{\infty}\langle a_n a_m\rangle \frac{T_n(\eta_1)T_m(\eta_2)+T_n(\eta_2)T_m(\eta_1)}{2}$$

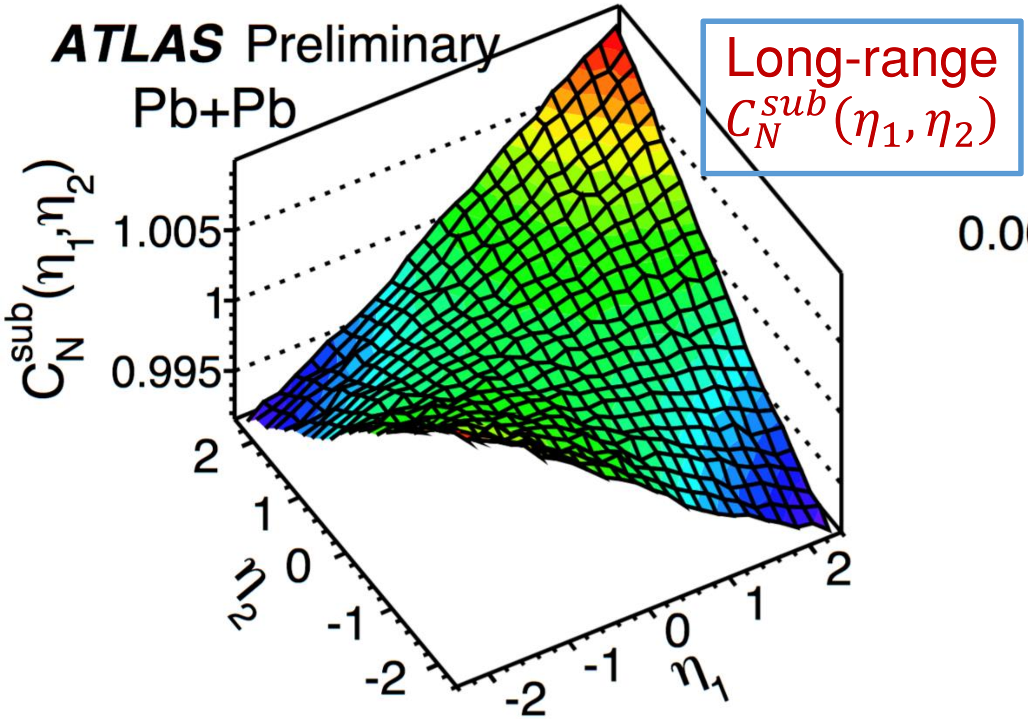

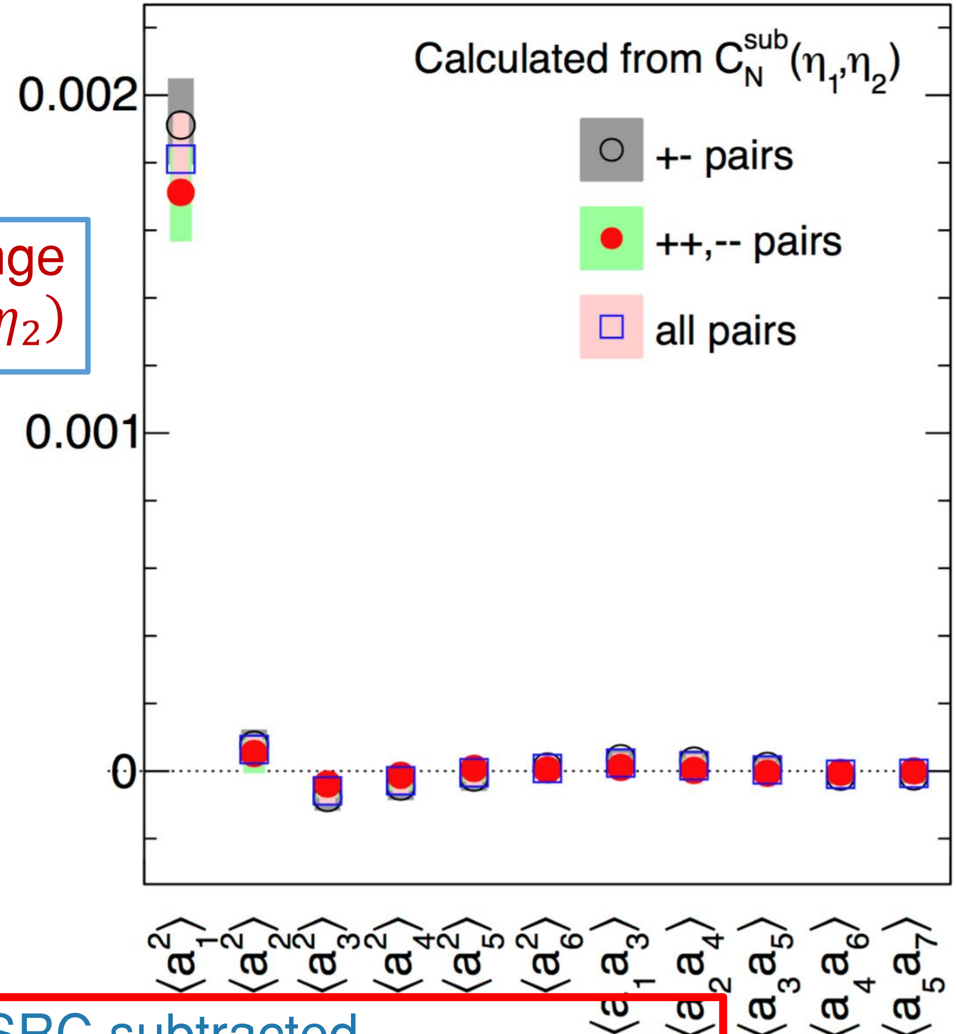

- Much simpler picture after SRC subtracted
  - LRC is dominated by linear multiplicity fluctuation in η;
  - LRC is independent of charge combination.

How stable are the results?

- Four largely independent methods are applied to determine $\langle a_1^2 \rangle$;
- Different methods have different sensitivity to the analysis procedures;

How stable are the results?

- Four largely independent methods are applied to determine $\langle a_1^2 \rangle$;
- Different methods have different sensitivity to the analysis procedures;

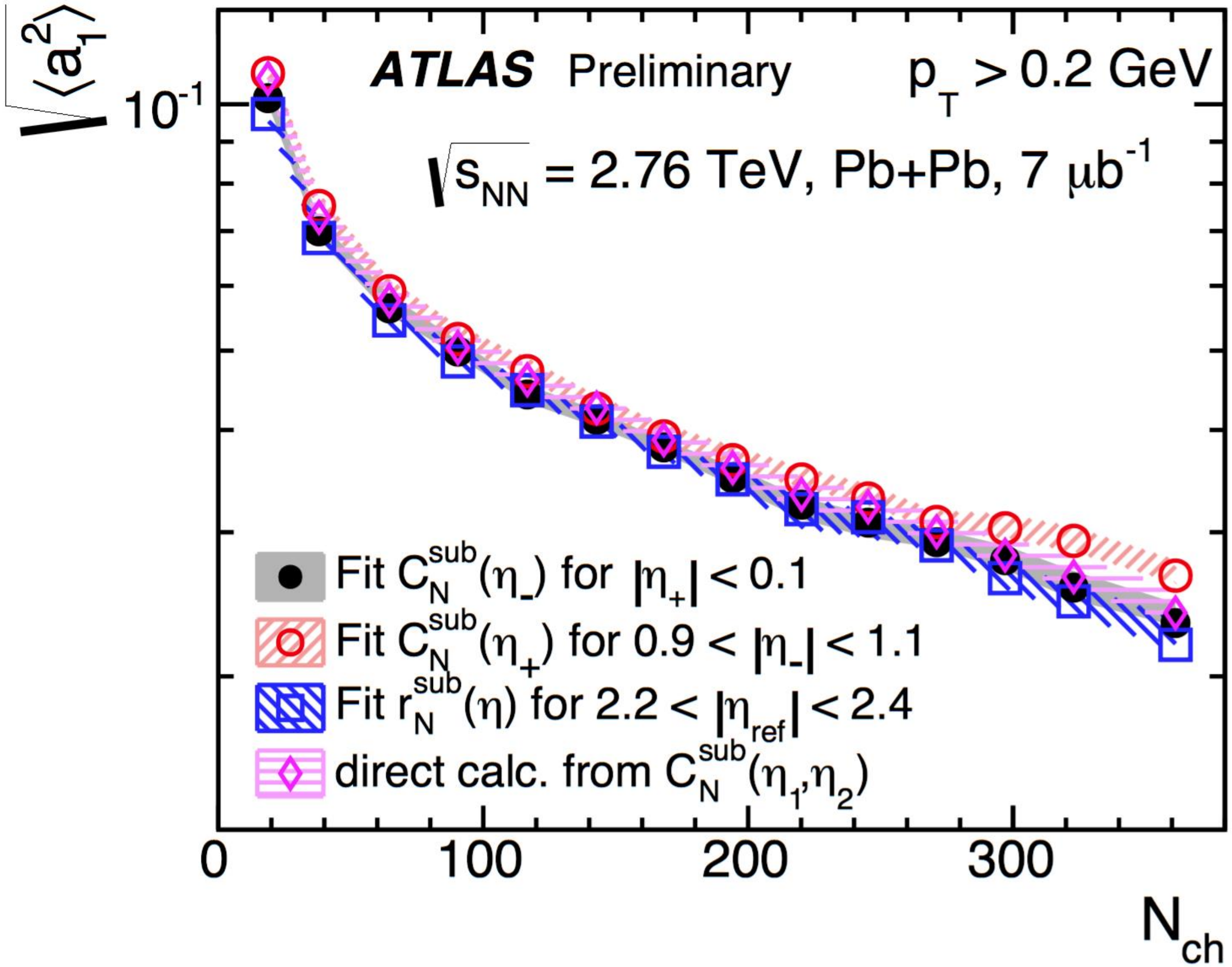

- Four methods give consistent a_1: conclusions are insensitive to the procedure.

Dependence on N_{ch} and collision systems

SRC

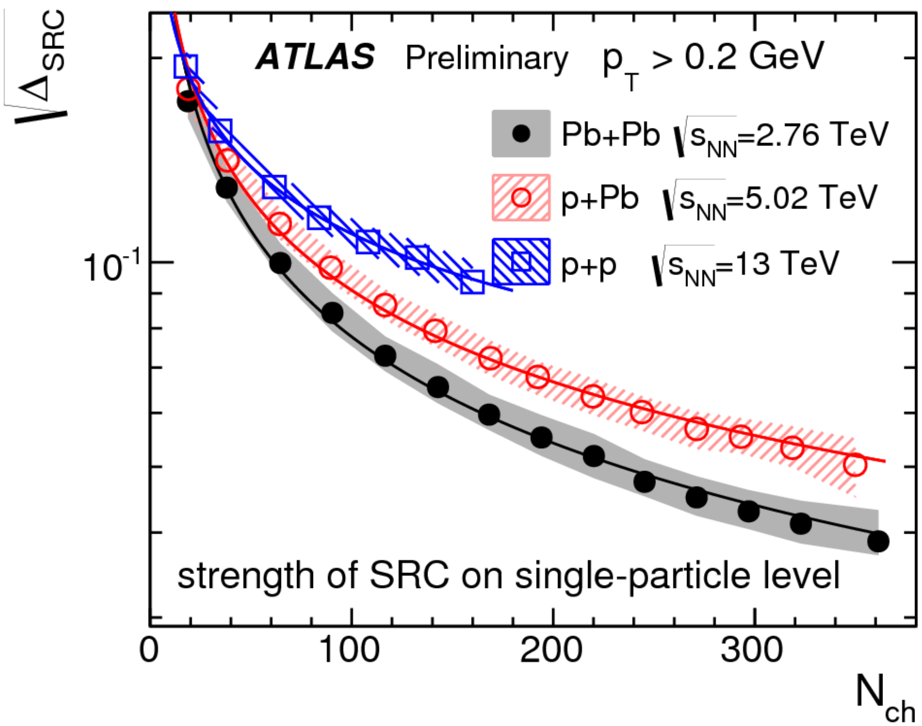

- Strength of SRC defined as: $\sqrt{\Delta_{SRC}} \equiv \sqrt{\frac{\int \delta_{SRC}(\eta_1,\eta_2)d\eta_1 d\eta_2}{4Y^2}}$;
- Depends on N_{ch}: strength of SRC increases towards peripheral;
- Depends on system size: SRC is stronger in small system.

Dependence on N_{ch} and collision systems

SRC

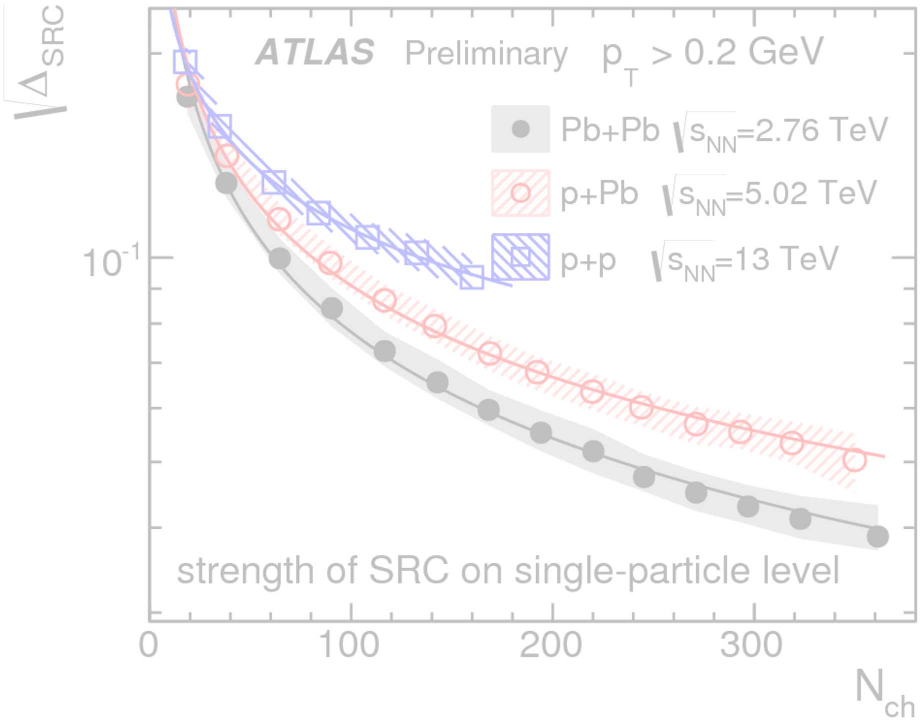

LRC

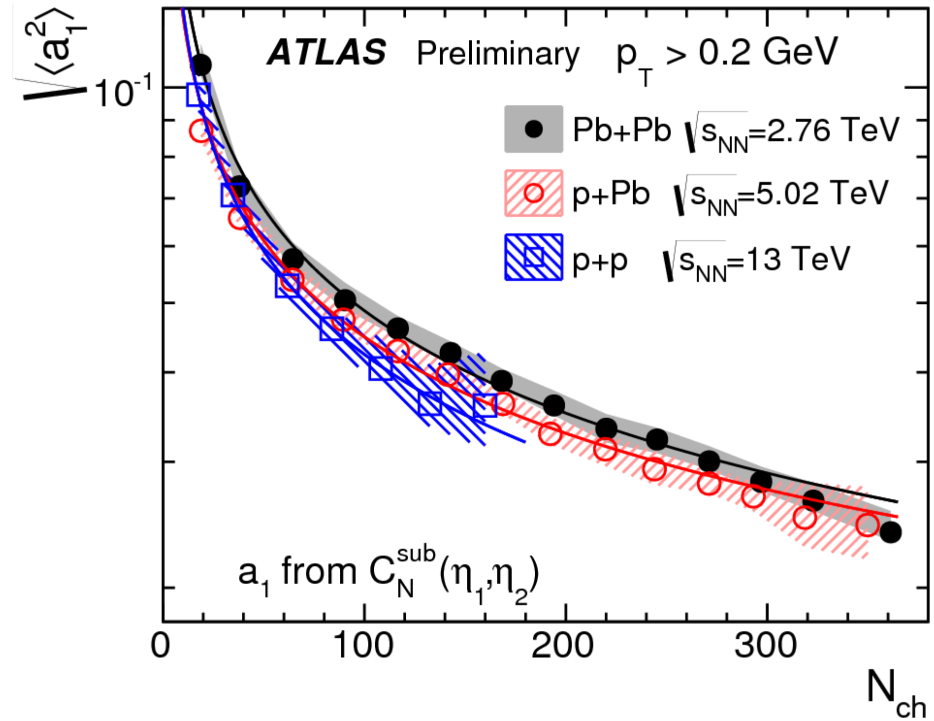

- Strength of LRC is characterized by dominating coefficient $\sqrt{a_1^2}$;
- Depends on N_{ch}: FB multiplicity fluctuation is larger in peripheral;
- Independent of system size: require sources at partonic level!
- Strength of SRC and LRC also follow pow-law function: why?

Dependence on N_{ch} and collision systems

SRC **LRC**

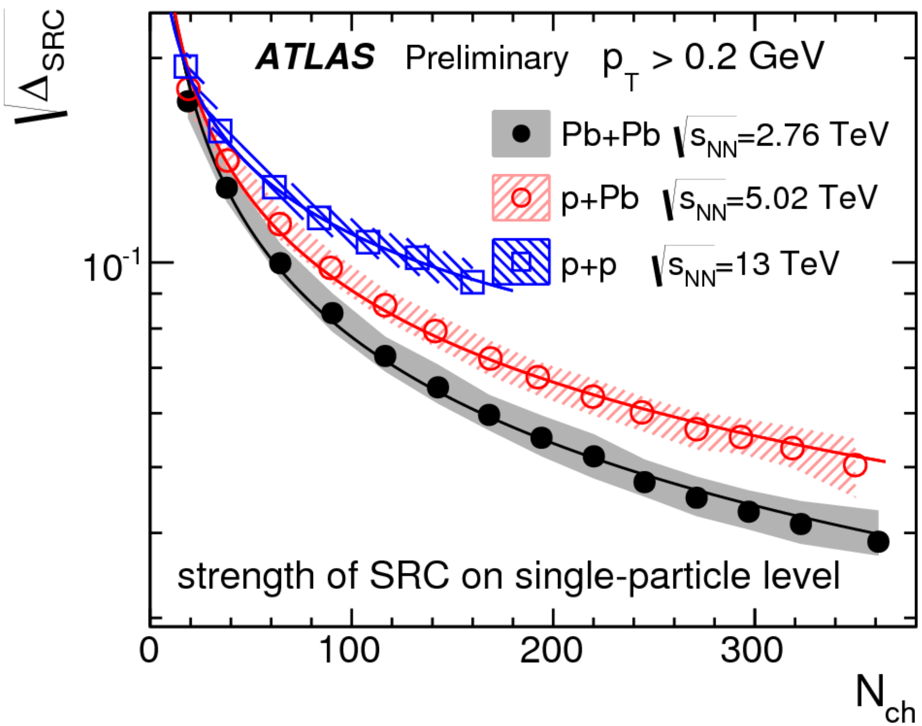

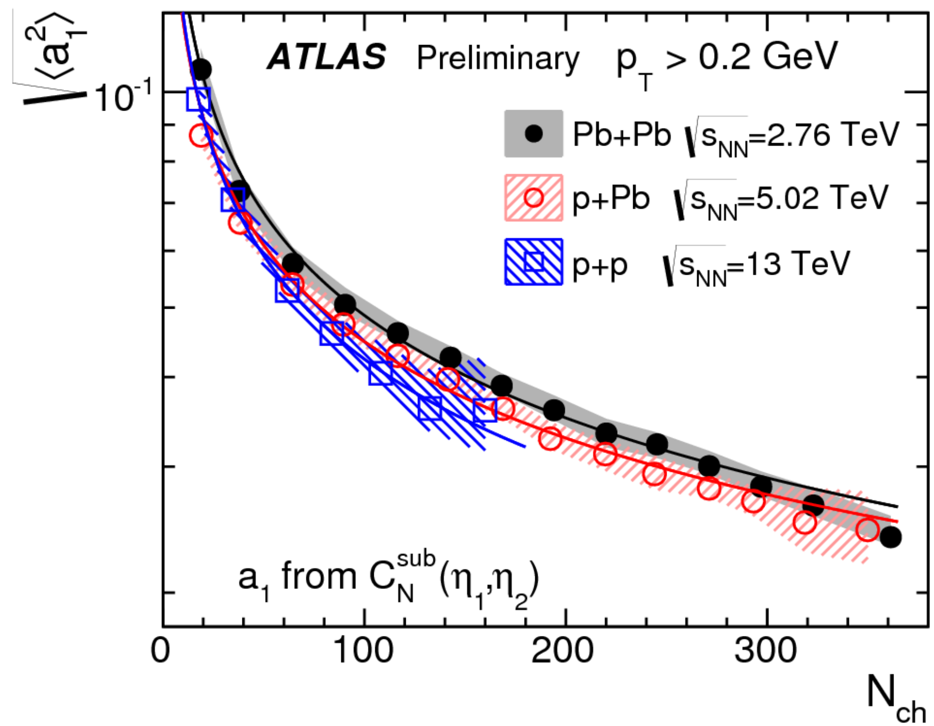

- In an independent cluster model, each cluster emits same number of pairs;
- Both SRC and LRC scale approximately as the inverse of number of clusters n;

$$\sqrt{\Delta_{SRC}} \sim \sqrt{a_1^2} \sim \frac{1}{n^{\alpha}}$$

Dependence on N_{ch} and collision systems

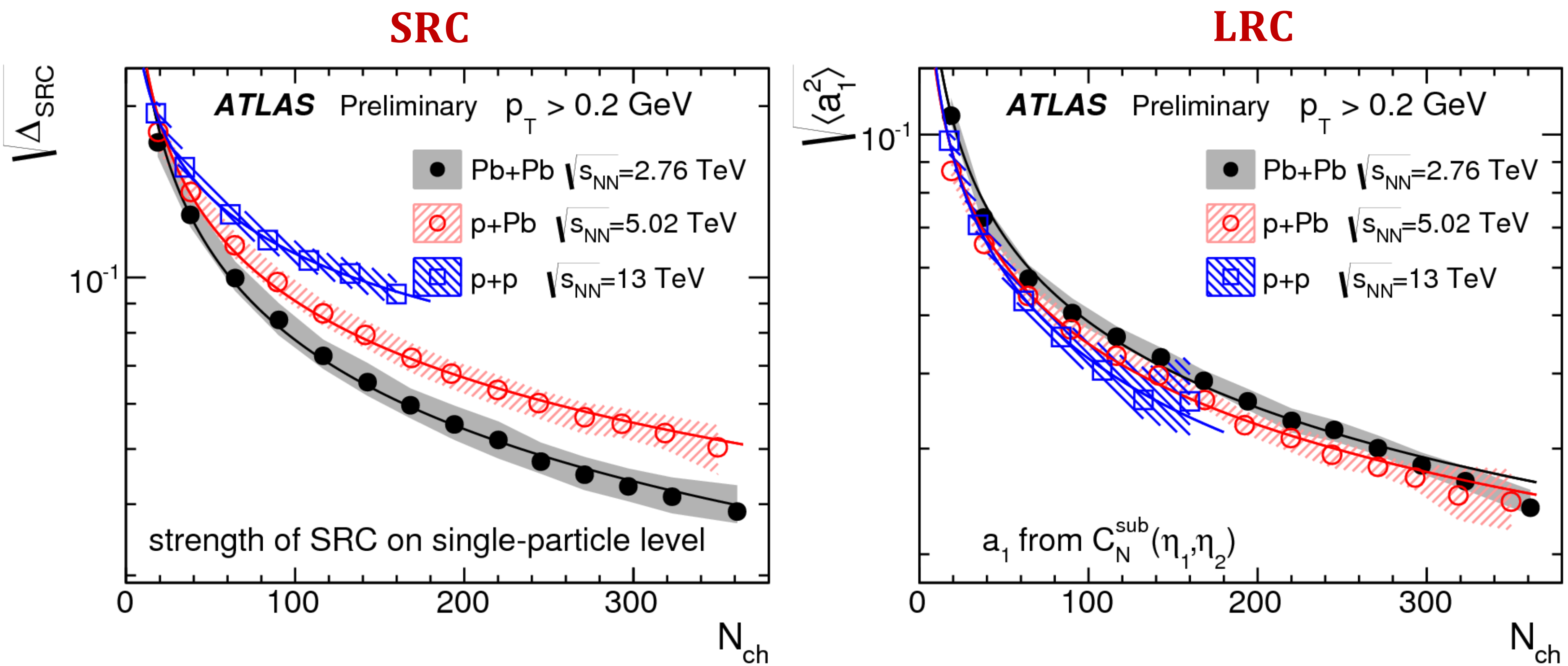

- In an independent cluster model, each cluster emits same number of pairs;
- Both SRC and LRC scale approximately as the inverse of number of clusters n;
- Assuming n and N_{ch} are directly related, then

$$\sqrt{\Delta_{SRC}} \sim \sqrt{a_1^2} \sim \frac{1}{n^\alpha} \sim \frac{1}{N_{ch}^\alpha}$$

Dependence on N_{ch} and collision systems

SRC **LRC**

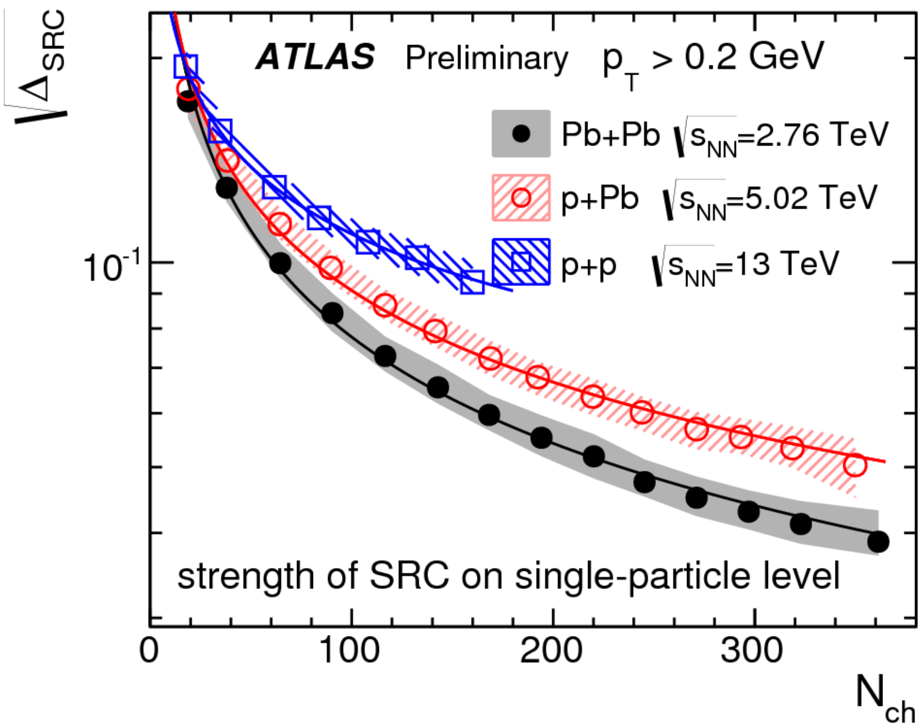

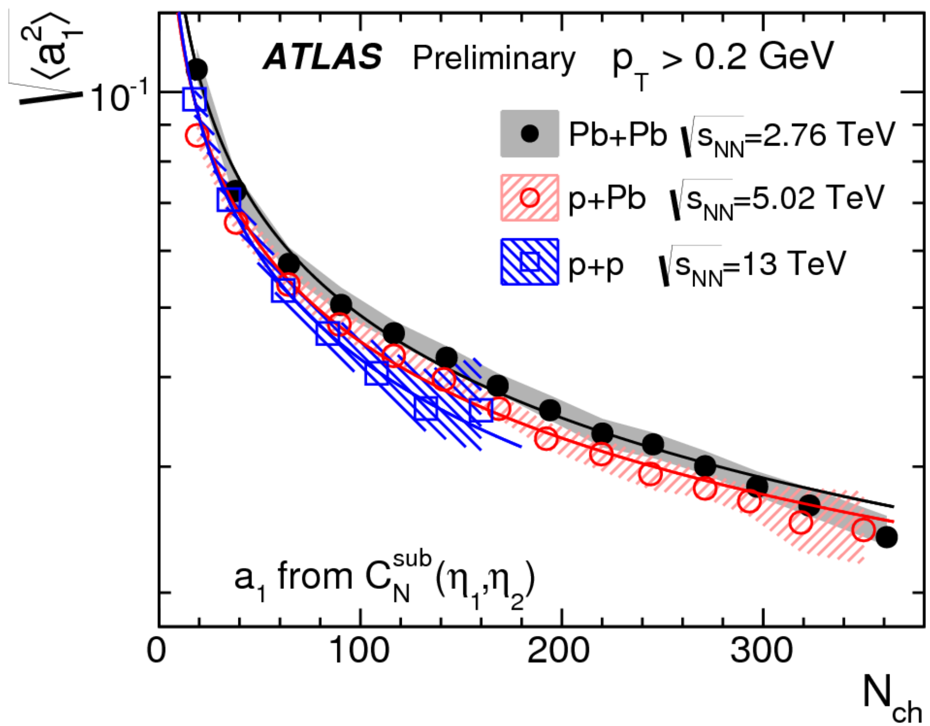

Fit with $\frac{c}{N_{ch}^{\alpha}}$

	Pb+Pb	p+Pb	pp
α for $\sqrt{\Delta_{SRC}}$	0.505 ± 0.011	0.450 ± 0.010	0.365 ± 0.014
α for $\sqrt{\langle a_1^2 \rangle}$	0.454 ± 0.011	0.433 ± 0.014	0.465 ± 0.018

$$\sqrt{\Delta_{SRC}} \sim \sqrt{a_1^2} \sim \frac{1}{n^{\alpha}} \sim \frac{1}{N_{ch}^{\alpha}}, \alpha \sim 0.5$$

Asymmetry in *p*+Pb collision

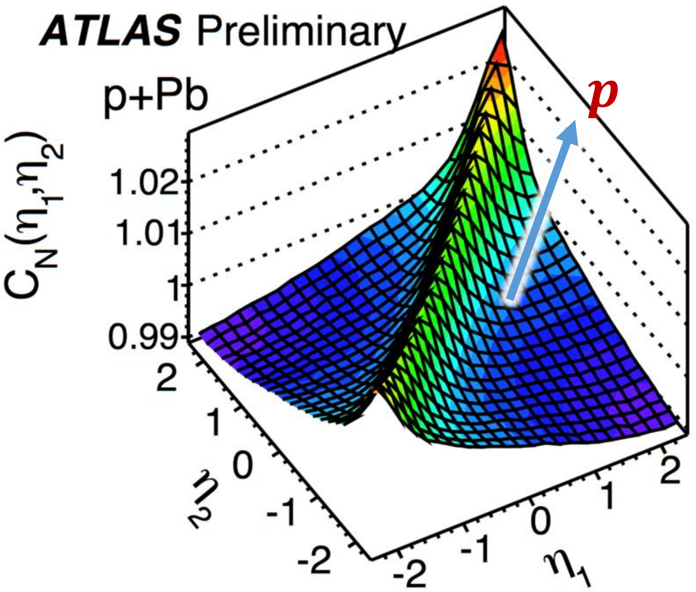

- Asymmetry observed in *p*+Pb collision: stronger correlation in the proton-going side.

Asymmetry in *p*+Pb collision

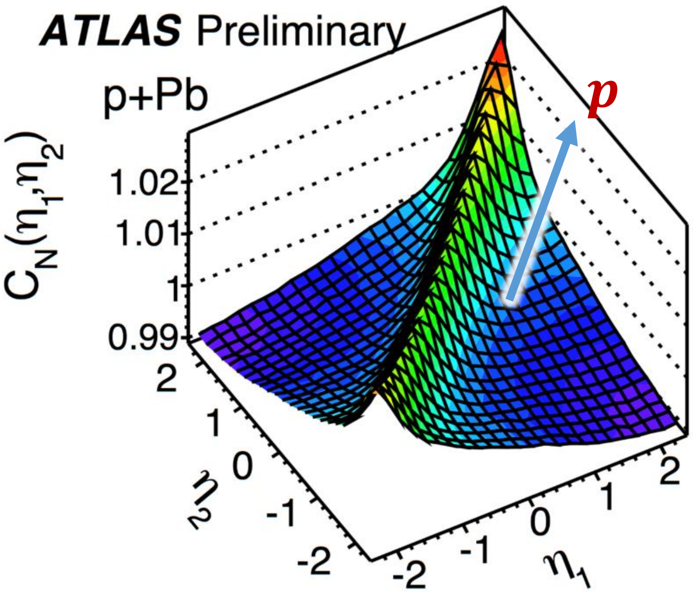

- Asymmetry observed in *p*+Pb collision: stronger correlation in the proton-going side.

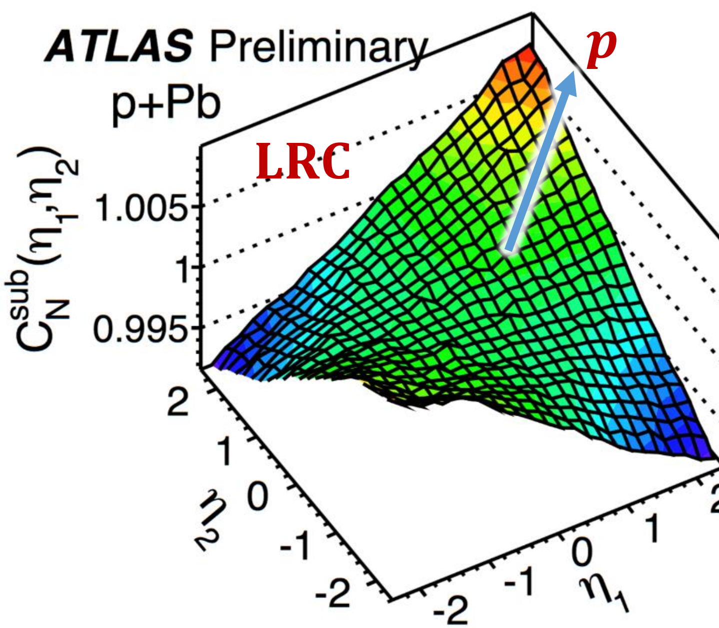

- LRC is symmetric.

Asymmetry in *p*+Pb collision

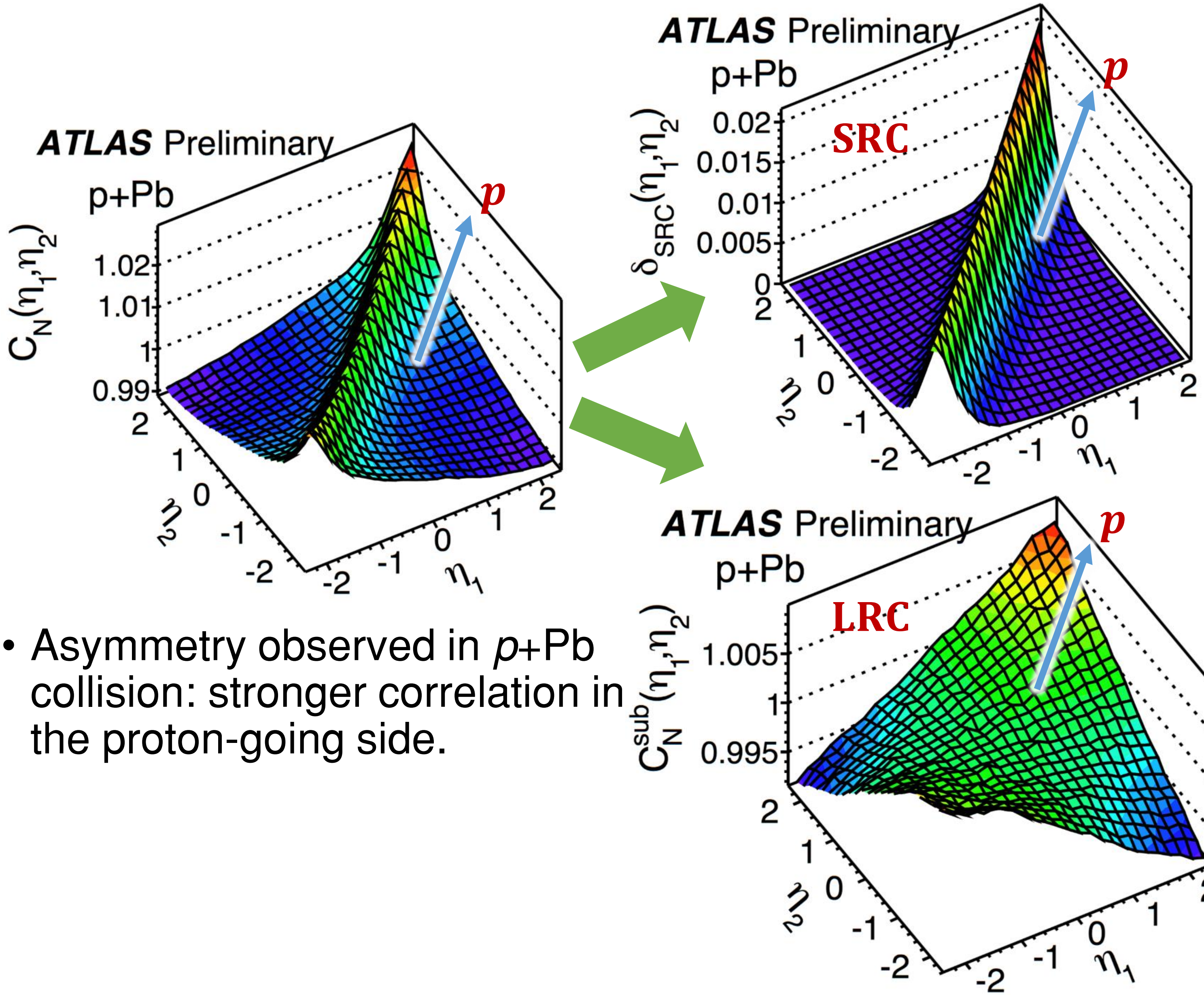

- Asymmetry entirely due to SRC!

- Asymmetry observed in *p*+Pb collision: stronger correlation in the proton-going side.

- LRC is symmetric.

Asymmetry in *p*+Pb collision

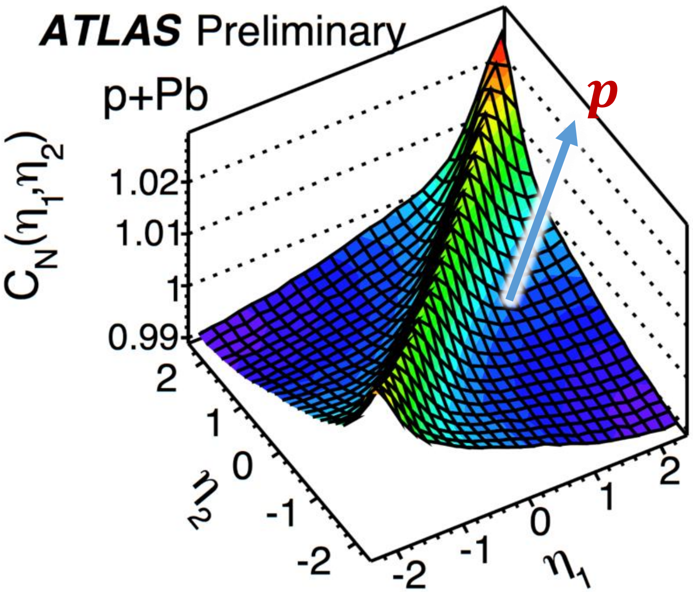

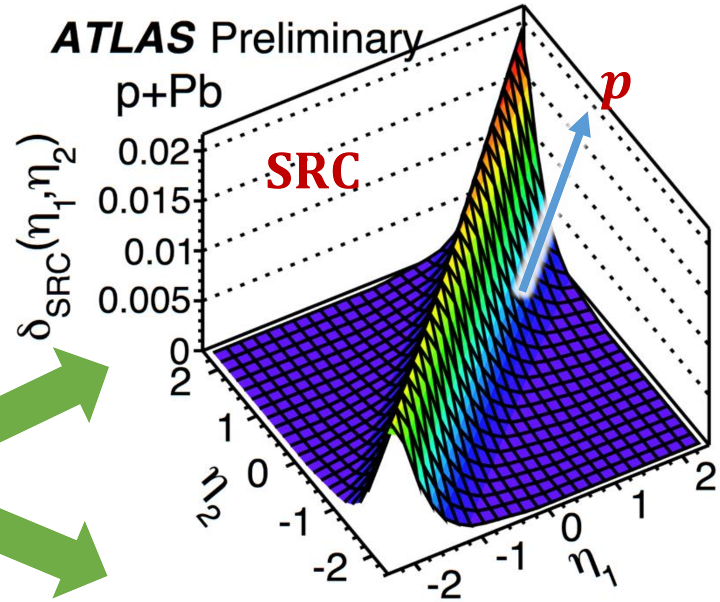

- Asymmetry entirely due to SRC!

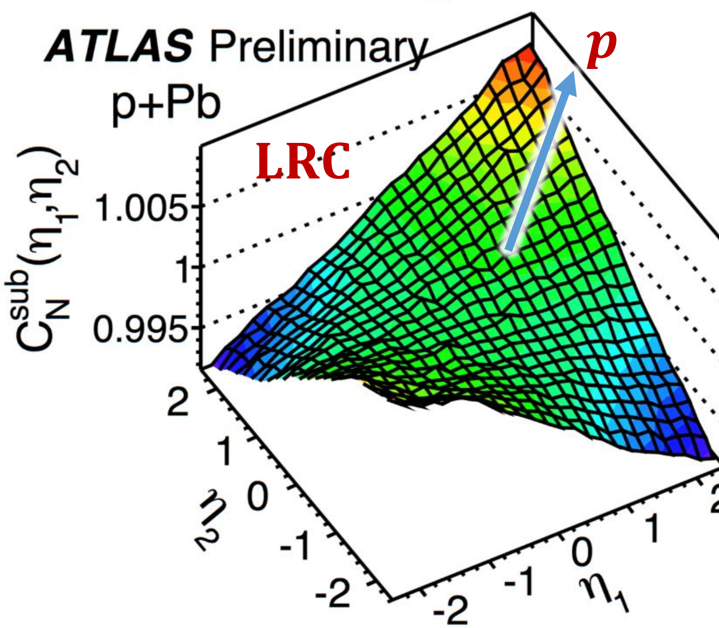

- LRC is symmetric.

- Asymmetry observed in *p*+Pb collision: stronger correlation in the proton-going side.

- Why the asymmetric collision causes asymmetric SRC?

SRC asymmetry in *p*+Pb collision

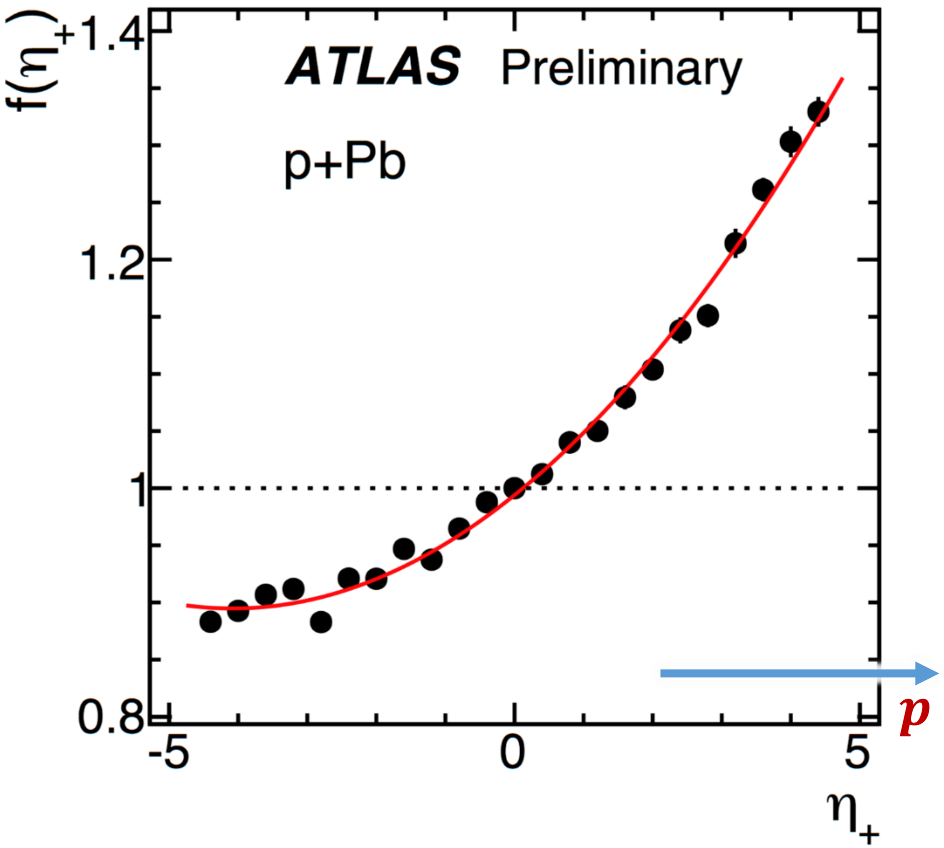

SRC asymmetry in *p*+Pb collision

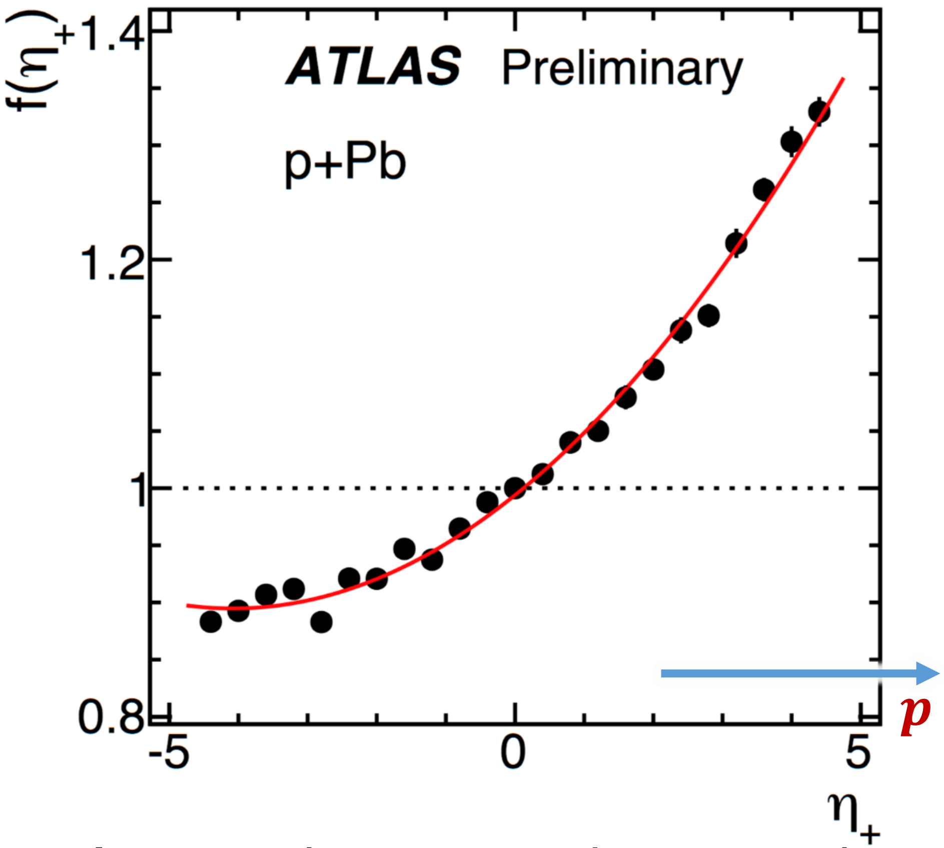

- Assume there are n clusters and each one emits m particles on average;

$$\delta_{SRC} \propto \frac{n\langle m(m-1)\rangle}{(n\langle m\rangle)^2} = \frac{1}{n}$$

SRC asymmetry in p+Pb collision

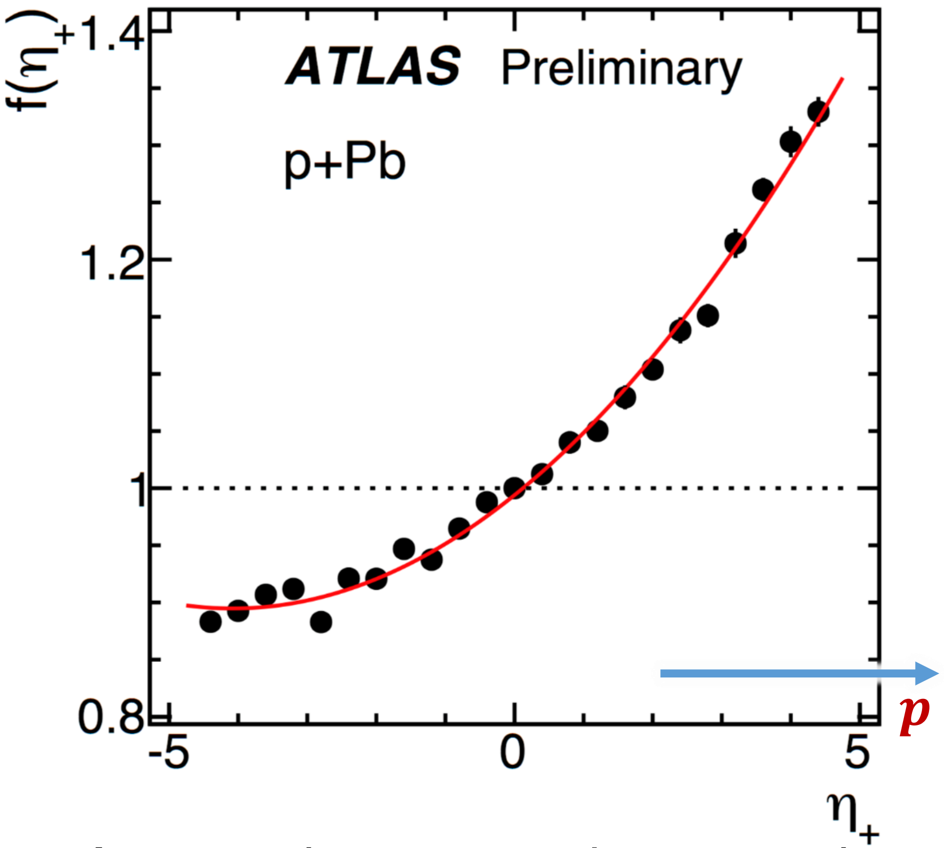

- Assume there are n clusters and each one emits m particles on average;
- Assume n is proportional to local particle density $dN_{ch}/d\eta$;

$$\delta_{SRC} \propto \frac{n\langle m(m-1)\rangle}{(n\langle m\rangle)^2} = \frac{1}{n} \propto \frac{1}{dN_{ch}/d\eta}$$

SRC asymmetry in p+Pb collision

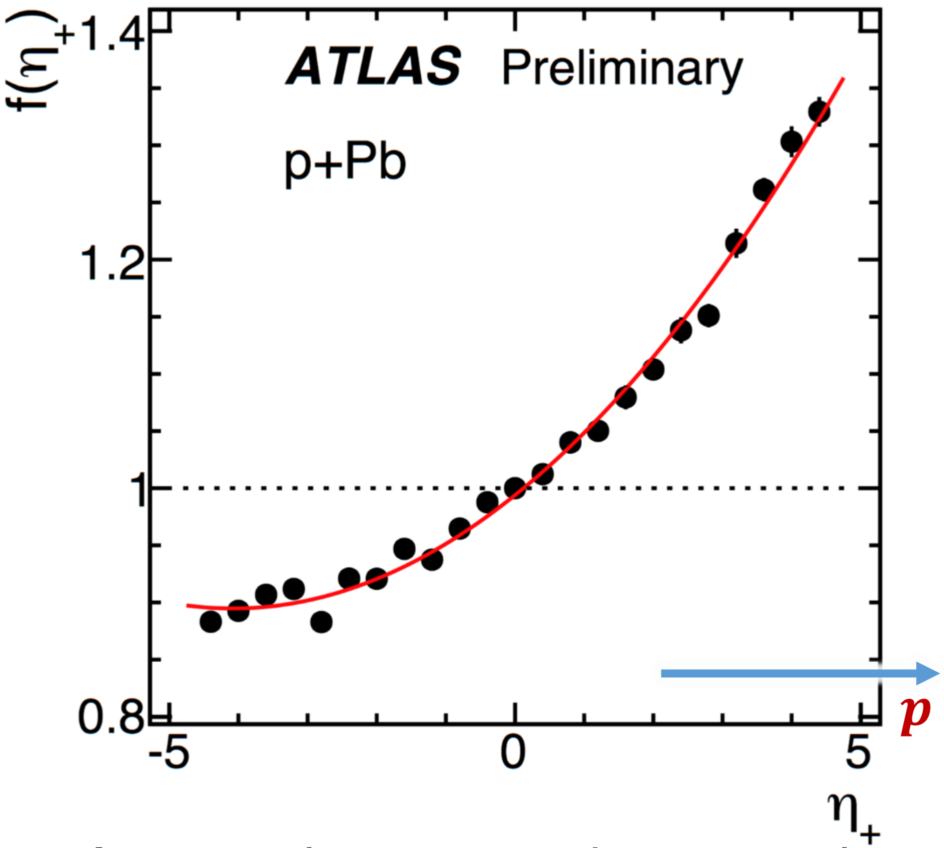

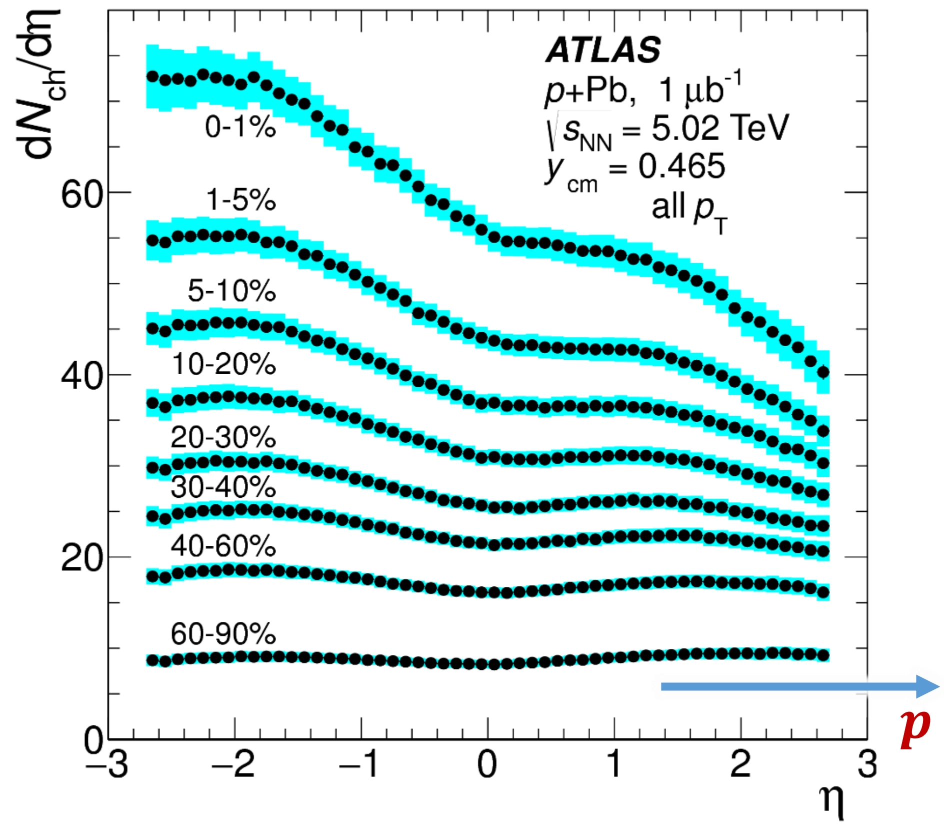

- Assume there are n clusters and each one emits m particles on average;
- Assume n is proportional to local particle density $dN_{ch}/d\eta$;

$$\delta_{SRC} \propto \frac{n\langle m(m-1)\rangle}{(n\langle m\rangle)^2} = \frac{1}{n} \propto \frac{1}{dN_{ch}/d\eta}$$

Inverse to multiplicity distribution

Compare SRC shape in three systems

Symmetrized *p*+Pb

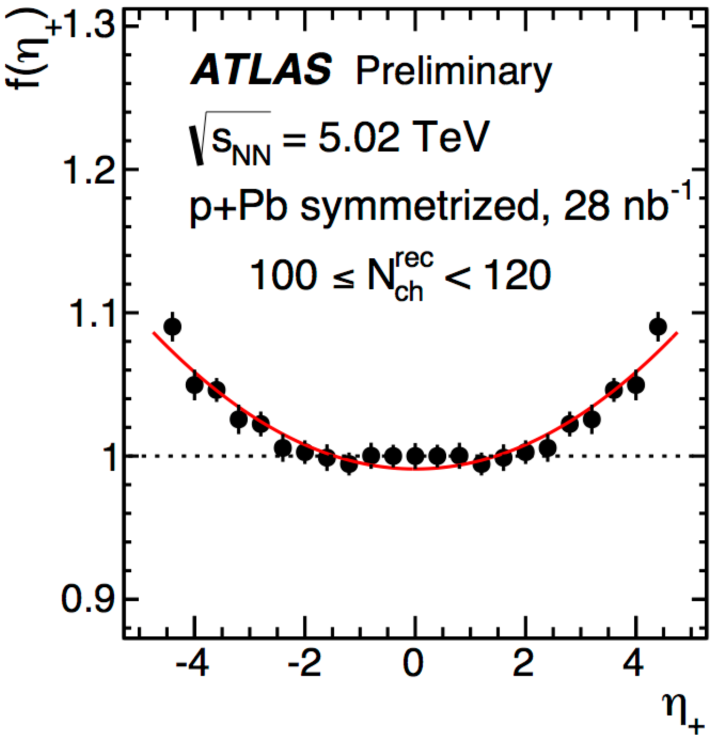

- For better comparison with *pp* and Pb+Pb, *p*+Pb is symmetrized;

Compare SRC shape in three systems

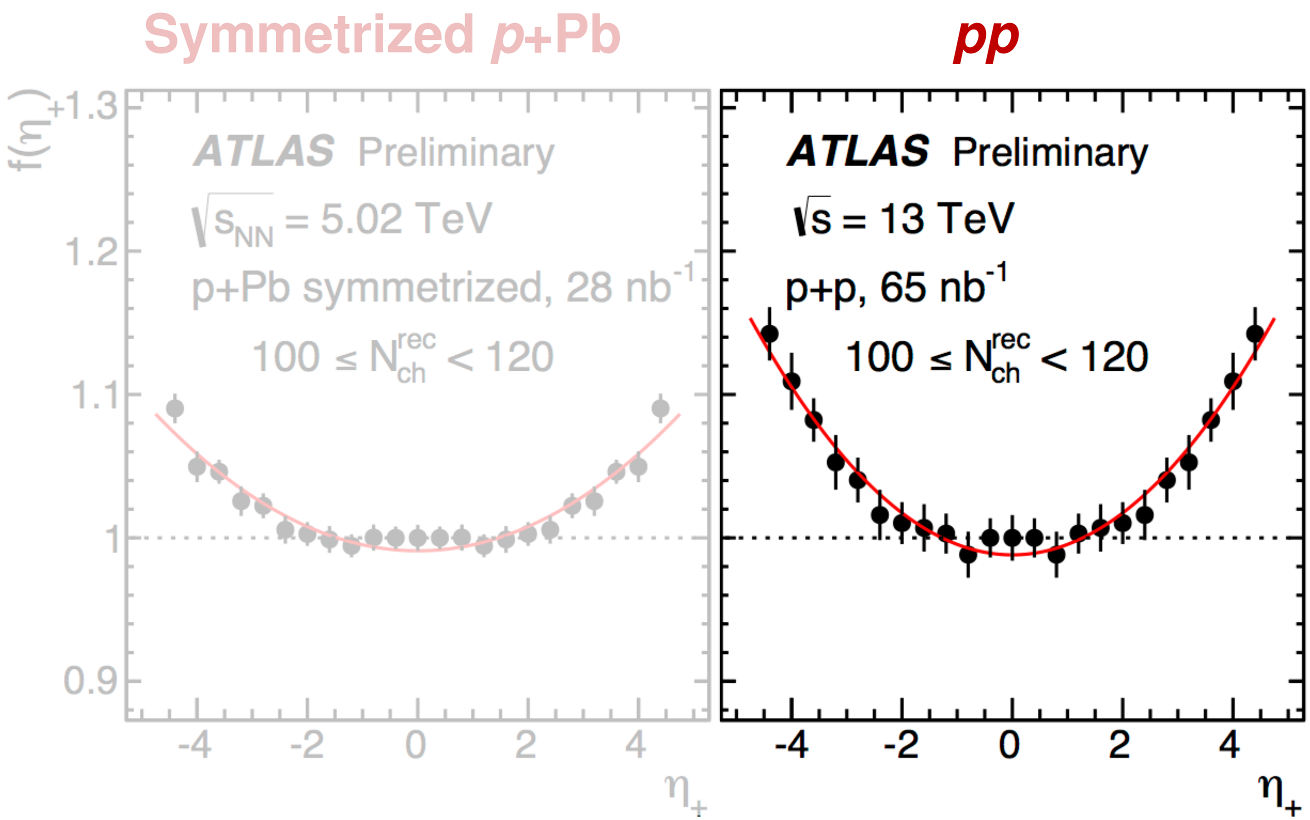

- For better comparison with *pp* and Pb+Pb, *p*+Pb is symmetrized;
- In high-multiplicity *pp*, SRC shape is slightly larger than *p*+Pb;

Compare SRC shape in three systems

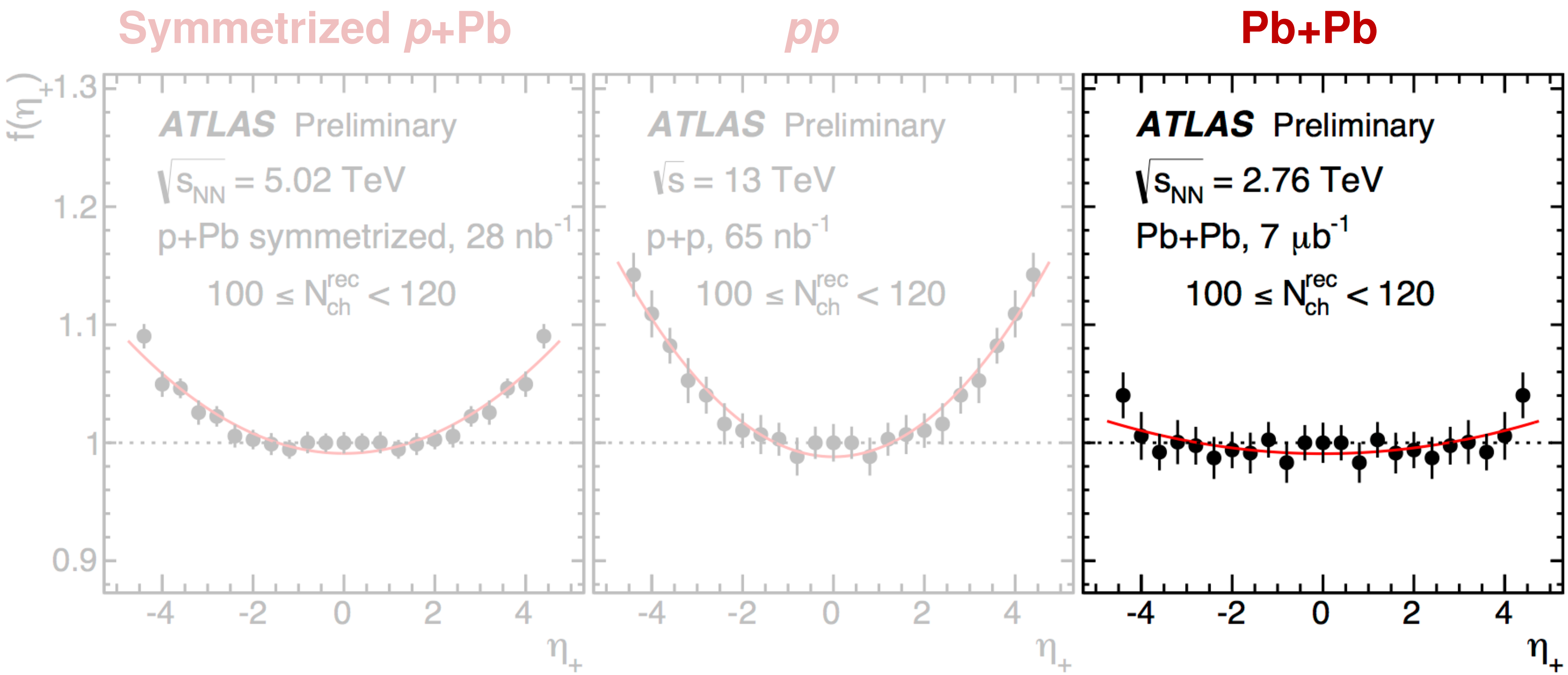

- For better comparison with pp and Pb+Pb, *p*+Pb is symmetrized;
- In high-multiplicity *pp*, SRC shape is slightly larger than *p*+Pb;
- However in Pb+Pb, SRC shape is more flat.

Compare SRC shape in three systems

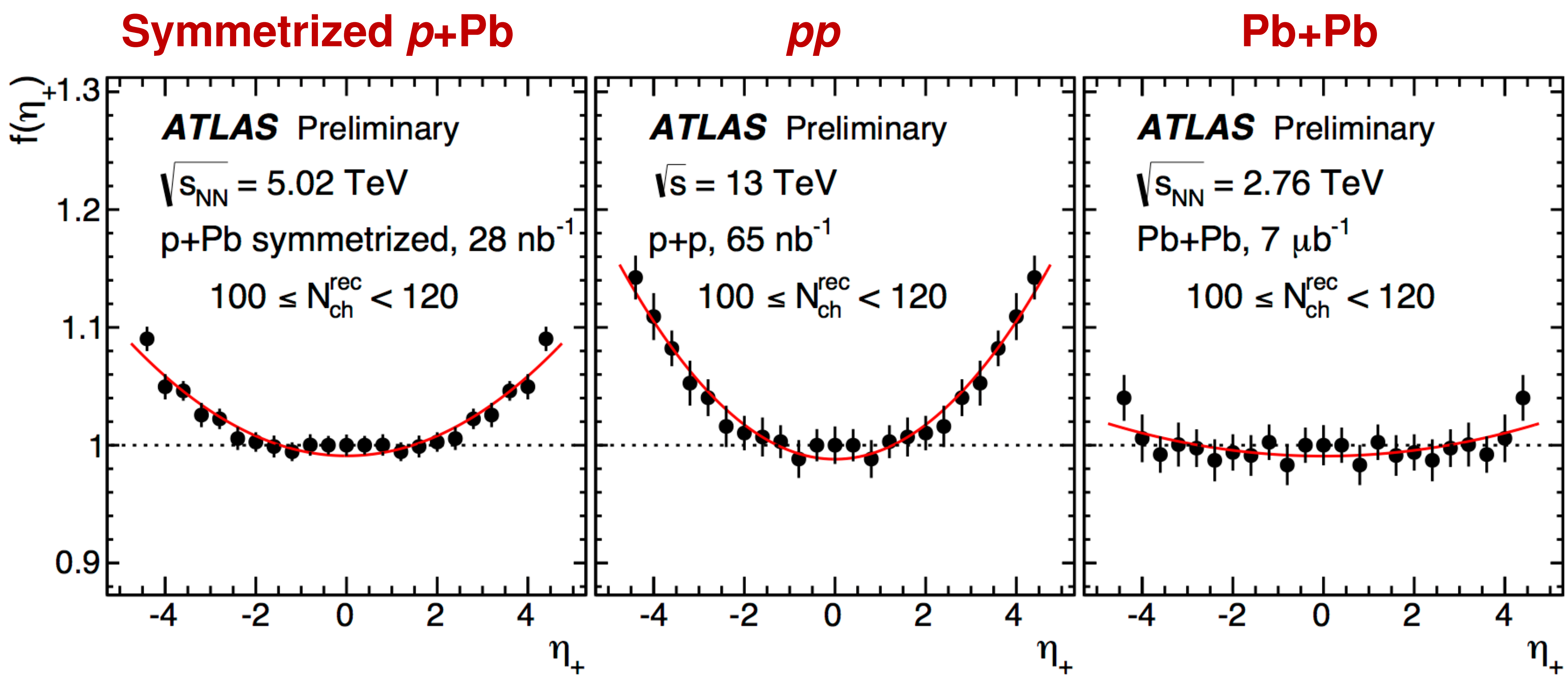

- For better comparison with pp and Pb+Pb, *p*+Pb is symmetrized;
- In high-multiplicity *pp*, SRC shape is slightly larger than *p*+Pb;
- However in Pb+Pb, SRC shape is more flat.
- EbyE asymmetry of multiplicity (relative to average multiplicity) in high-multiplicity *pp* is larger than *p*+Pb while Pb+Pb collision is more symmetric.

Summary

- Forward-backward multiplicity correlation $C_N(\eta_1, \eta_2)$ is measured in Pb+Pb, *p*+Pb and *pp* collisions at similar event multiplicity.
  - Correlation function consistent of a strong short-range component and a long-range component.

- A data-driven method is used to estimate SRC based on the fact that SRC has strong charge dependence, while LRC does not.

- Legendre expansion as well as other three independent methods shows that shape of LRC is dominated by leading linear fluctuation $1 + \langle a_1^2 \rangle \eta_1 \eta_2$.

- The N_{ch}-scaling of LRC and SRC across three systems are studied.
  - SRC depends strongly on collision systems and decrease with N_{ch};
  - LRC decrease with N_{ch} but independent of system size;
  - Both follows power-law of N_{ch} with an index close to 0.5: information on the number of sources for particle production?

- EbyE asymmetry of multiplicity (relative to the average) in high-multiplicity *pp* is larger than *p*+Pb, while Pb+Pb collision is more symmetric.

Summary

- Forward-backward multiplicity correlation $C_N(\eta_1, \eta_2)$ is measured in Pb+Pb, *p*+Pb and *pp* collisions at similar event multiplicity.
  - Correlation function consistent of a strong short-range component and a

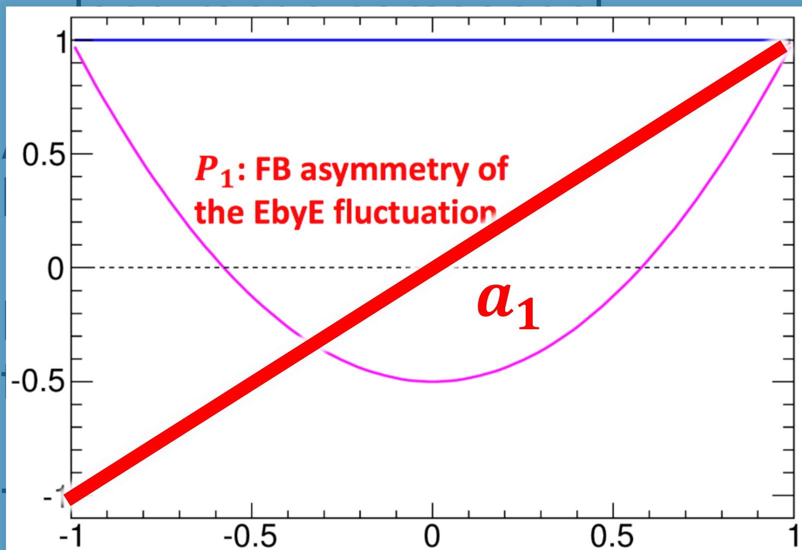

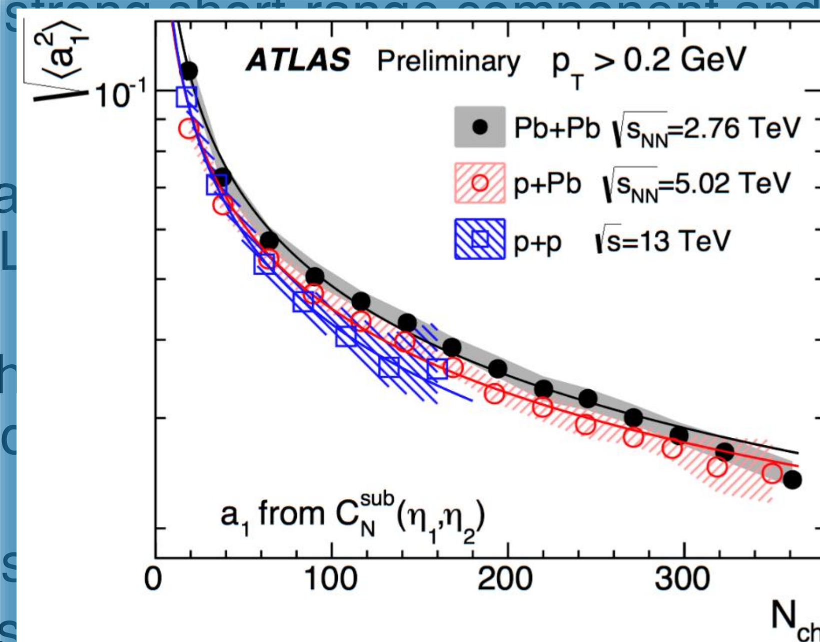

  - SRC depends strongly on collision systems and decrease with N_{ch};
  - LRC decrease with N_{ch} but independent of system size;
  - Both follows power-law of N_{ch} with an index close to 0.5: information on the number of sources for particle production?

- EbyE asymmetry of multiplicity (relative to the average) in high-multiplicity *pp* is larger than *p*+Pb, while Pb+Pb collision is more symmetric.

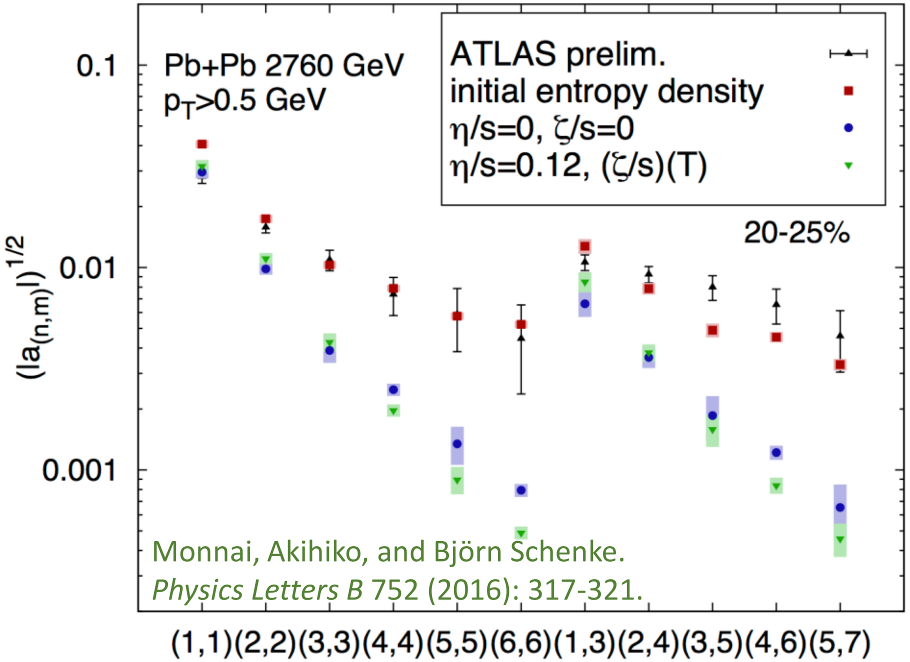

- Results show the viscous hydro compared with data (LRC+SRC);
- Initial entropy density (modified Glauber) describe the data quite well;
- Hydro-expansion damps the coefficients.

Outlook

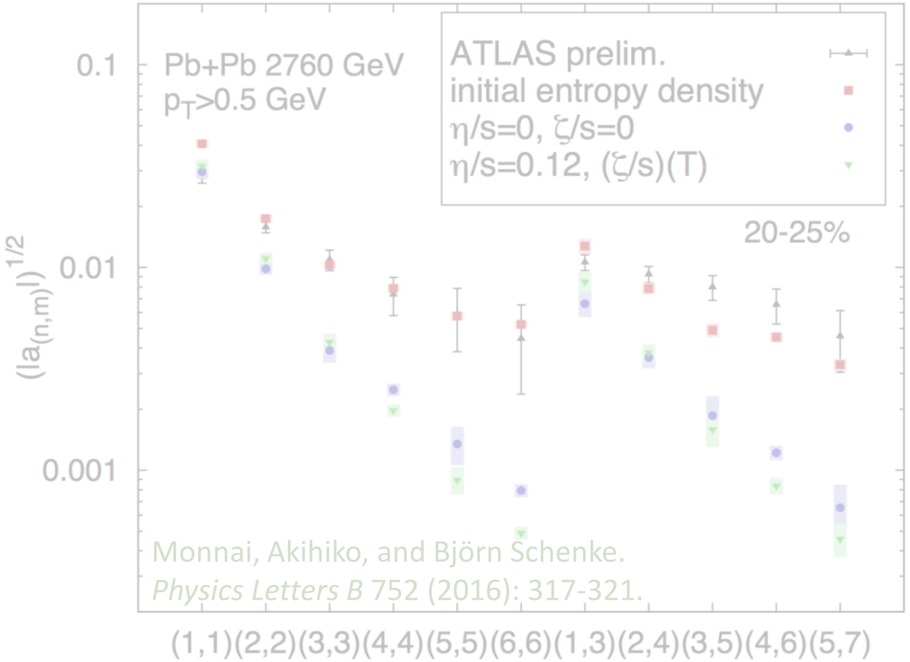

- Results show the viscous hydro compared with data (LRC+SRC);
- Initial entropy density (modified Glauber) describe the data quite well;
- Hydro-expansion damps the coefficients.

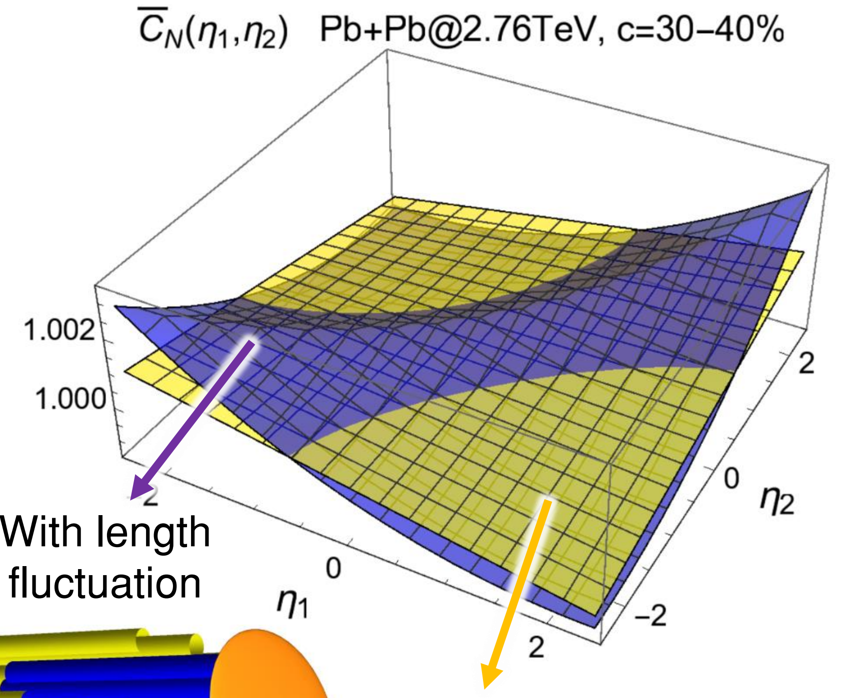

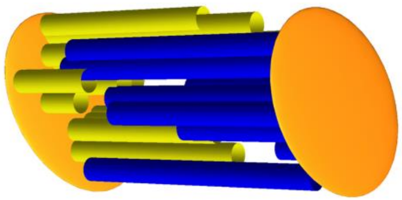

Broniowski, Wojciech, and Piotr Bozek. *arXiv:1512.01945* (2015).

- Length of sources fluctuation could also explain the shape observed in data.

Outlook

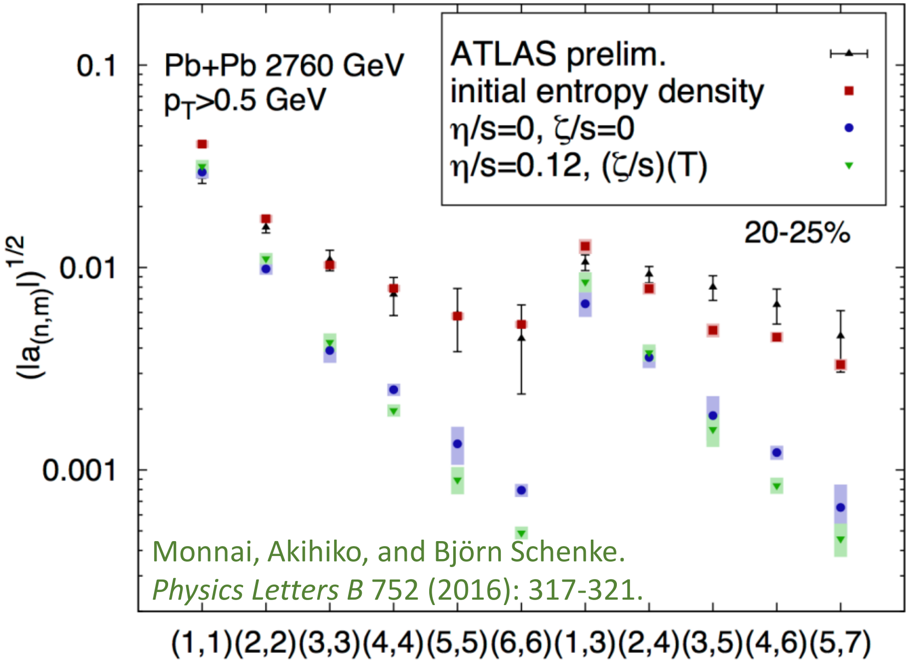

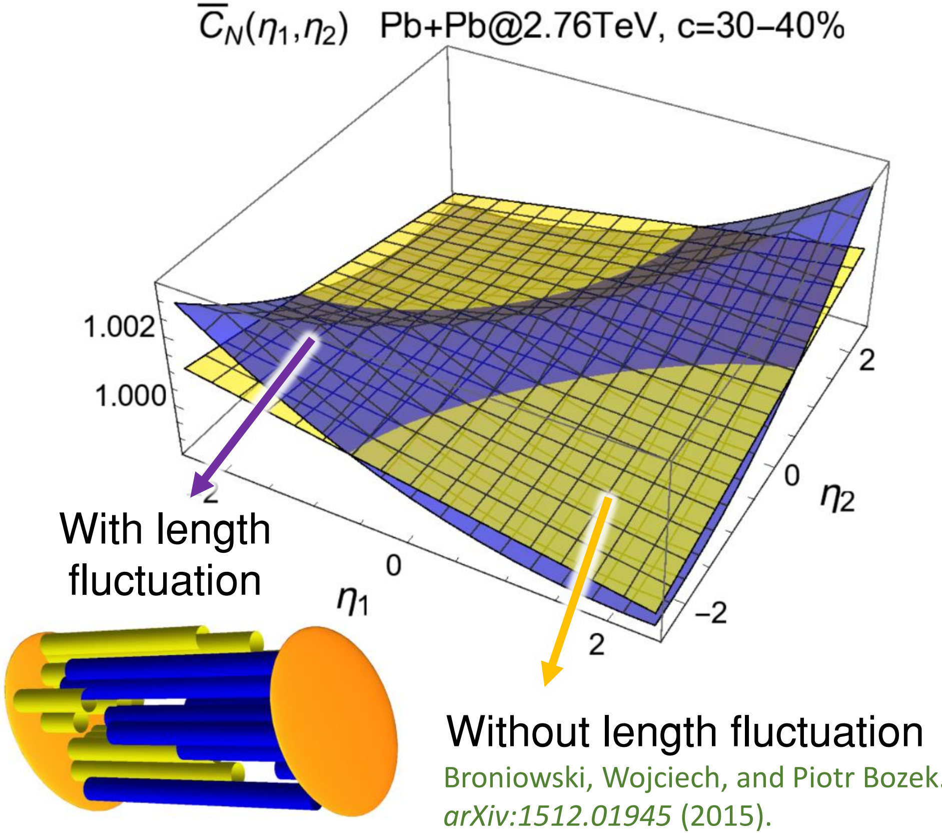

- Results show the viscous hydro compared with data (LRC+SRC);
- Initial entropy density (modified Glauber) describe the data quite well;
- Hydro-expansion damps the coefficients.

- Length of sources fluctuation could also explain the shape observed in data.

- With SRC separated from LRC, these results will provide better constrains to various initial models.

Outlook 2

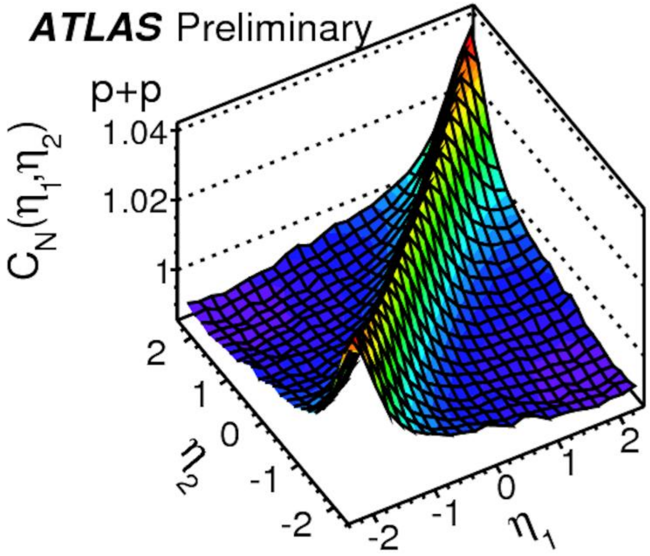

- $C(\eta_1, \eta_2)$ is a very comprehensive observable.

Outlook 2

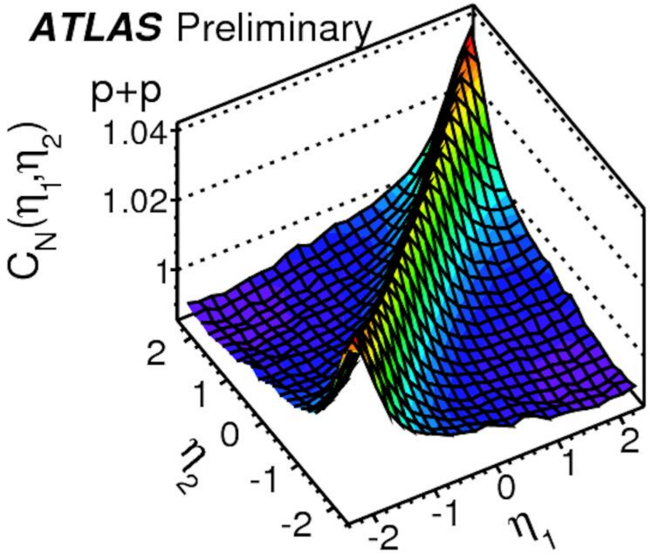

- $C(\eta_1, \eta_2)$ is a very comprehensive observable.
- Reconstruct balance function

$$2B(\Delta\eta) \equiv 2C^{+-}(\Delta\eta) - C^{++}(\Delta\eta) - C^{--}(\Delta\eta)$$

Outlook 2

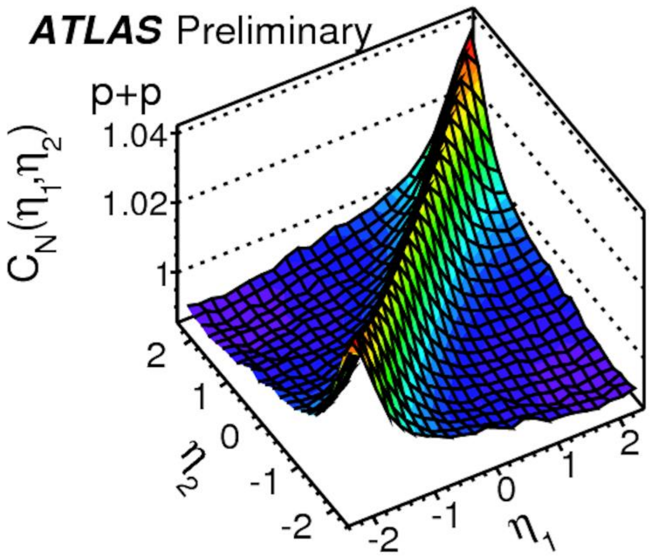

- $C(\eta_1,\eta_2)$ is a very comprehensive observable.
- Reconstruct balance function

$$2B(\Delta\eta) \equiv 2C^{+-}(\Delta\eta) - C^{++}(\Delta\eta) - C^{--}(\Delta\eta)$$

- Test factorization: high-p_T a_n^H and low-p_T a_n^L

$$r_n \equiv \frac{\langle a_n^H a_n^L \rangle}{\sqrt{\langle a_n^H a_n^H \rangle}\sqrt{\langle a_n^L a_n^L \rangle}}$$

Outlook 2

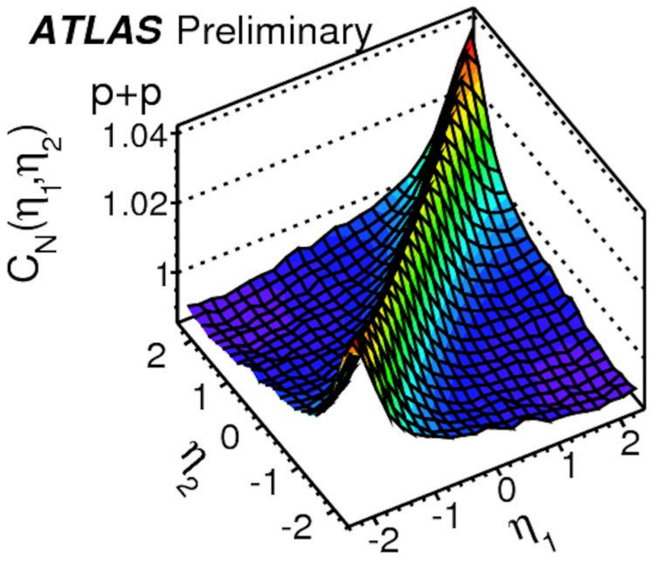

- $C(\eta_1, \eta_2)$ is a very comprehensive observable.
- Reconstruct balance function

$$2B(\Delta\eta) \equiv 2C^{+-}(\Delta\eta) - C^{++}(\Delta\eta) - C^{--}(\Delta\eta)$$

- Test factorization: high-p_T a_n^H and low-p_T a_n^L

$$r_n \equiv \frac{\langle a_n^H a_n^L \rangle}{\sqrt{\langle a_n^H a_n^H \rangle}\sqrt{\langle a_n^L a_n^L \rangle}}$$

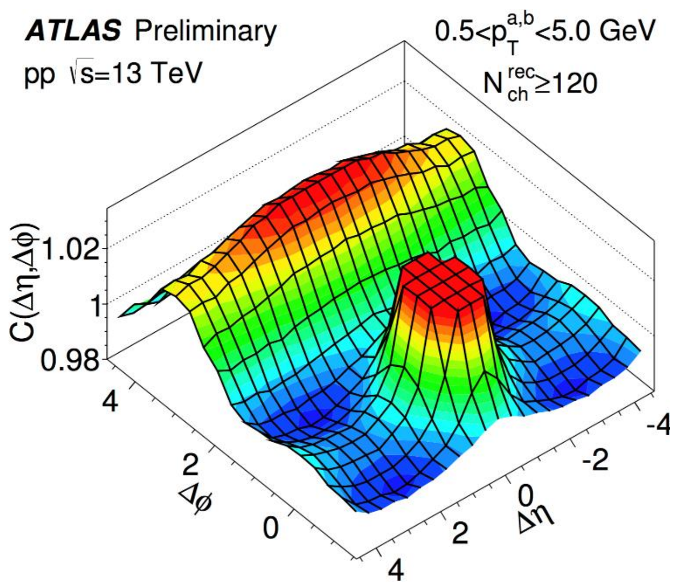

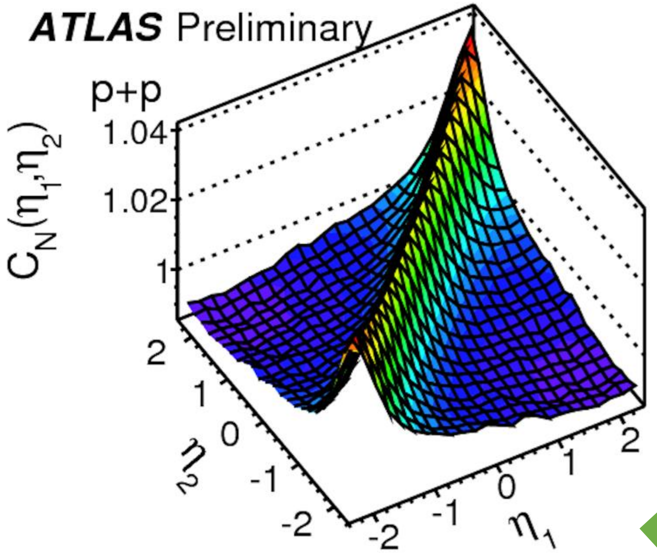

- $C(\eta_1, \eta_2)$ is a very comprehensive observable.
- Reconstruct balance function

$$2B(\Delta\eta) \equiv 2C^{+-}(\Delta\eta) - C^{++}(\Delta\eta) - C^{--}(\Delta\eta)$$

- Test factorization: high-p_T a_n^H and low-p_T a_n^L

$$r_n \equiv \frac{\langle a_n^H a_n^L \rangle}{\sqrt{\langle a_n^H a_n^H \rangle}\sqrt{\langle a_n^L a_n^L \rangle}}$$

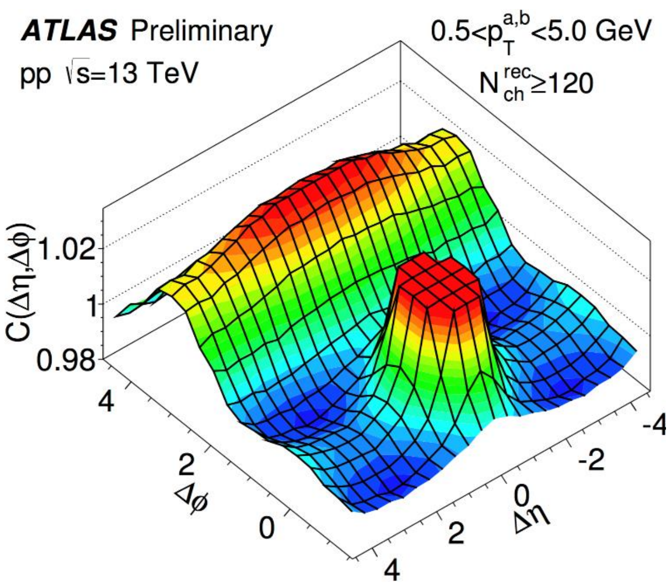

$C(\eta_1, \eta_2)$

+

$C(\Delta\eta, \Delta\phi)$

$C(\eta_1, \eta_2, \Delta\phi)$!

Back-up

Residual centrality dependence

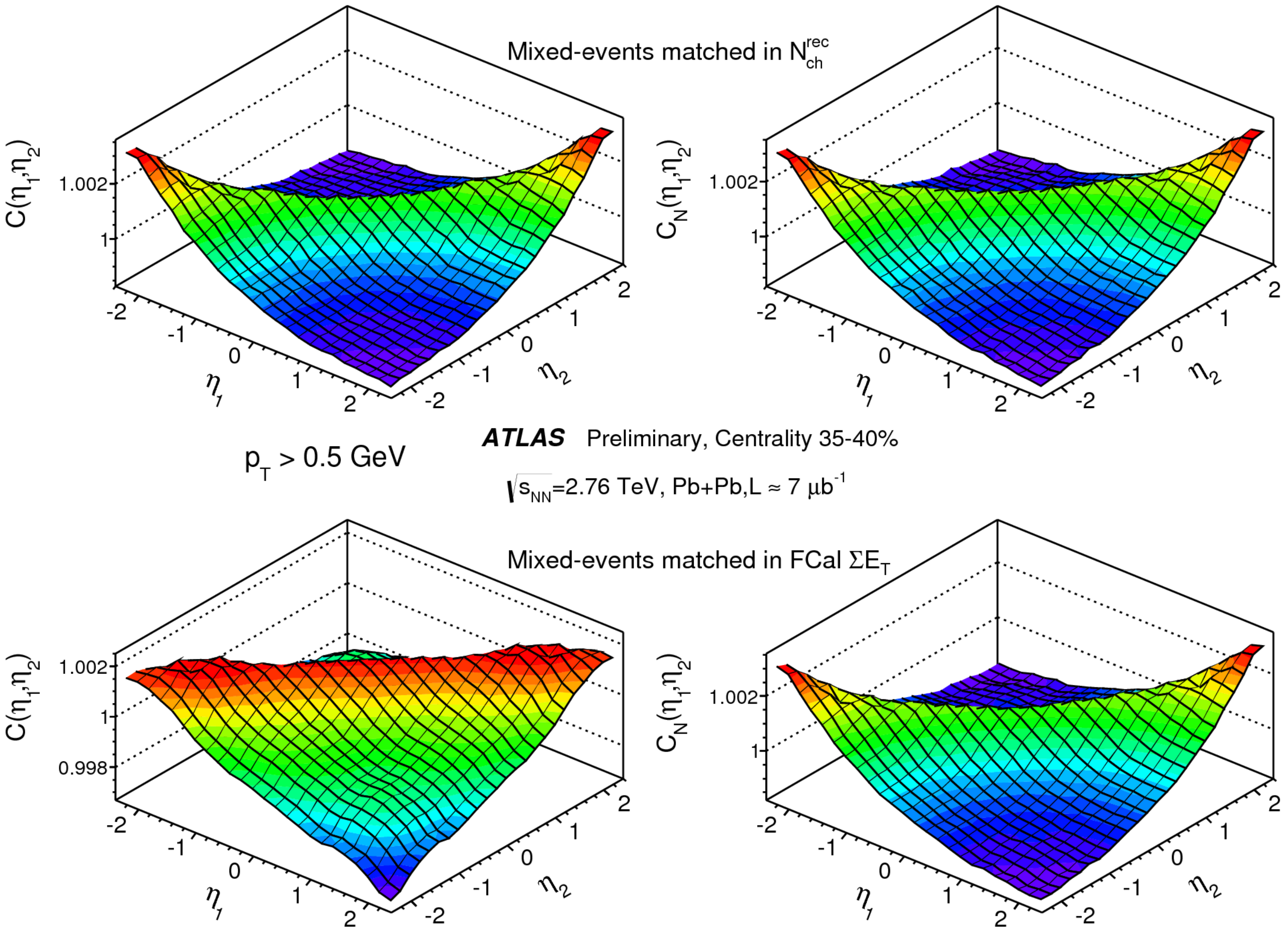

Spectrum: before and after SRC subtraction

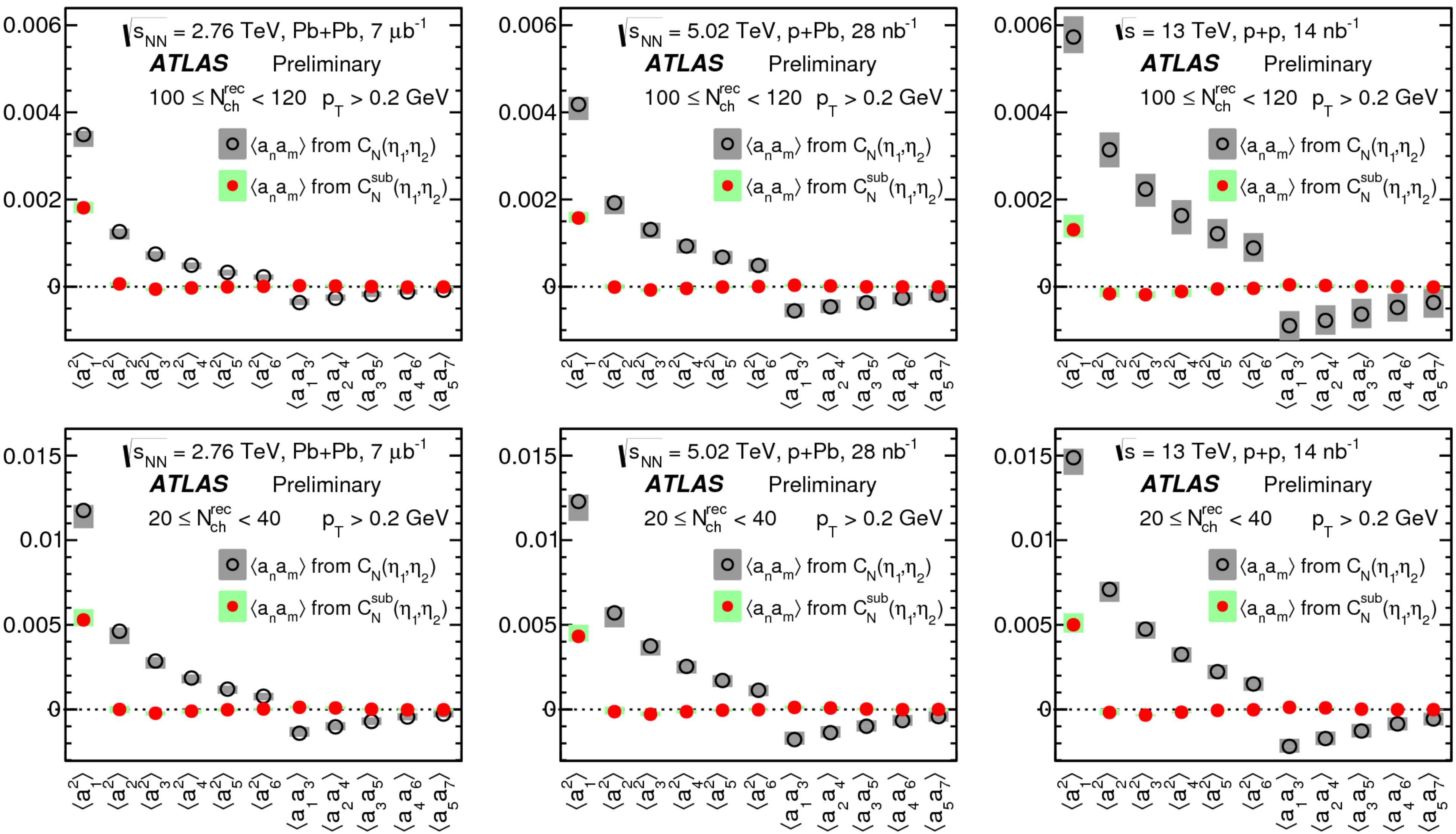

Other methods to measure $\langle a_1^2 \rangle$

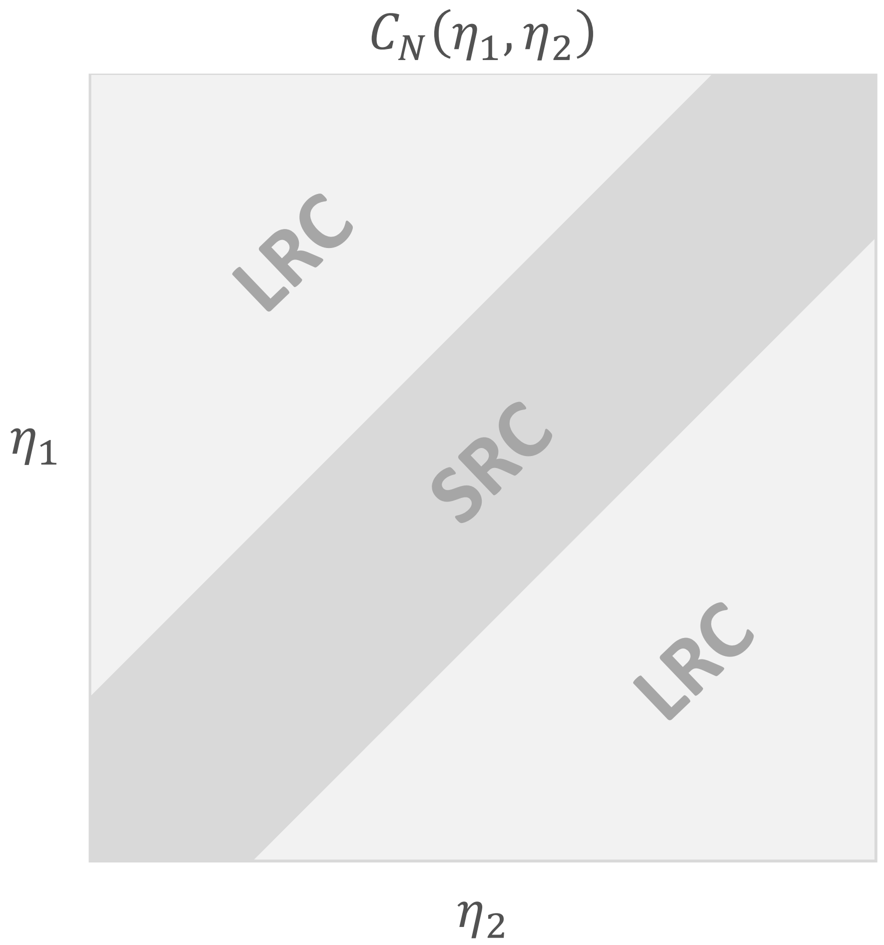

Other methods to measure $\langle a_1^2 \rangle$

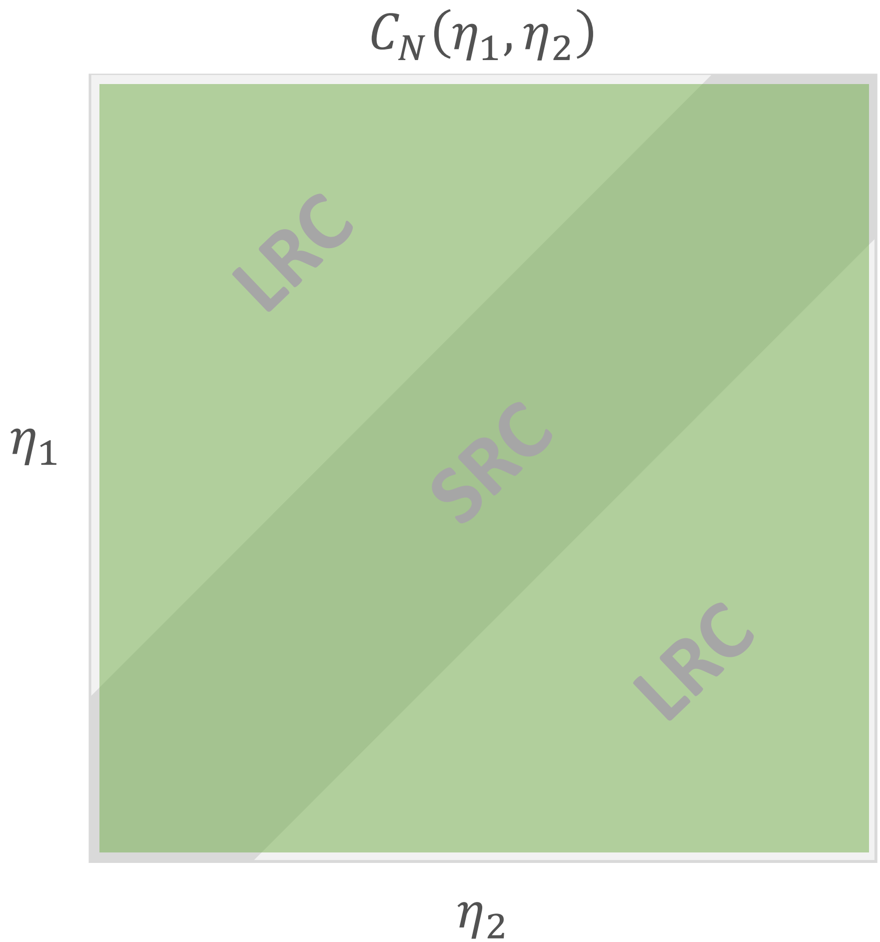

- Expansion of $C_N^{sub}(\eta_1, \eta_2)$

$$C_N^{sub}(\eta_1, \eta_2) = 1 + \langle a_1^2 \rangle \eta_1 \eta_2$$

- Use whole (η_1, η_2) space.

Other methods to measure $\langle a_1^2 \rangle$

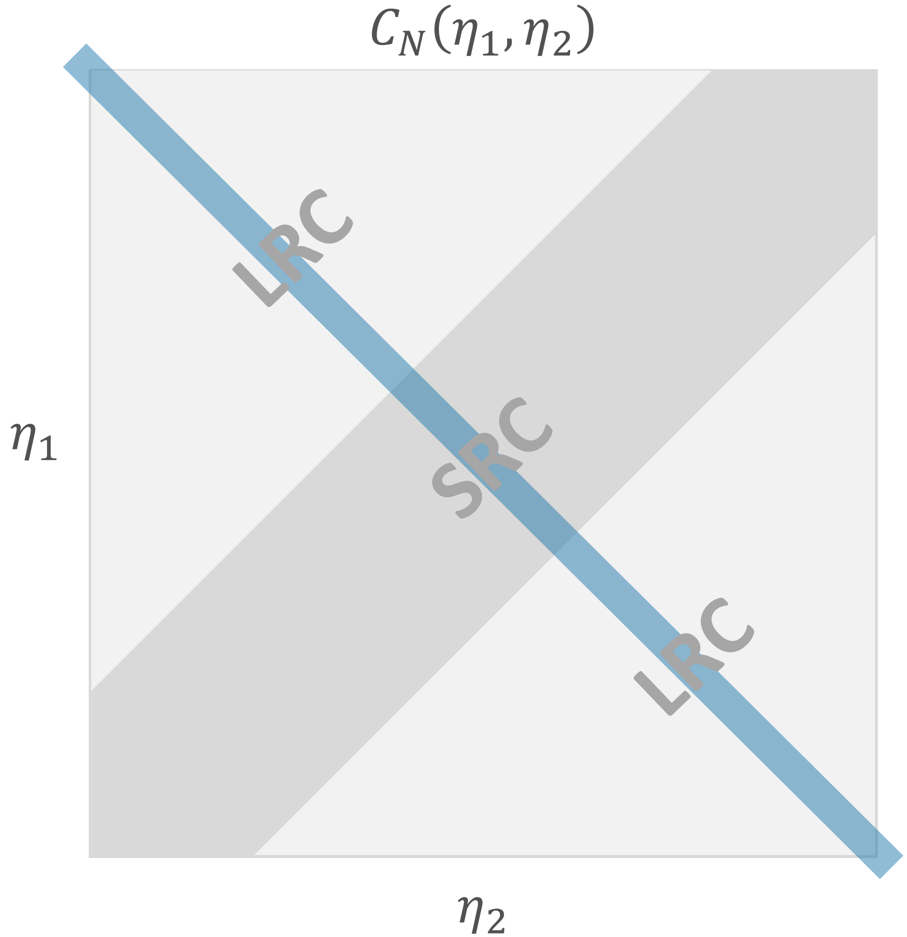

- Expansion of $C_N^{sub}(\eta_1, \eta_2)$

$$C_N^{sub}(\eta_1, \eta_2) = 1 + \langle a_1^2 \rangle \eta_1 \eta_2$$

- Quadratic fit along $C_N^{sub}(\eta_-)$

$$C_N^{sub}(\eta_-) = 1 + \frac{\langle a_1^2 \rangle}{4}(\eta_+^2 - \eta_-^2)$$

- Longest level arm for SRC estimation.

Other methods to measure $\langle a_1^2 \rangle$

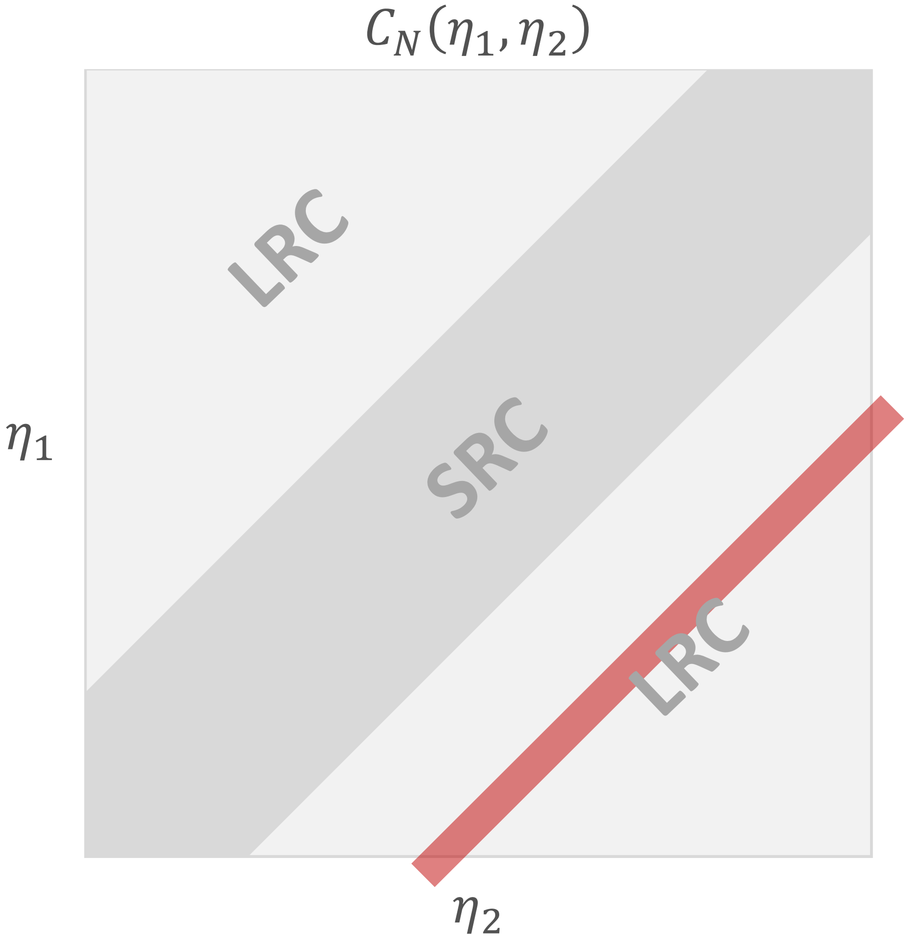

- Expansion of $C_N^{sub}(\eta_1,\eta_2)$

$$C_N^{sub}(\eta_1,\eta_2) = 1 + \langle a_1^2 \rangle \eta_1 \eta_2$$

- Quadratic fit along $C_N^{sub}(\eta_-)$

$$C_N^{sub}(\eta_-) = 1 + \frac{\langle a_1^2 \rangle}{4}(\eta_+^2 - \eta_-^2)$$

- Quadratic fit along $C_N^{sub}(\eta_+)$

$$C_N^{sub}(\eta_-) = 1 + \frac{\langle a_1^2 \rangle}{4}(\eta_+^2 - \eta_-^2)$$

- Outside the SRC region, not affected by the SRC removal procedure.

Other methods to measure $\langle a_1^2 \rangle$

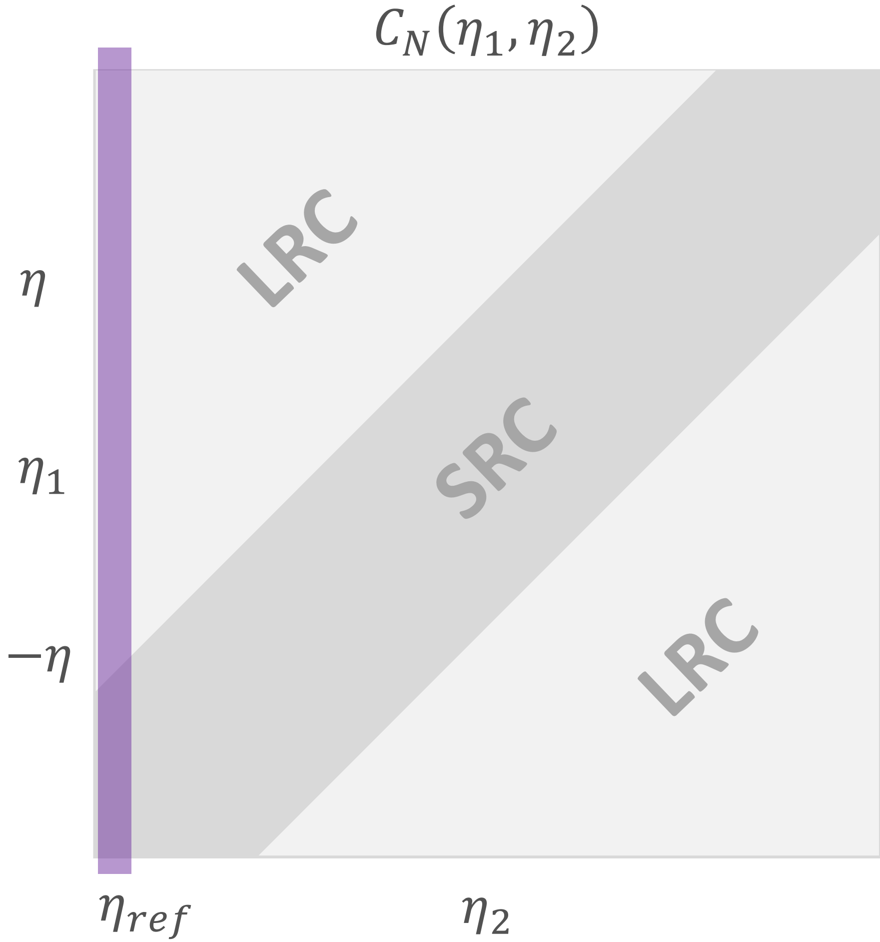

- Residual centrality dependence cancels out.

- Expansion of $C_N^{sub}(\eta_1, \eta_2)$

$$C_N^{sub}(\eta_1, \eta_2) = 1 + \langle a_1^2 \rangle \eta_1 \eta_2$$

- Quadratic fit along $C_N^{sub}(\eta_-)$

$$C_N^{sub}(\eta_-) = 1 + \frac{\langle a_1^2 \rangle}{4}(\eta_+^2 - \eta_-^2)$$

- Quadratic fit along $C_N^{sub}(\eta_+)$

$$C_N^{sub}(\eta_-) = 1 + \frac{\langle a_1^2 \rangle}{4}(\eta_+^2 - \eta_-^2)$$

- Linear fit of $r_N^{sub}(\eta, \eta_{ref}) \equiv \frac{C_N^{sub}(-\eta, \eta_{ref})}{C_N^{sub}(\eta, \eta_{ref})}$

$$r_N^{sub}(\eta, \eta_{ref}) = 1 - 2\langle a_1^2 \rangle \eta \eta_{ref}$$

Other methods to measure $\langle a_1^2 \rangle$

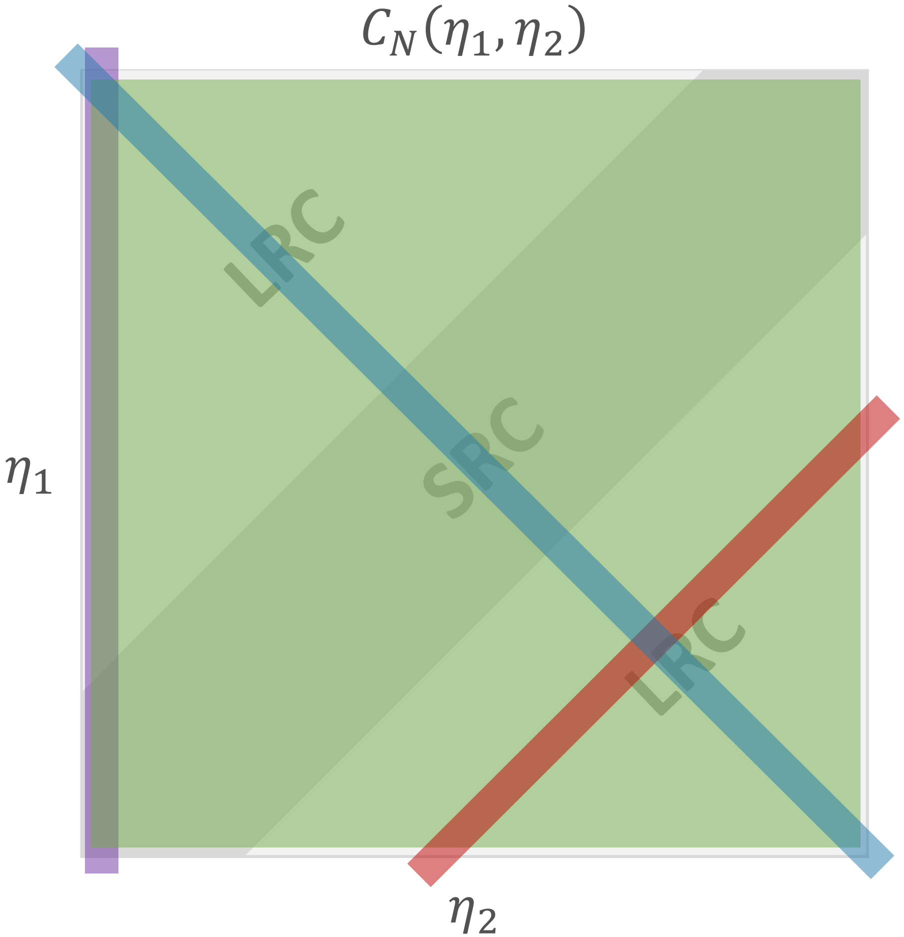

- Expansion of $C_N^{sub}(\eta_1, \eta_2)$

$$C_N^{sub}(\eta_1, \eta_2) = 1 + \langle a_1^2 \rangle \eta_1 \eta_2$$

- Quadratic fit along $C_N^{sub}(\eta_-)$

$$C_N^{sub}(\eta_-) = 1 + \frac{\langle a_1^2 \rangle}{4}(\eta_+^2 - \eta_-^2)$$

- Quadratic fit along $C_N^{sub}(\eta_+)$

$$C_N^{sub}(\eta_-) = 1 + \frac{\langle a_1^2 \rangle}{4}(\eta_+^2 - \eta_-^2)$$

- Linear fit of $r_N^{sub}(\eta, \eta_{ref}) \equiv \frac{C_N^{sub}(-\eta, \eta_{ref})}{C_N^{sub}(\eta, \eta_{ref})}$

$$r_N^{sub}(\eta, \eta_{ref}) = 1 - 2\langle a_1^2 \rangle \eta \eta_{ref}$$

- Four methods have different responses of the analysis procedures, and are largely independent.

Projection of $C_N(\eta_1, \eta_2)$: position 1

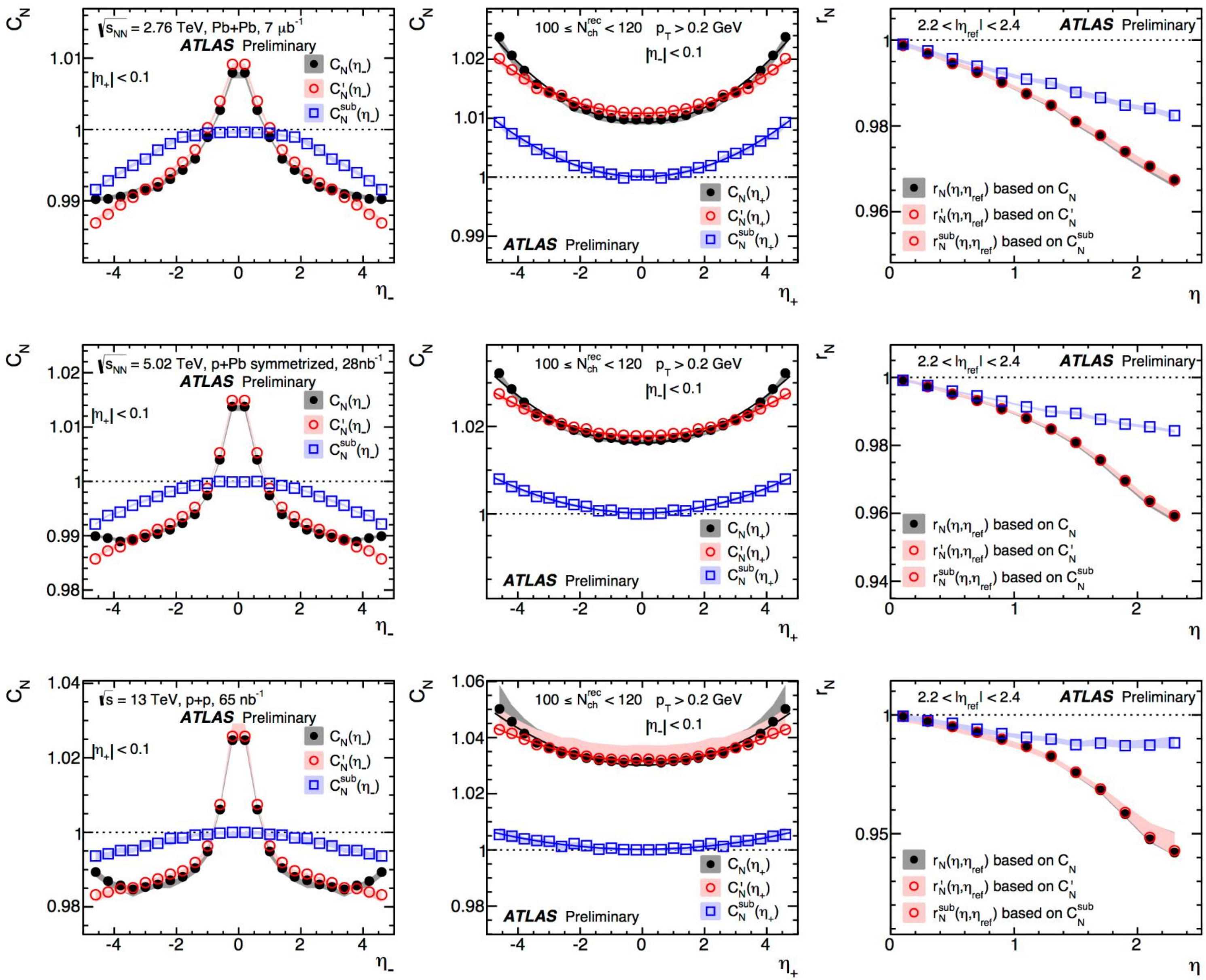

Projection of $C_N(\eta_1, \eta_2)$: position 2

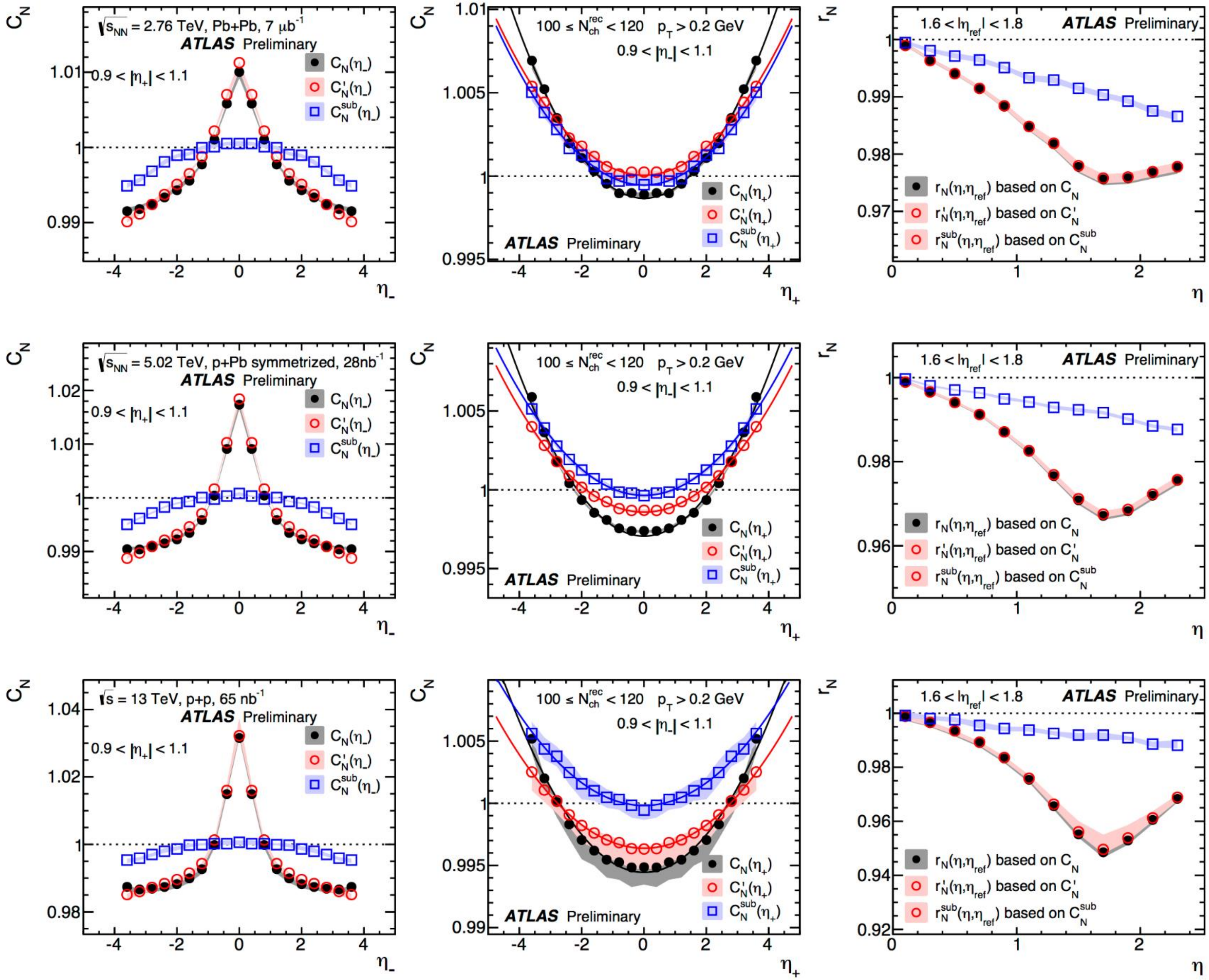

Projection of $C_N(\eta_1, \eta_2)$: position 3

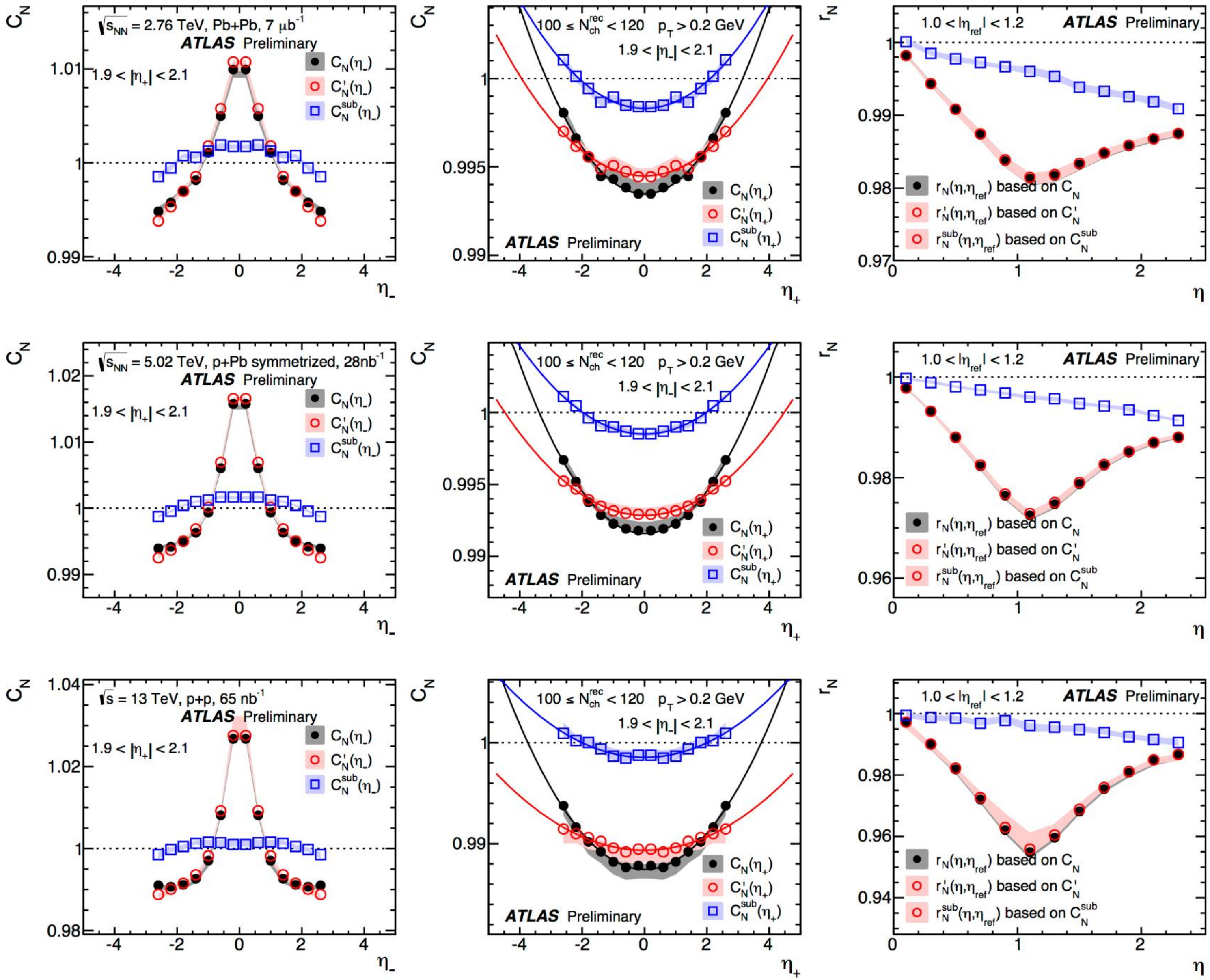

Gaussian width of fitting $R(\eta_1, \eta_2)$

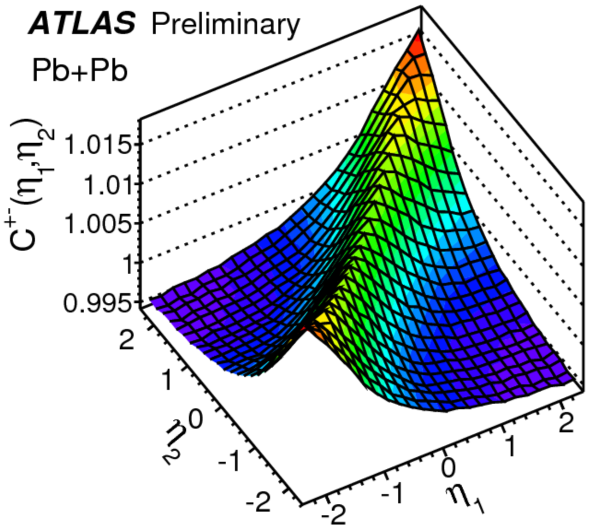

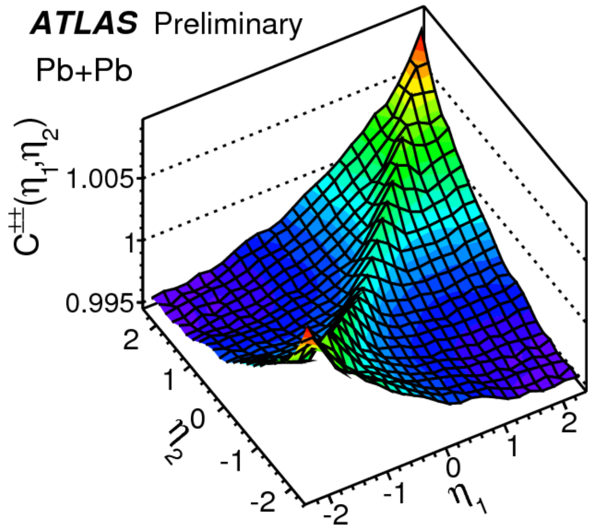

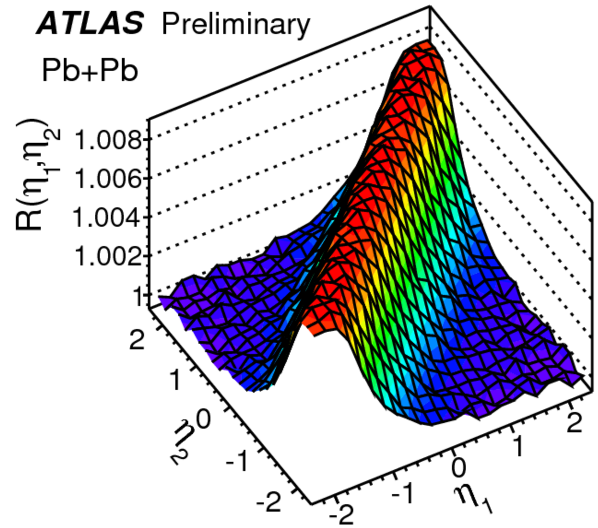

ATLAS Preliminary

$200 \leq N_{ch}^{rec} < 220$

$\sqrt{s_{NN}}$ = 2.76 TeV, Pb+Pb, 7 μb^{-1}

$p_T > 0.2$ GeV

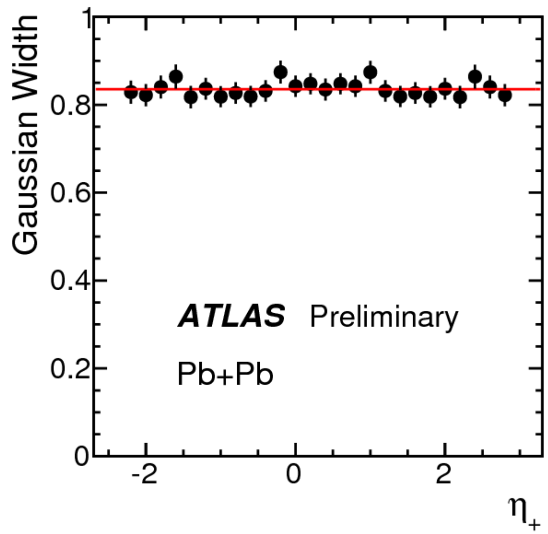

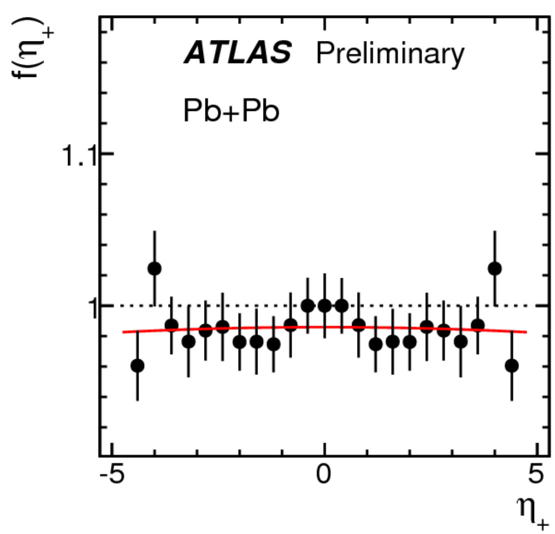

Gaussian width as a function of N_{ch}

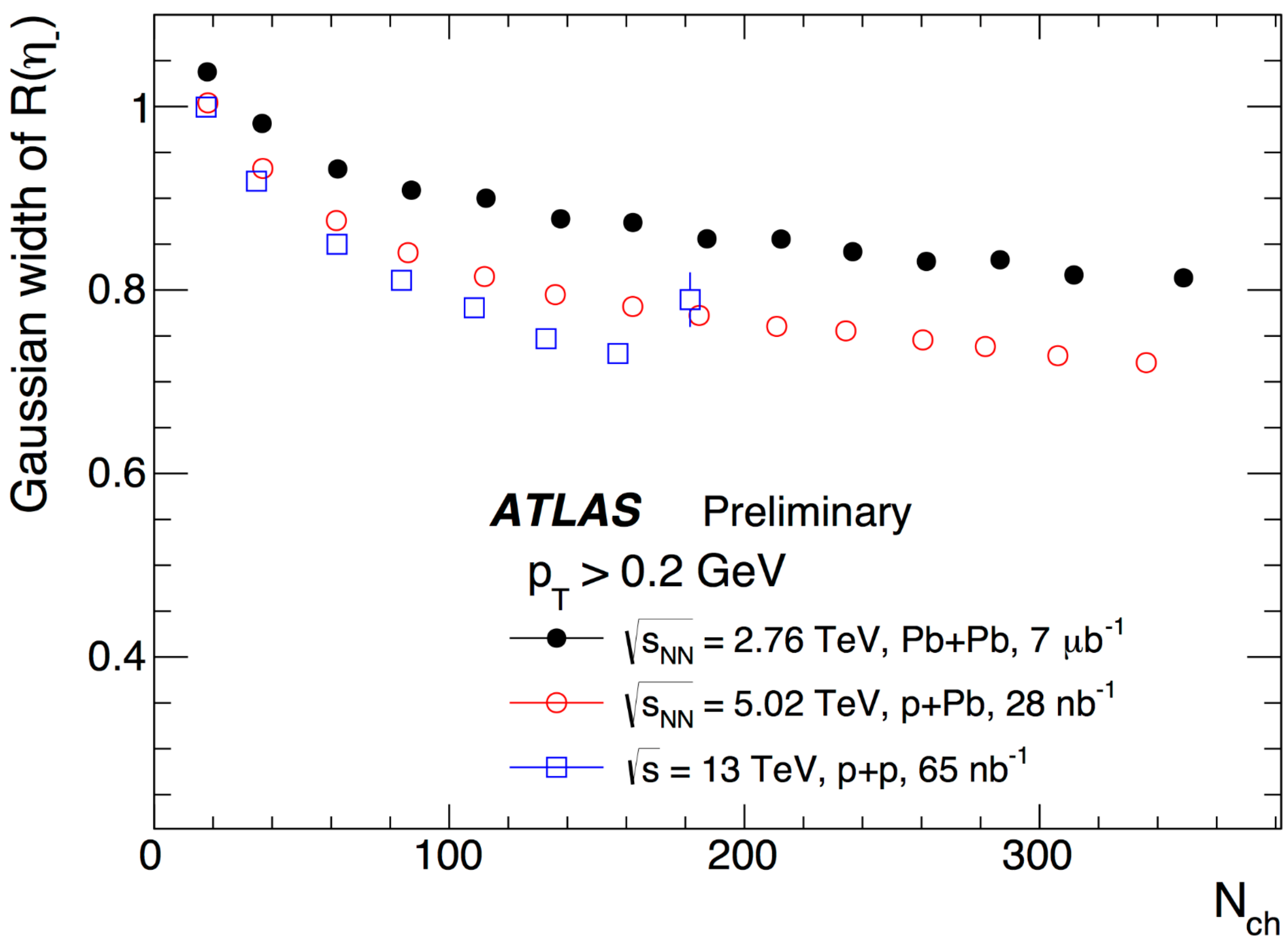

Detector acceptance from SRC

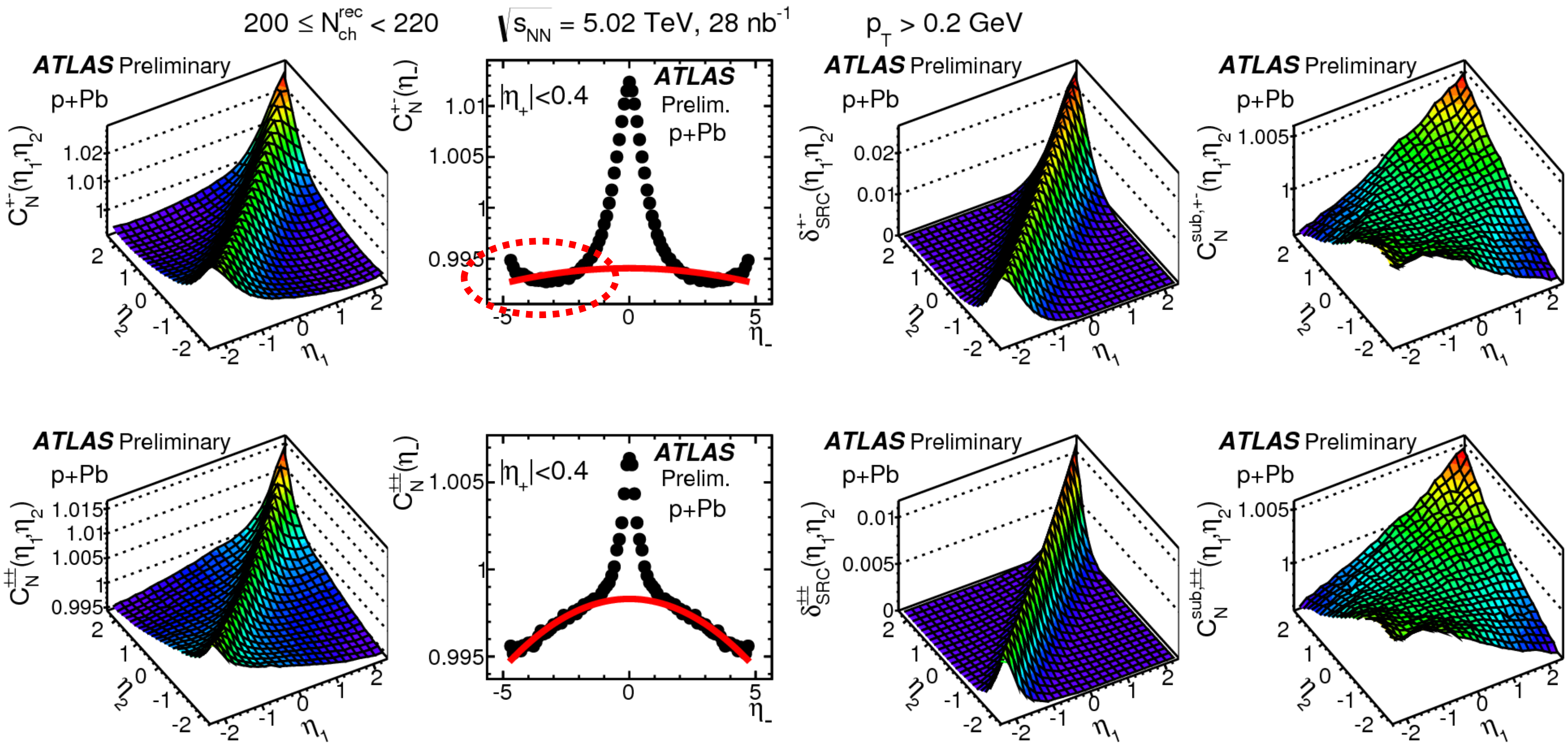

Detector acceptance from SRC

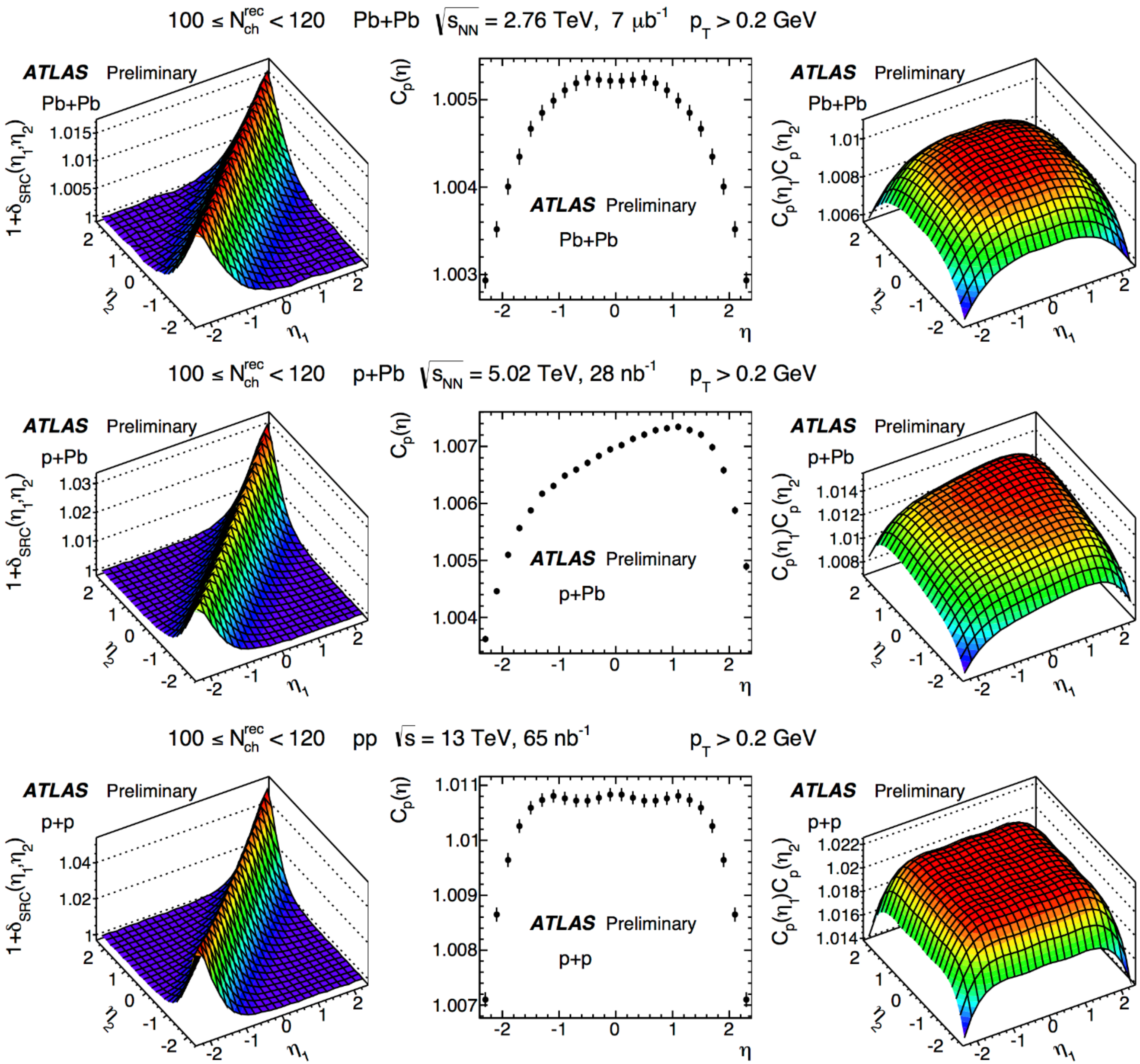

Detector acceptance from SRC

- In general, the raw CF $C(\eta_1,\eta_2)$ could be decomposed as

$$C = C_{LRC} + C_{SRC} + C_{SPM}$$

where C_{SPM} is the contribution from single particle mode, and it could be removed through normalizing C_{RAW} by the projections of itself C_{RAW}^{proj}, where

$$C^{proj} = C_{LRC}^{proj} + C_{SRC}^{proj} + C_{SPM}^{proj}$$

- Notice here $C_{LRC}^{proj} = 1$ because $\langle a_m a_n \rangle_{m,n\neq 0}^{proj} = 0$, and because C_{SPM} is supposed to be factorized in the (η_1,η_2) plane, so $C_{SPM} = C_{SPM}^{proj}$. Then we have

$$C_N \equiv C/C^{proj} \approx C_{LRC} + C_{SRC} - C_{SRC}^{proj}$$

where C_{SRC}^{proj} didn't vanish due to the acceptance effects;

- Because of the presence of C_{SRC}^{proj}, the estimated SRC C_{SRC}^{est} will be biased

$$C_{SRC}^{est} = C_{SRC} + C_{SRC}^{bias}$$

where C_{SRC}^{bias} denotes the bias;

- However, if we calculate the projections of C_{SRC}^{est}

$$[C_{SRC}^{est}]^{proj} = C_{SRC}^{proj} + [C_{SRC}^{bias}]^{proj} \approx C_{SRC}^{proj}$$

where $[C_{SRC}^{bias}]^{proj}$ is negligible as long as the $C_{SRC}^{bias} \ll C_{SRC}$ (it is true in this analysis, if not, more iteration required until this relation holds);

- Finally, the contamination term $-C_{SRC}^{proj}$ could be subtracted from C_N

$$C_N' \equiv C_N + [C_{SRC}^{est}]^{proj} = C_{LRC} + C_{SRC}$$

Scan of projections: Pb+Pb

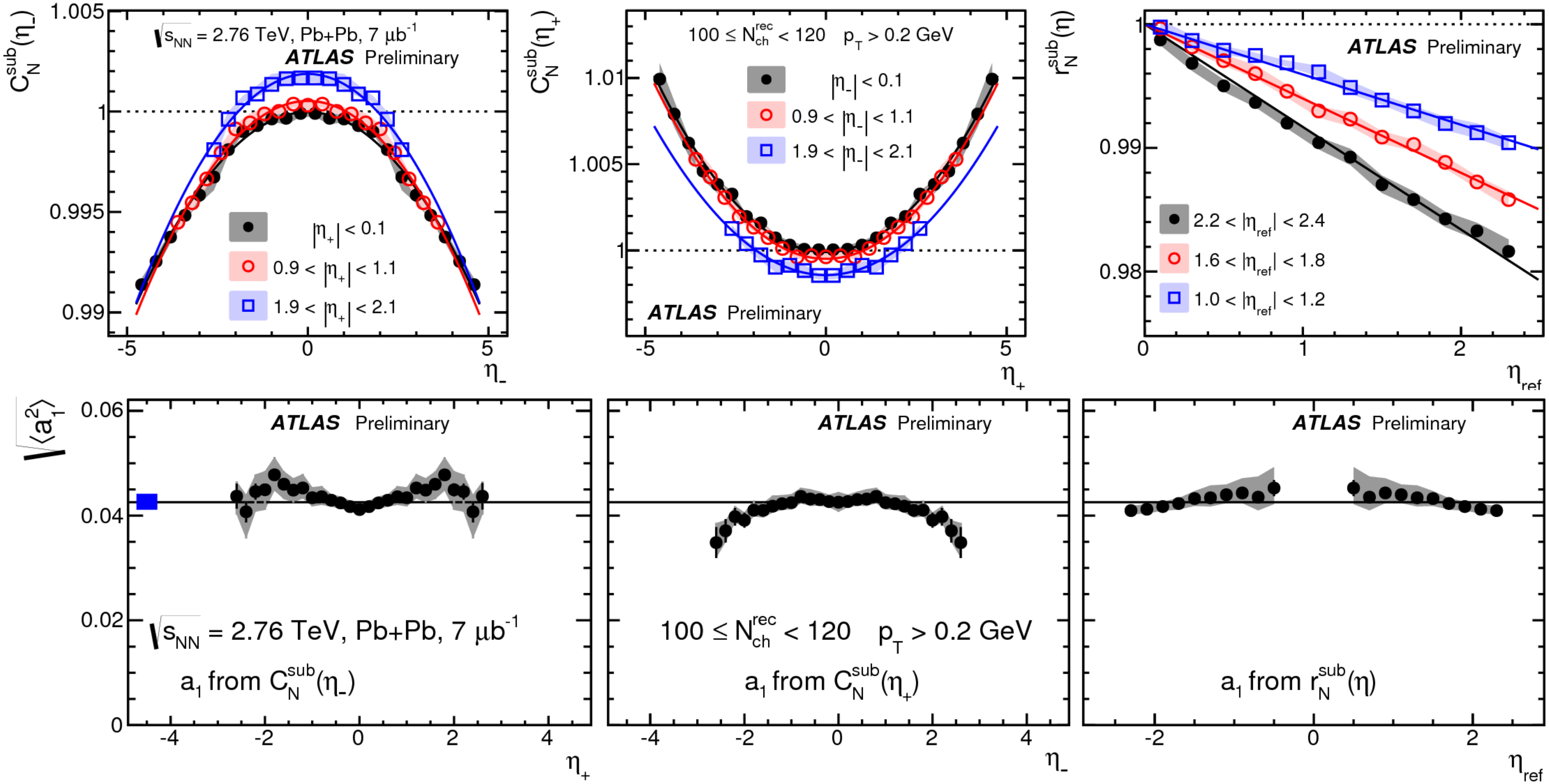

Scan of projections: *p*+Pb

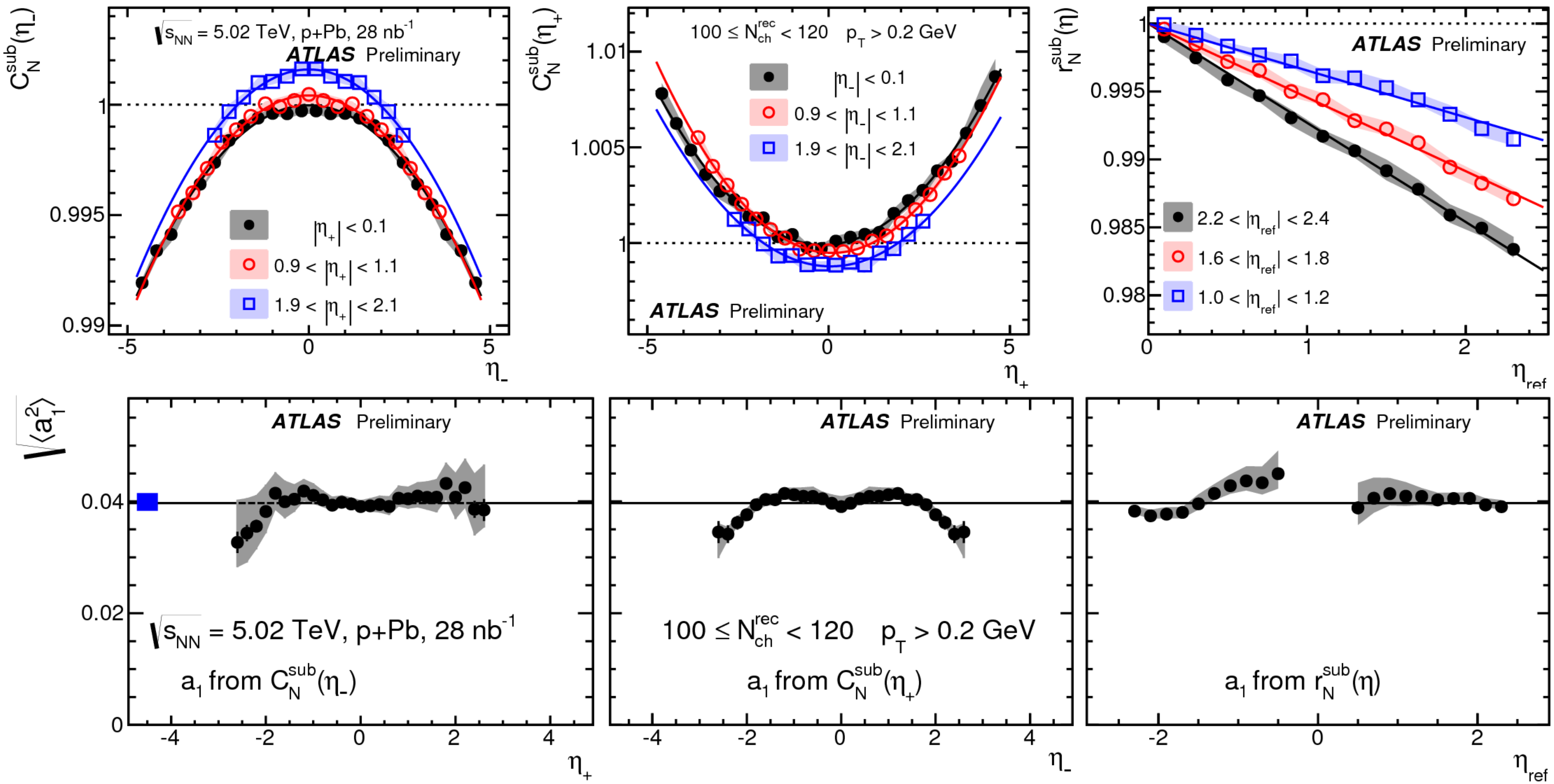

Scan of projections: *pp*

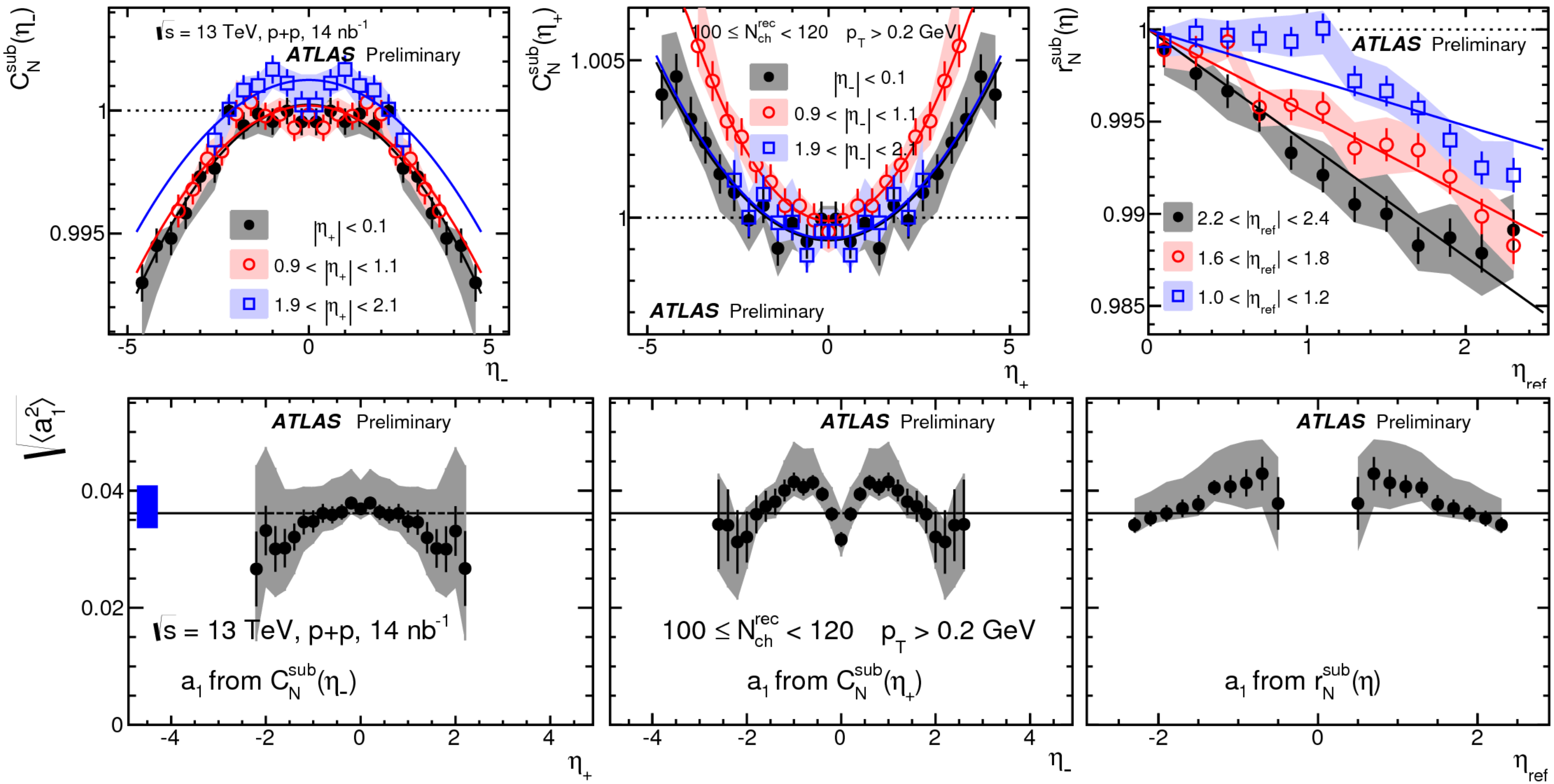

Charge dependence

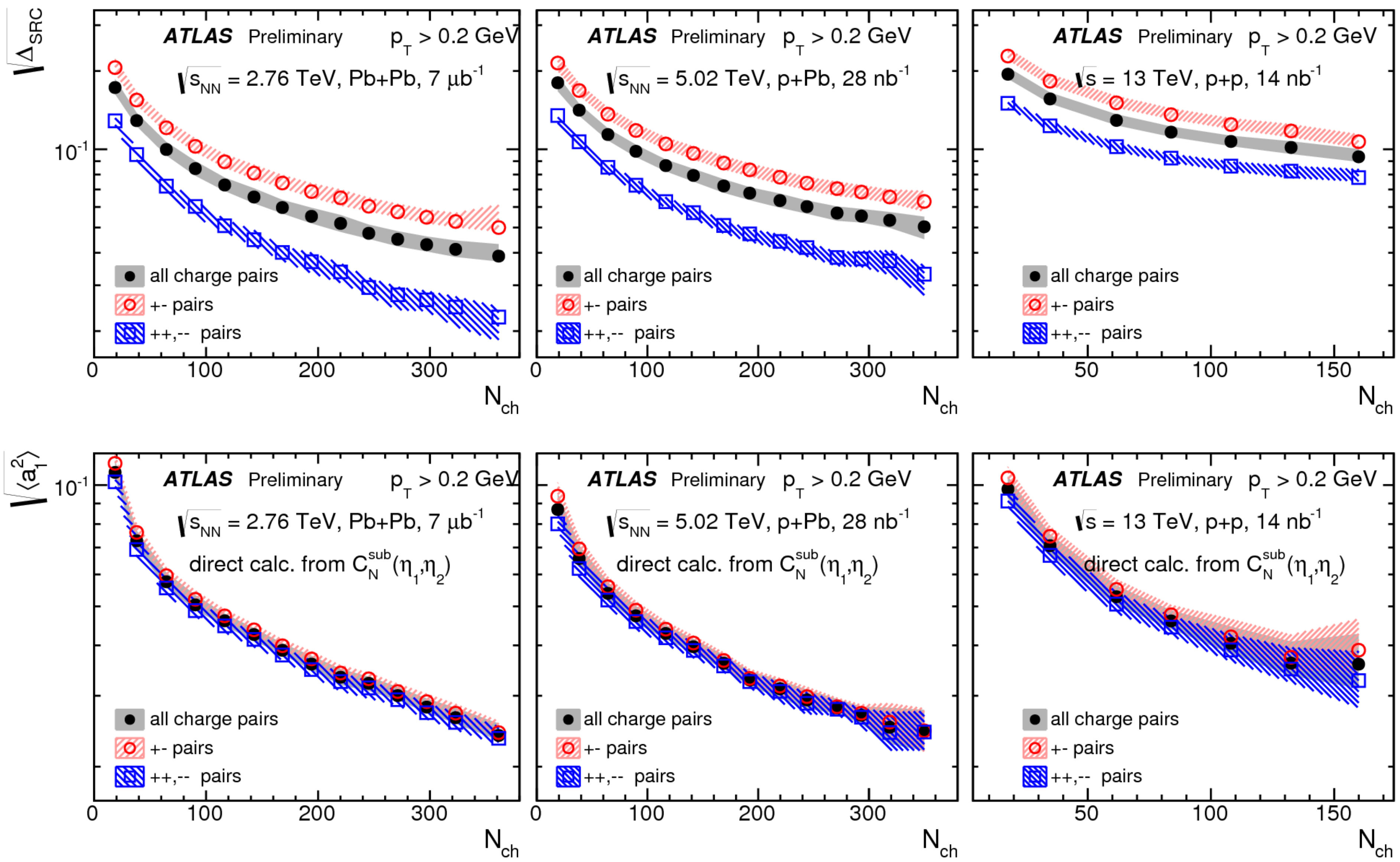

Systematic uncertainty: correlation function

Collision system	Pb+Pb	p+Pb	pp
Event-mixing [%]	0.4–0.7	0.4–2.2	0.2–1.4
Run-by-run stability [%]	0.3–0.5	0.3–1.5	0.2–1.5
z_{vtx} variation [%]	0.3–0.6	0.3–1.5	0.2–1.6
Track selection & efficiency [%]	0.6–1.2	0.2–1.3	0.3–0.7
MC consistency [%]	0.2–1.6	0.5–2.5	0.7–3.3
Charge dependence [%]	1.0–1.8	0.8–3.8	1.5–2.5
SRC subtraction [%]	1.1–2.1	1.0–5.9	1.2–5.0
Total [%]	1.7–3.2	2.1–7.6	2.5–6.9

Systematic uncertainty: a_1

	Quadratic fit to the $C_N^{sub}(\eta_-)\|_{\|\eta_+\|<0.1}$			Quadratic fit to the $C_N^{sub}(\eta_+)\|_{0.9<\|\eta_-\|<1.1}$		
Collision system	Pb+Pb	p+Pb	pp	Pb+Pb	p+Pb	pp
Event-mixing [%]	0.5–2.2	0.3–1.8	0.2–2.8	0.2–1.7	0.2–1.6	0.2–2.7
Run-by-run stability [%]	0.2–1.3	0.2–1.7	0.2–2.8	0.2–1.5	0.2–1.1	0.2–1.6
z_{vtx} variation [%]	0.3–1.9	0.1–2.2	0.1–1.6	0.1–1.8	0.2–0.7	0.1–0.9
Track selec.& efficiency[%]	0.4–2.1	0.3–0.9	0.8–2.2	0.8–3.7	1.0	0.9–1.2
MC consistency [%]	0.2–3.6	0.4–3.9	0.2–10.0	0.2–4.3	0.2–2.4	0.2–4.7
Charge dependence [%]	0.9–4.2	1.0–10.2	2.8–4.6	0.4–3.8	0.6–3.1	1.2–6.2
SRC subtraction [%]	0.9–2.5	1.2–6.3	1.3–4.8	1.4–2.5	1.2–3.7	1.2–4.6
Total [%]	2.1–5.2	2.7–10.3	10–12	2.4–5.5	2.5–6.8	3.5–11.2

	Linear fit to the $r_N^{sub}(\eta)\|_{2.2<\|\eta_{ref}\|<2.4}$			Global Legendre expansion of C_N^{sub}		
Collision system	Pb+Pb	p+Pb	pp	Pb+Pb	p+Pb	pp
Event-mixing [%]	0.3–2.3	0.3–1.4	0.1–1.5	0.2–1.8	0.1–1.7	0.1–0.9
Run-by-run stability [%]	0.1–1.2	0.1–1.7	0.2–2.8	0.2–0.7	0.1–1.3	0.1–2.1
z_{vtx} variation [%]	0.2–1.2	0.2–2.1	0.2–2.6	0.1–1.3	0.2–2.5	0.2–1.7
Track selec.& efficiency[%]	0.4–1.3	0.6–0.9	0.7–1.7	0.3–0.9	0.4–0.7	0.8–2.4
MC consistency [%]	0.2–2.6	0.2–3.7	0.8–7.6	0.2–2.5	0.4–3.2	0.1–6.7
Charge dependence [%]	0.4–4.9	0.1–8.8	1.6–5.3	2.3–5.3	1.0–12.7	3.4–8.1
SRC subtraction [%]	1.4–3.2	2.2–3.4	1.7–5.0	1.7–4.3	2.0–8.9	2.7–9.6
Total [%]	2.4–6.2	2.9–8.9	4.4–9.8	3.4–6.4	4.1–12.9	6.2–12.5